A Market and Engineering Study of a 3-Kilowatt Class Gas Turbine Generator

by

Mark A. Monroe

Submitted to the Department of Aeronautics and Astronautics in partial fulfillment of the requirements for the degree of

Master of Science in Aerospace Engineering

at the

MASSACHUSETTS INSTITUTE OF TECHNOLOGY

September 2003

Author .....
Department of Aeronautics and Astronautics
August 22, 2003

Certified by ....
Alan H. Epstein
R.C. Maclaurin Professor of Aeronautics and Astronautics
Thesis Supervisor

Accepted by ....
Edward M. Greitzer
H.N. Slater Professor of Aeronautics and Astronautics
Chair, Department Committee on Graduate Students

AERO

A Market and Engineering Study of a 3-Kilowatt Class Gas Turbine Generator

by

Mark A. Monroe

Submitted to the Department of Aeronautics and Astronautics
on August 22, 2003, in partial fulfillment of the
requirements for the degree of
Master of Science in Aerospace Engineering

Abstract

Market and engineering studies were performed for the world's only commercially available 3 kW class gas turbine generator, the IHI Aerospace Dynajet. The objectives of the market study were to determine the competitive requirements for small generators in various U.S. applications, assess the unit's current suitability for these applications, and recommend ways to modify performance or marketing practices to make it more competitive. Engineering study goals included developing an accurate cycle model and assessing the potential for performance improvement.

The market study found that the current high selling price precludes competitiveness in most segments of the U.S. civil market. One potential exception may be the marine market, where price sensitivity is less of an issue and a premium is paid for quiet operation, a distinct advantage of the Dynajet. A gas turbine generator solution has more potential in the military market, where the difference from incumbent prices is smaller than in the civil market. The Dynajet is also an appealing military solution because of its high reliability and quiet operation. The market study concluded that increasing power output and efficiency while reducing purchase price would be the most effective approach to improved competitiveness. Alternatively, the current strengths could be leveraged by adapting it for use with an absorption cooler and by emphasizing its superior emission characteristics to consumers and regulators.

The engineering study discovered that cycle performance is degraded by secondary nonidealities including flow leakage, heat leakage, and thermal flow distortion. Although these nonidealities are present to some degree in all gas turbines, their impacts are larger in small-scale engines. The net effect of all nonidealities is a 61 percent reduction in power and 12 point decrease in overall efficiency.

Analysis concluded that the best way to enhance Dynajet competitiveness is to reduce or remove those nonidealities that are straightforward to fix while increasing power output to either 3 or 5 kW. Output of 5 kW is most promising in terms of cost and weight competitiveness; however, such an improvement may require turbomachinery redesign. A short-term increase of power output to 3 kW appears practical from an engineering standpoint.

Thesis Supervisor: Alan H. Epstein
Title: R.C. Maclaurin Professor of Aeronautics and Astronautics

Acknowledgements

This thesis would not have been possible without the help of many people. Most notably, I would like to thank my advisor, Prof. Alan Epstein, for his support and innumerable contributions to this research. I was quite fortunate to walk into his office looking for a research topic on the very day he received an email from IHI Aerospace proposing this one.

In addition to Prof. Epstein, other GTL faculty and research staff who provided valuable guidance include Prof. Edward Greitzer, Dr. Choon Tan, Dr. Yifang Gong, Prof. Zoltan Spakovsky, Prof. Jack Kerrobrock, and Dr. Norihisa Miki. I am grateful for their assistance.

I would also like to thank the support staff at the GTL for their contributions to the successful completion of this research. Lori Martinez provided a crucial line of communication with Prof. Epstein. She also made waiting for meetings more enjoyable with her cheerful conversation and tasty candy tray. Diana Park was indispensable when it came time to prepare presentations and reports, and several of the figures in this thesis were made with her help. Thanks also to Mary McDavitt, Holly Anderson, Susan Parker, Julie Finn, and Paul Warren.

My friends inside and outside the GTL helped make the past year and a half a great time. Thanks to my roommate Shana for adding levity at home and at work. Thanks to my other roommates Andrew, Dan, and Alicia for making 7 Granite a fine place to live. Thanks to Shana, Garrett, Todd, Mike, Alex, and Nate for bowling, poker, road trips, and other diversions. Graduate school would not have been the same without them. Finally, thanks to my fraternity brothers for their unique contributions to my graduate school experience. Particularly Rob, Gabe, Matt, Corey, Luke, John B., and Tony.

I am grateful to my family for their love and support during my education. Home was a welcoming retreat from the sometimes-stressful MIT environment. I owe them a great deal.

Finally, I would like to recognize and thank IHI Aerospace for funding this research and my graduate studies. In particular, thanks to Dr. Kousuke Isomura and Mr. Hirotaka Kumakura for spearheading the project. The engine data and personal insight they provided

were critical to success. I am also thankful for the hospitality they showed me at the IHI facilities in Yokohama and Tomioka, Japan.

Contents

List of Figures

List of Tables

Nomenclature

Roman

A	flow area / thermocouple cross-sectional area
c	specific heat / critical condition (Mach number = 1)
C	velocity / thermcouple rod circumference
C_D	discharge coefficient
H	convective heat transfer film coefficient
i	square root of negative one / ideal
k	thermal conductivity
K	fluid property for seal analysis
L	exposed thermocouple length
m	mass
M	Mach number
n	harmonic number of the velocity nonuniformity Fourier component
P	pressure
Q	heat energy per unit area
Q	heat energy
r	radius
t	time
T	temperature
U	flow disturbance propagation speed
v	specific volume
V	velocity
w	axial flow velocity
W	rotor power
x	axial coordinate

Greek

α	bypass ratio
β	impeller exit angle
ε	heat exchanger effectiveness
γ	specific heat ratio, c_p/c_v
η	efficiency
π	pressure ratio
θ	cylindrical coordinate
ρ	flow density
σ	circular frequency of flow nonuniformity
τ	temperature ratio
ω	rotational speed
ξ	magnitude of velocity nonuniformity

Superscripts

$'$	relative frame / perturbation
$\cdot$	time derivative

Subscripts

0	engine inlet / reference condition
1	compressor scroll inlet / general inlet condition
1.1	effective compressor inlet with heat addition
2	compressor exit / general exit condition
3	air-side heat exchanger inlet

4	air-side heat exchanger exit
5	combustor inlet
6	combustor exit
7	turbine nozzle guide vane inlet
8	turbine exit
11	gas-side heat exchanger inlet
12	gas-side heat exchanger exit
a	adiabatic
c	compressor
C	cold flow
Corr	corrected quantity
des	design condition
f	flow
H	hot flow
Mean	average of hot and cold quantities
n	nonadiabatic
p	constant pressure
r	regenerator / thermocouple rod
t	stagnation quantity / turbine
Total	sum of hot and cold quantities
v	constant volume
w	wall

Chapter 1

Introduction

1.1 Background and Motivation

The IHI Aerospace (IA) Dynajet gas turbine generator is a unique product [1]. It is the world's only gas turbine generator in production in the under-10 kW size range. This thesis is motivated by IA's interest in entering the U.S. generator market. To do so, IA partnered with the Massachusetts Institute of Technology Gas Turbine Laboratory (MIT GTL) to perform a two-phase study for improved Dynajet competitiveness. First, a market study was performed to identify the requirements for competitiveness in the U.S. market. Second, an engineering study of the Dynajet was performed to determine potential avenues for engine improvement. These studies are presented herein.

1.2 Objectives

The main objective of this thesis is to present a set of options for Dynajet improvement that will optimize its competitiveness in the U.S. generator market. To establish the knowledge base necessary for achieving this objective, market and engineering studies were performed.

The principal objective of the market study is to define the U.S. market potential for the current Dynajet and any subsequent derivatives. Such information can be used to guide marketing strategies and future product development.

The principal objective of the engineering study is to develop a cycle model of the Dynajet that accurately represents the engine's performance. The model must be consistent with measurements and provide a detailed accounting of all cycle nonidealities. The ultimate goal of the cycle model is utility as a guide to engine modifications for performance improvement.

To conclude, the findings of the market and engineering studies will be evaluated together to make recommendations for Dynajet improvement. These recommendations will give consideration to the cost and difficulty of modifications as well as their expected impact on market competitiveness.

1.3 Dynajet Overview

The Dynajet is a single-shaft, regenerative gas turbine generator capable of producing 2.6 kW of alternating current power. A cutaway side-view of the system is shown in Figure 1-1. A single-stage centrifugal compressor, single-stage centrifugal turbine, single-can combustor, and counterflow heat exchanger comprise the engine. The ideal Dynajet cycle diagram is shown in Figure 1-2. The numbering convention used in this diagram will be referred to throughout this thesis. A permanent magnet synchronous generator is utilized for power production. Output from the generator is converted to 50 or 60 Hz by an integrated inverter, allowing for variable speed operation and better efficiency at low output. The rated speed for maximum power output is 100,000 RPM.

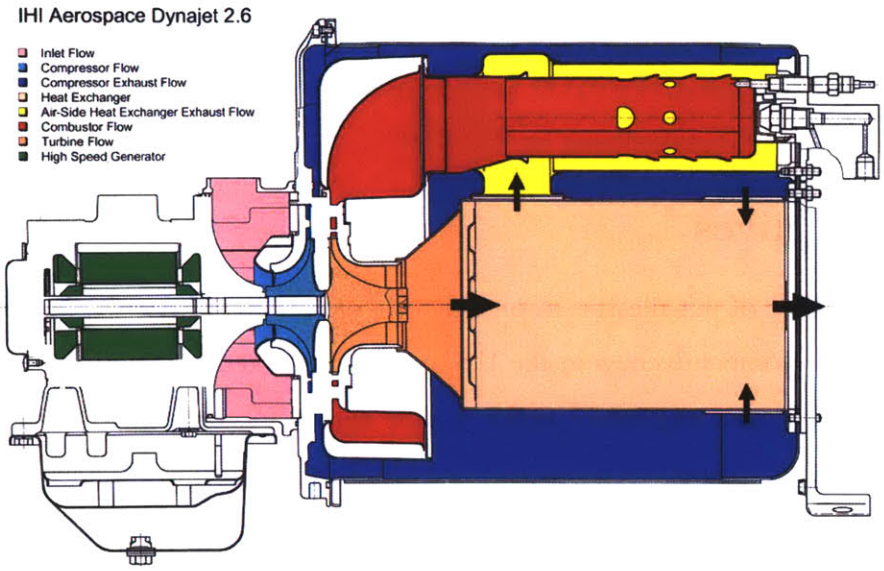

Figure 1-1: Dynajet cutaway side-view.

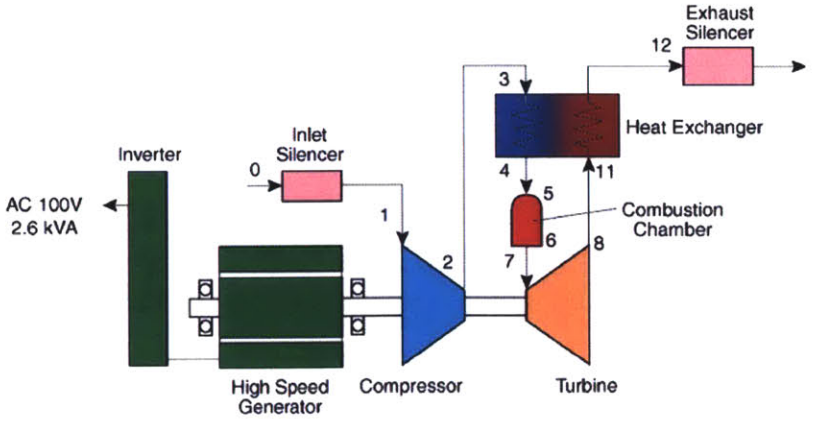

Figure 1-2: Ideal Dynajet cycle diagram.

A three-dimensional solid model of the Dynajet was created in SolidWorks to facilitate understanding of the engine's complex geometry. Isometric and three-view representations of the model are shown in Figure 1-3 and Figure 1-4, respectively. The model is not detailed to the level of fittings and tolerances, nor is it intended to be. Rather, the model is meant to be useful for such applications as wall and flow area estimation for heat transfer calculations and for input to computational fluid dynamics software for rigorous flow analysis.

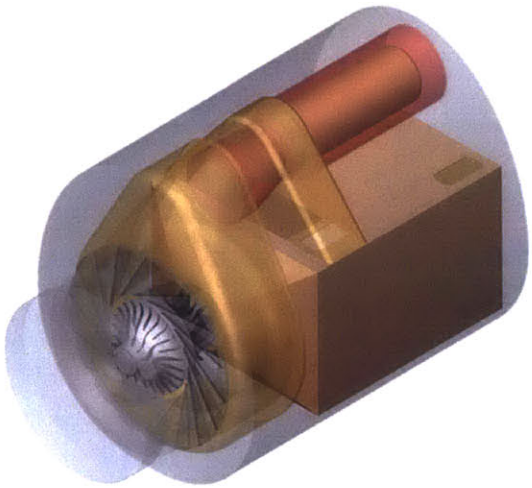

Figure 1-3: Isometric-view of Dynajet 3-D solid model.

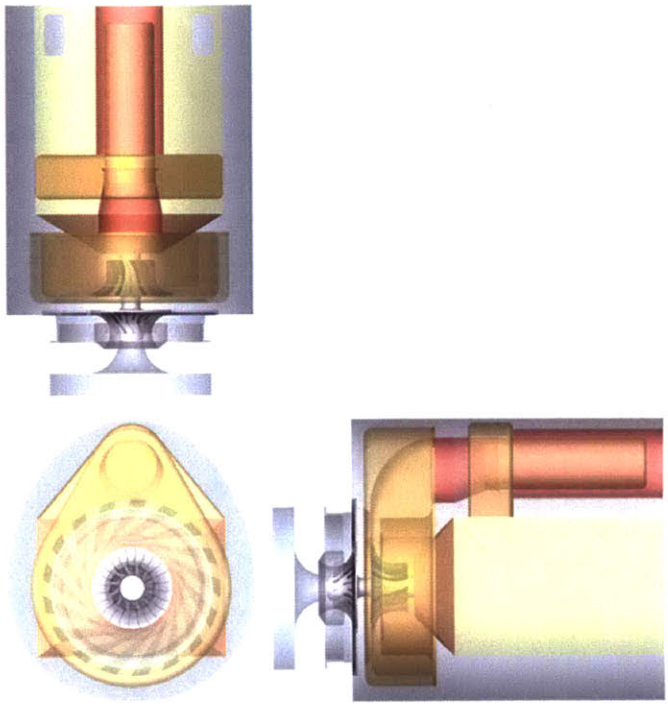

Figure 1-4: Three-view of Dynajet 3-D solid model.

Chapter 2

Market Study

As a unique product, the Dynajet has unique characteristics and unique engineering challenges. As such, a one for one comparison with existing compact power sources in its size range runs the risk of being misleading. Therefore, rather than concentrate on specific product comparisons, this market study describes efforts in the following areas: (1) identifying existing markets and delineating the requirements of those markets; (2) exploring new and possibly emerging opportunities in the 2-5 kW generator set size range; and (3) describing the role that government regulation may play in defining the changing marketplace.

2.1 Generator Market Overview

As a product, the Dynajet falls into the category of portable power generators. Generators are considered portable below about 6 kW in output (as opposed to mobile generators which are larger, can provide tens of kilowatts, and may be skid or vehicle mounted). At this time, the vast majority of this market consists of internal combustion (IC) engine generators powered by either spark-ignition or compression-ignition engines, although there are minor sales of solar systems for specialized applications. The Freedonia Group estimates the total market for portable power generators at just under $500M per year and projects it will grow by about 5.8 percent per year between now and 2005 [2].

In addition to its current portable functionality, the Dynajet could potentially be modified to operate across the entire spectrum of small power generation applications: portable, marine, and recreational vehicle (RV). As shown by Figure 2-1, the U.S. Department of Commerce (DoC) reported a 1998 wholesale market value for all gasoline and diesel generator sets below 15 kilowatts of approximately $400M [3]. While this value differs from the Freedonia Group estimate, the disparity can be attributed to wholesale versus retail value differences and the inclusion of non-generator set power sources such as batteries and fuel cells in the Freedonia estimate. In terms of shipments for generator sets below 15 kilowatts, the DoC reported approximately 600,000 for the year 1998 (Figure 2-2

and Figure 2-3). Ten companies surveyed by the Electrical Generating Systems Association (EGSA) reported shipments of 20,000 units for the last quarter of 2001 [4].

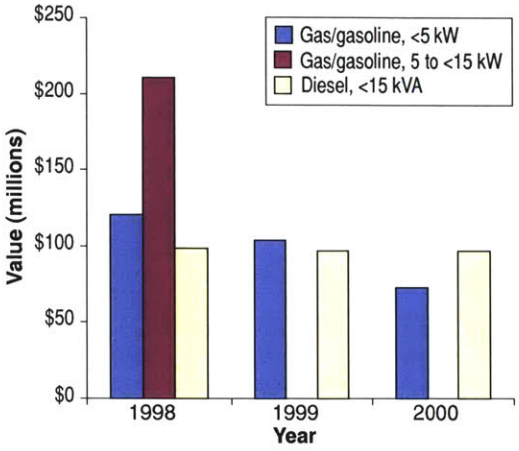

Figure 2-1: U.S. generator set shipment value [3].

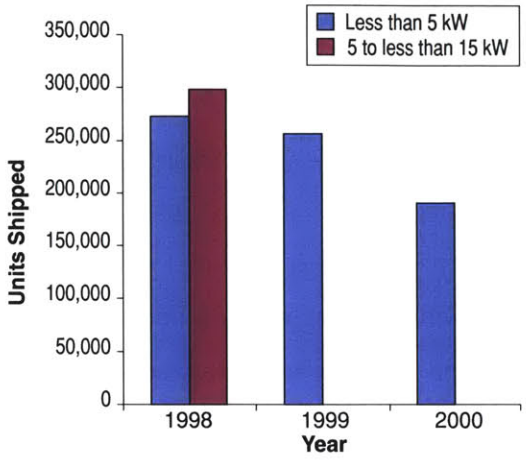

Figure 2-2: U.S. gasoline generator set shipments [3].

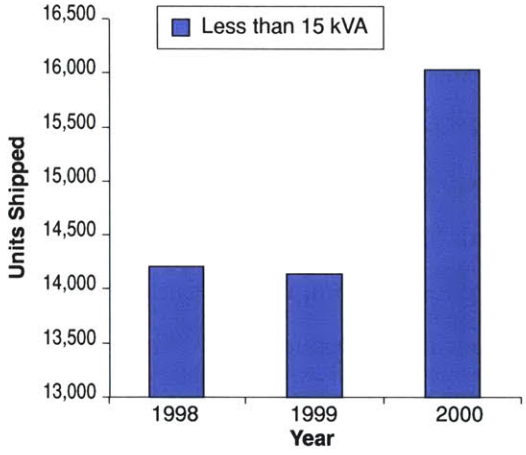

Figure 2-3: U.S. diesel generator set shipments [3].

For many years the portable power generator market in the U.S. was static, changing little year-by-year in either sales or technology. This is now a market in the process of transformation, a transformation fuelled by both changing market demands and new technological opportunities. The changing market demand stems largely from new emissions standards coupled with the unexpected fallout of electricity deregulation in states across the U.S., especially California.

Tightening emissions standards affect the portable power generator market in two ways. First, the mandated reduction of emissions in California over the next two years will force replacement or at least upgrading of most of the internal combustion-driven generator

sets now on the market. (Historically, emissions standards in the U.S. are most strict in California. The California standards are then slowly adopted by other states, usually in the Northeast first, and eventually by the federal government.) Second, the recent power outages in California have prompted a re-examination of the current exemption of emergency power generators from emissions licensing requirements. This is because the former rationale of exempting emergency generators because they are very infrequently operated (and thus have minimal environmental impact) is clearly invalid if the utility-supplied power continues to be unreliable for whatever reason. Independent of the rationale, the net effect is that emissions restrictions on engines below 20 kW will become much more demanding. As discussed in Section 2.3.1, regulations are in place that mandate significant emissions improvements in small engines between now and 2005. This regulatory market pull is also reflected in evolving U.S. military requirements that generally reflect the U.S. military's desire to stay within U.S. Environmental Protection Agency (EPA) guidelines, which they must do by law when operating in the U.S.

Much of the new interest in the small end of the power generation market is driven by the perception that new, emerging technologies offer both new opportunities for existing markets and open up all-new markets such as distributed generation. There is considerable research around the world on fuel-efficient, compact, environmentally friendly power sources and conversion equipment. The underlying theory is that new technology will permit small power producers to approach the efficiencies of large central plants, perhaps in a more environmentally benign manner. The one that is currently receiving the most attention at both the basic research and product development levels is the fuel cell. While the majority of present investment is aimed at the automotive market, companies have announced units for the portable generation and residential marketplaces. "Microturbines" (gas turbine generators in the 30-200 kW size range) have been the source of much interest and investment as well. Persisting, long-term investment in solar power is continuing to improve its efficiency and drive down its cost, but it is still a very expensive option. One projection of the cost of generating power in the 2000-2015 time frame is shown in Figure 2-4. The Economist reports that about $800M of U.S. venture capital was invested in such technologies in the year 2000 (Figure 2-5) [5].

The large investments reported above are mainly for power generators in sizes much greater than the 2-5 kW range of interest to this study. Nevertheless, much of the

technology under development can be applicable to this small end of the market. In fact, the Dynajet is derived from larger sized, automotive gas turbine technology and could thus be considered the low end of the microturbine size range applied to portable power. Similarly, there is considerable interest in fuel cells in this size range for both civil and military portable power applications, primarily due to their low noise and anticipated low fuel consumption. Later sections of this report will discuss the current state of fuel cell technology for this market.

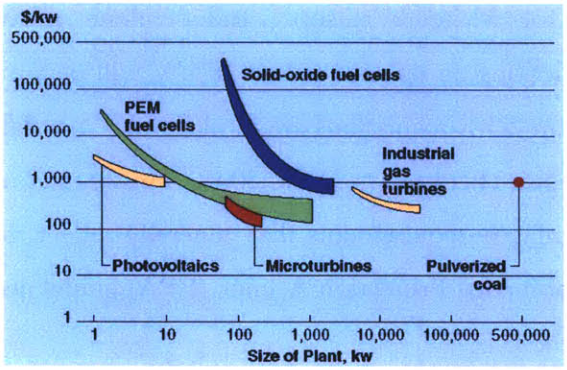

Figure 2-4: Projection of the cost of generating capacity, 2000-15 [5].

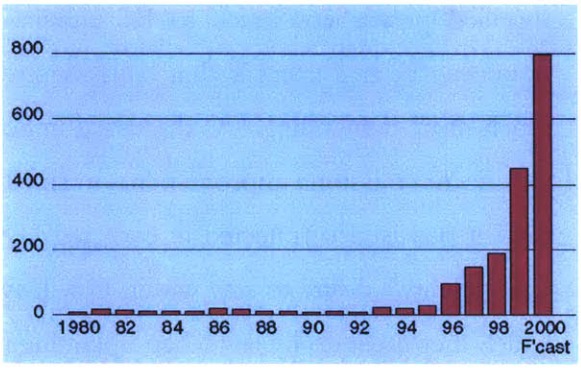

Figure 2-5: U.S. venture capital investment in micropower technology, $M [5].

2.1.1 Residential

Two types of generators currently comprise the residential market: stationary standby generators and portable gasoline or diesel generators. Stationary standby generators typically provide power in excess of 10 kW, and thus are beyond the scope of this study. The current Dynajet is a portable generator. Specifications for a sample of portable generators, including the Dynajet, are summarized in Table 2.1.

As shown in the table, portable generators are loosely classified as either light duty (occasional use) or heavy duty (commercial). However, what separates one from the other in terms of specifications is not clearly defined. Diesels are always classified as heavy duty but gasoline engines are only sometimes. The Honda EB5000XK1, for example, is advertised as "commercial grade." Generators have different warranty durations for residential and commercial use. The Honda is warranted for 1 year under commercial use and 2 years under residential use. A common characteristic among most portables is that they have four-stroke engine cycles to achieve the required emission standards explained in Section 2.3.1.

Table 2.1: Portable and Dynajet generator specifications.

		Engine Maker	Rated Output (kW)	Price (US Dollars)	Price per Unit Power ($US/kW)	Fuel Type	Dry Mass (kg)	Fuel Consumption (liters/h)	PSFC (kg/kW-hr)	Noise (dB) from 7m	Volume (m^3)
IHI Aerospace Dynajet		IHI Aerospace	2.6	$9,000	$3,462	multiple	65	4.5	1.45	60	0.152
Light Duty Portable	**Yamaha EF-2800i**	Yamaha	2.5	$1,100	$440	unleaded regular	29	1.7	0.48	67	0.081
	Kawasaki GE500AS	Kawasaki	4.4	$1,727	$393	unleaded regular	74	2.75	0.46	71.5	0.216
	Mitsubishi MGA-2900FOU	Mitsubishi, 6hp	2.5	$694	$278	unleaded regular	43	2	0.58	70	0.104
	Honda EN2500 AL	Honda, 5hp	2.3	$600	$261	unleaded regular	32	1.75	0.55	76	0.106
Heavy Duty Portable	**Honda EB5000XK1**	Honda, 11hp	4.5	$1,625	$361	unleaded regular	89	3.47	0.56	72	0.534
	Robin RGD5000	Robin, 8.5hp	4.5	$2,149	$478	diesel	99	2.2	0.41	76	0.182
	Yanmar YDG2700	Yanmar, 4.8hp	2.5	$1,915	$766	diesel	63	1.35	0.45	80	0.136

2.1.2 Commercial

The commercial market for generator sets is satisfied by the same set of portables found in the residential market. The major difference is that commercial buyers generally use their generators more frequently and for longer durations, so durability and fuel consumption are greater concerns. Commercial uses for generators include such applications as tool power at work sites and power for other outdoor commercial activities such as food stands.

Light-duty generator set population estimates compiled by the California Air Resources Board for environmental impact analysis are shown in Table 2.2 [6]. Rough estimates of the total U.S. generator market can be derived by extrapolation from this data. For example, there are approximately 50,000 four-stroke gasoline generators in California that output less than 3.75 kilowatt. An average lifetime of 16 years implies that 3,125 are replaced each year. Assuming that generator population scales with human population, the total U.S. market can then be estimated at 8 times the California total – 25,000 per year.

Table 2.2: Inventory of light-duty generator sets in California [6].

Engine Type	Power (kW)	1990 Pop.	2010 Pop.	Life (yrs)	Average Power (kW)	PSFC (kg/kW-hr)	Activity (hrs/yr)
Gasoline (4 cycle)	0–3.75	46918	54255	16	3	0.66	115
	3.75–11.25	128874	149028	12	6.75	0.54	115
Gasoline (2 cycle)	0–1.5	3574	4132	16	0.75	0.78	115
	1.5–11.25	36	41	12	6.75	0.78	115
Diesel	0–11.25	4908	5627	16	8.25	0.43	338

2.1.3 Military

A Survey of Current Military Generators and Their Usage [7]

The U.S. Military has over 86,000 small generators in inventory ranging in size up to 100 kW. The distribution of these by power output is given in Figure 2-6. Most of the operation of these units is at power outputs considerably below the rated levels. As can be seen in Table 2.3, the average demand in peacetime is less than 28 percent while that in wartime is 60-70 percent. In peacetime, the average operating time is only 24 hours per month, rising to 400-700 in wartime. This data is shown in more detail in Figure 2-7 and Figure 2-8.

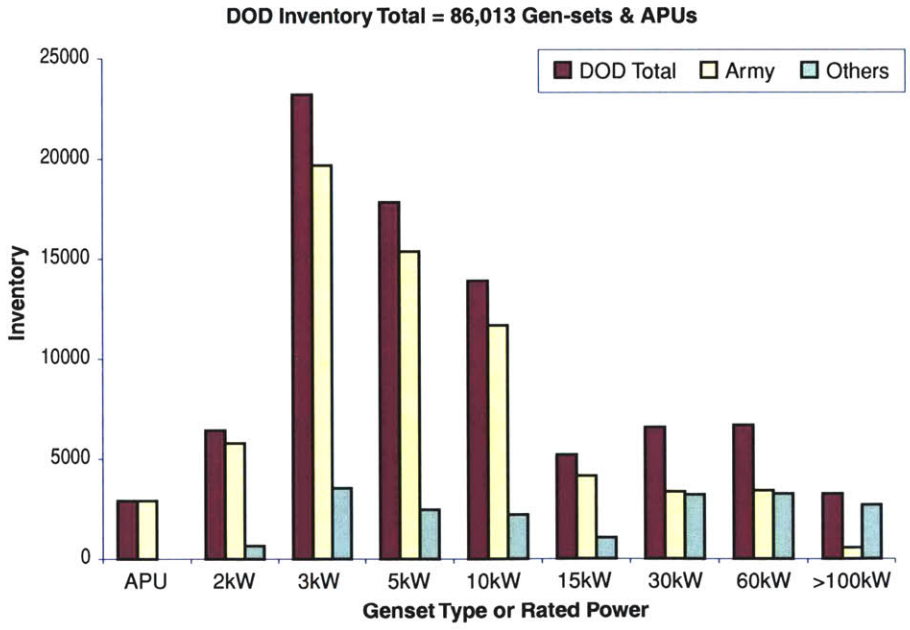

Figure 2-6: DoD generator set inventory by rated load capacity [7].

Table 2.3: Average demand power and operating time for DoD mobile electric generators [7].

Mission	Peacetime[2]	Wartime 15-d mission[2]	Wartime 30-d mission[1]
Generator rated power	5-60 k W	60 kW and under	Over 60 kW
Average demand power, % of rated	27.8	58.1	69.9
Average operating time, % of months	3.2	47.2	95.3
Average operating time, h/month	23.2	340	686

Note: Based on a 30-d month or 720 h.

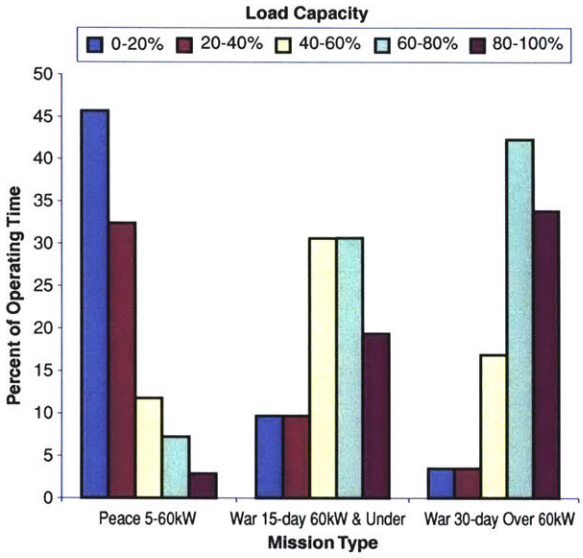

Figure 2-7: Generator set percent operating time at percent load capacity for average peacetime and projected wartime missions [7].

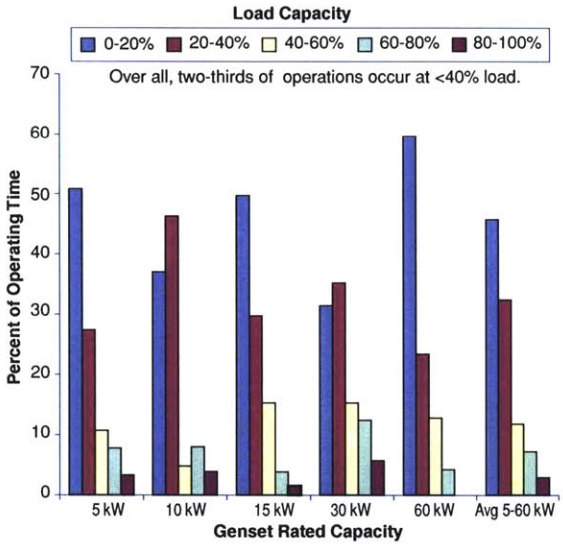

Figure 2-8: Peacetime utilization for 5-, 10-, 15-, 30-, and 60-kW DoD generator sets with percent of operating time at percent load capacity [7].

Fuel consumption is a major evaluation factor for mobile electric generators since it has a strong influence on life cycle costs and logistics demands. Data on the fuel consumption and thermal efficiency of selected generators are presented in Figure 2-9 and Figure 2-10.

Since these are mobile generators, weight is an important consideration. Generator weights are shown in Figure 2-11 and Figure 2-12 and Table 2.4 for existing generator sets. Projected weights for future units are given in Figure 2-13 and Table 2.5 and Table 2.6.

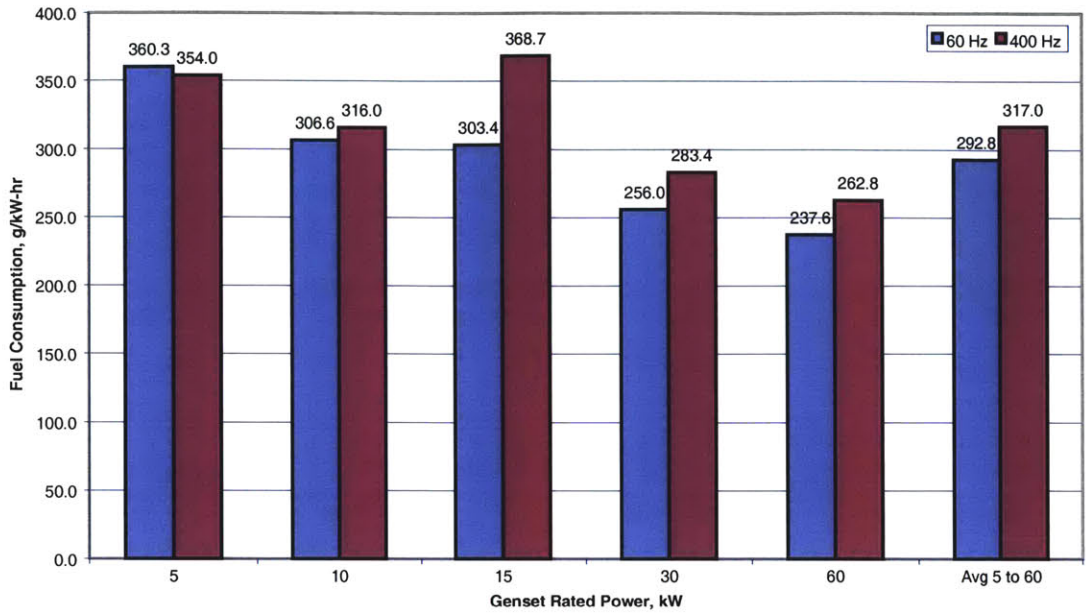

Figure 2-9: Fuel consumption rate for DoD TQG mobile electric generators, 5 to 60 kW [7].

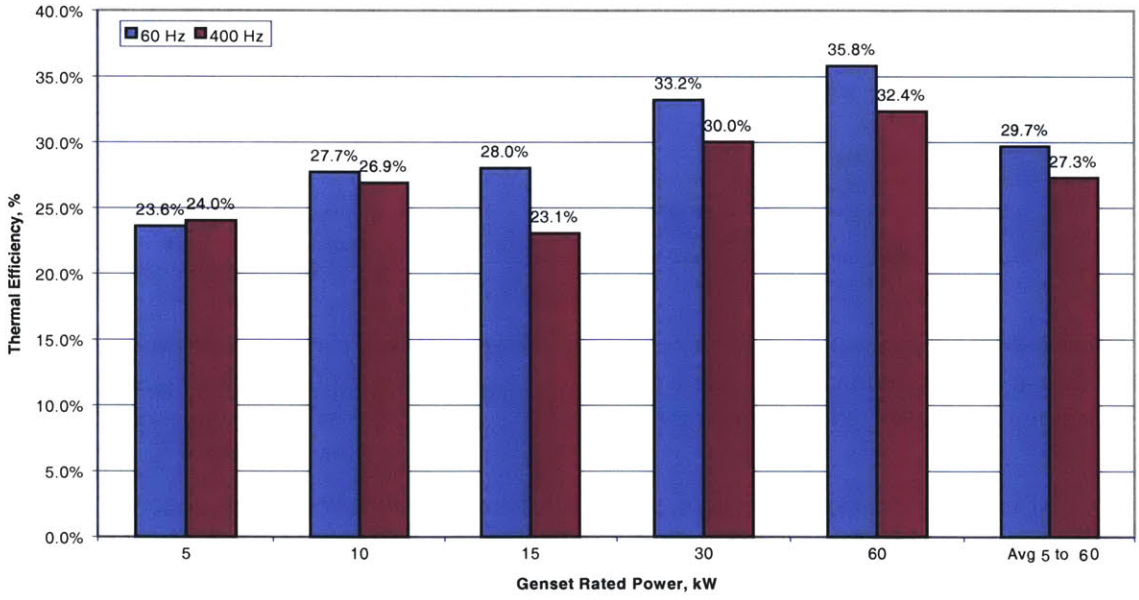

Figure 2-10: Thermal efficiency of DoD mobile electric generators, 5 to 60 kW [7].

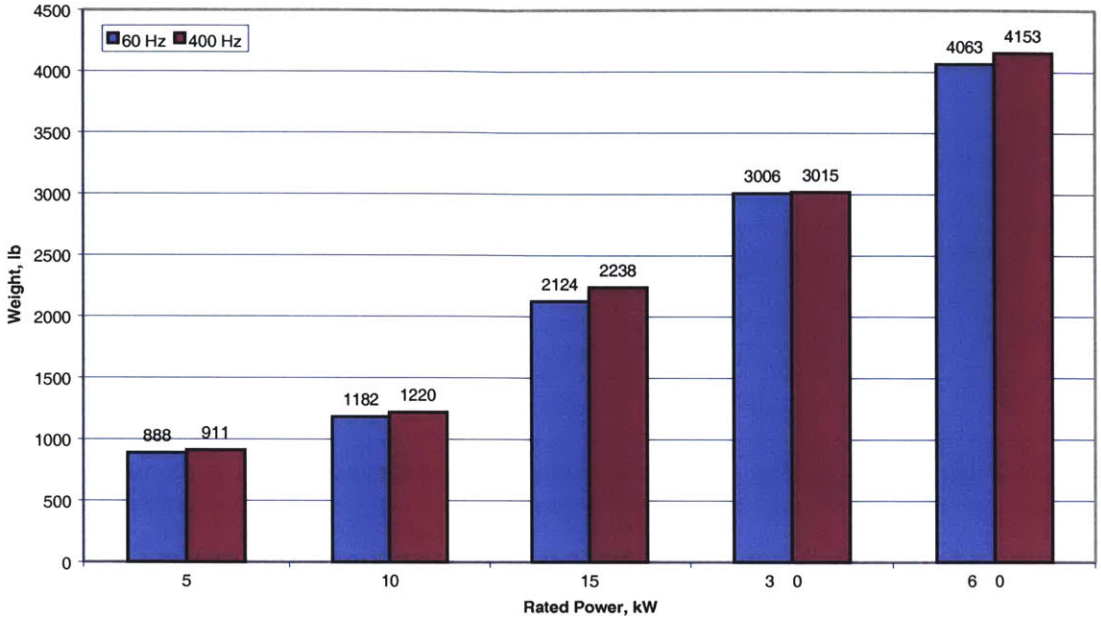

Figure 2-11: Weight for DoD TQG mobile electric generators, 5 to 60 kW [7].

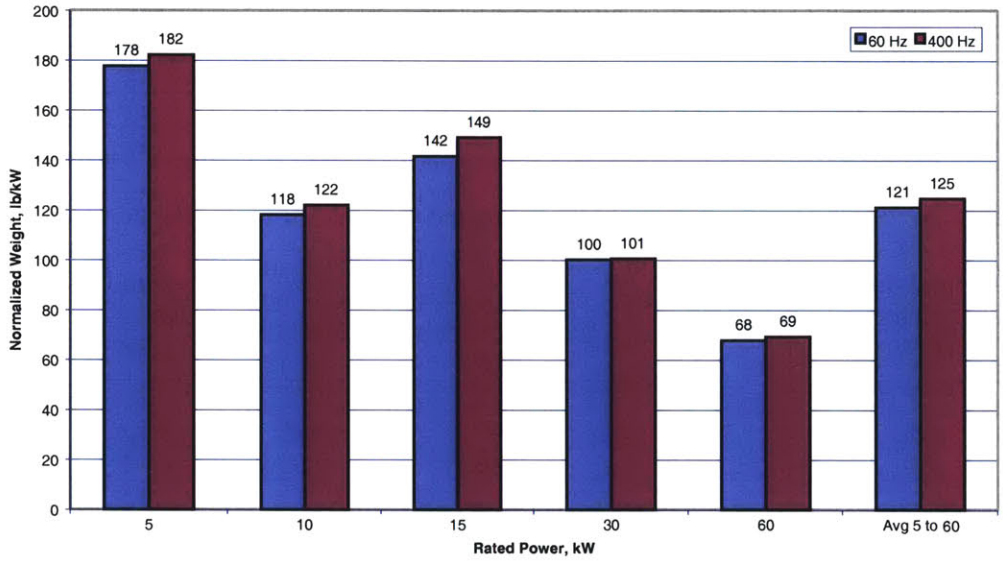

Figure 2-12: Normalized weight for DoD TQG mobile electric generators, 5 to 60 kW [7].

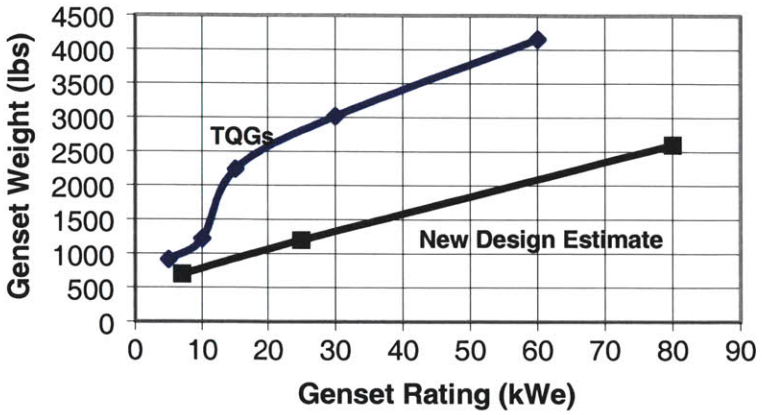

Figure 2-13: Weight estimates for proposed generator sets compared with current 400 Hz TQGs [7].

Table 2.4: Weight of generator set and frame for existing TQGs [7].

Unit	Estimated frame and housing weight (lb)	Total gen-set weight (lb)	Contribution of frame and housing to total weight (%)
5 kW	408	888	46
10 kW	465	1182	39
15 kW	1138	2124	54
30 kW	1329	3006	44
60 kW	1479	4063	36

Table 2.5: Breakdown of generator set estimated weights for proposed generator sets [7].

Normal gen-set rating (kWe)	Engine and accessories weight (lb)	Alternator and electronics and control system (lb)	Enclosure and frame weight (lb)	Fluid weight (lb)	Total weight (lb)
7.0	160	170	320	50	700
25	340	240	470	150	1200
80	760	540	890	410	2600

Table 2.6: Size and weight estimates for proposed generator sets compared with current 400 Hz TQGs [7].

Nominal gen-set rating (kW)	Estimated gen-set weight (lb)	Estimated length (in.)	Estimated width (in.)	Estimated height (in.)	Estimated volume (ft^3)
Proposed gen-sets based on conceptual design					
7	700	49	29	33	27
25	1200	55	37	34	40
80	2600	68	47	50	92
Existing 400-Hz TQGs					
5	911	50.3	31.8	36.2	33.5
10	1220	61.7	31.8	36.2	41.1
15	2238	69.2	35.3	54.1	76.5
30	3015	79.2	35.3	54.1	87.5
60	4153	87	35.3	58.2	103

The military cares about not only the weight of the generating set but also the total weight of the generator set plus its fuel since this is the total mass that is needed to supply electric power. It must be carried with the generator or supplied in the field by the logistics organization. Figure 2-14 and Figure 2-15 illustrate the total mission mass as a function of mission duration and power requirements for 5 kW and 10 kW generators, respectively.

Another important metric for any power generator is the cost of maintenance. For the U.S. Army, this cost has proven to be largely independent of the rated output of the generator, so that small generators are much more expensive per unit power to maintain. The costs, approximately $500-700 per hour of operation, are shown in Table 2.7.

The above data give an overview of current military mobile electric generators across a wide size range. In the next section, the procurement policy for small generators is discussed and three units under 5 kW in size are examined in more detail.

Current DoD Procurement Policy for Small Generators [8]

Entry to the military market for small generators is largely controlled by the U.S. Army Program Manager-Mobile Electric Power (PM-MEP), the program manager for generators less than 50 kW. Generators above this size are considered base power and are managed by the U.S. Air Force. PM-MEP tests and certifies generators in different size ranges that are then ordered by the services as needed. The program manager's goal is to provide a standard set of generators that can be used across services to reduce the costs of acquisition, operation, and support.

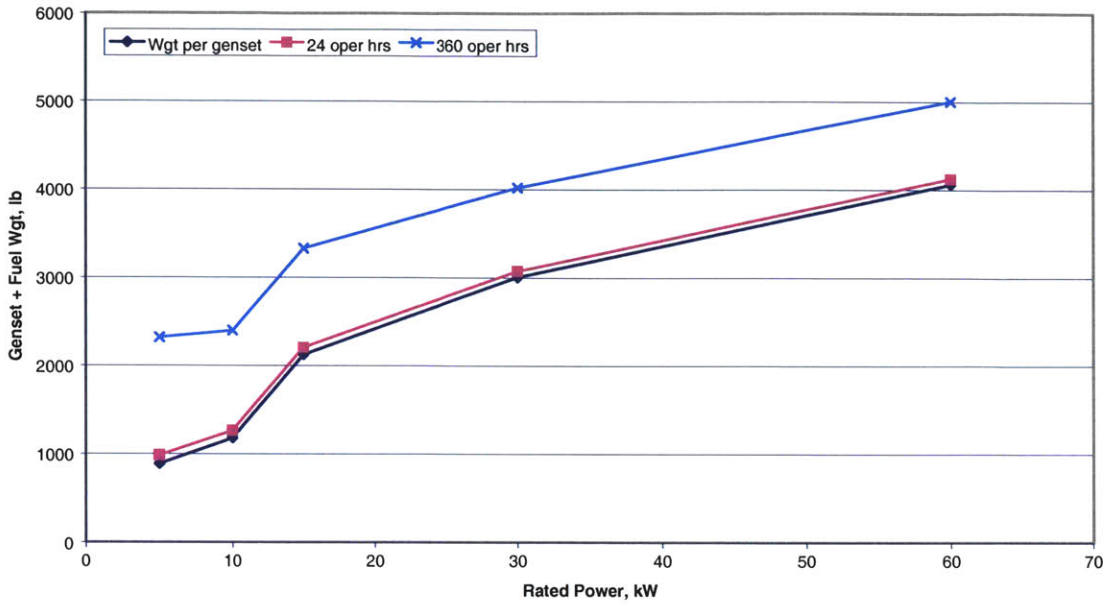

Figure 2-14: Mission weight for DoD mobile electric generators for 5 kW power demand and different mission durations [7].

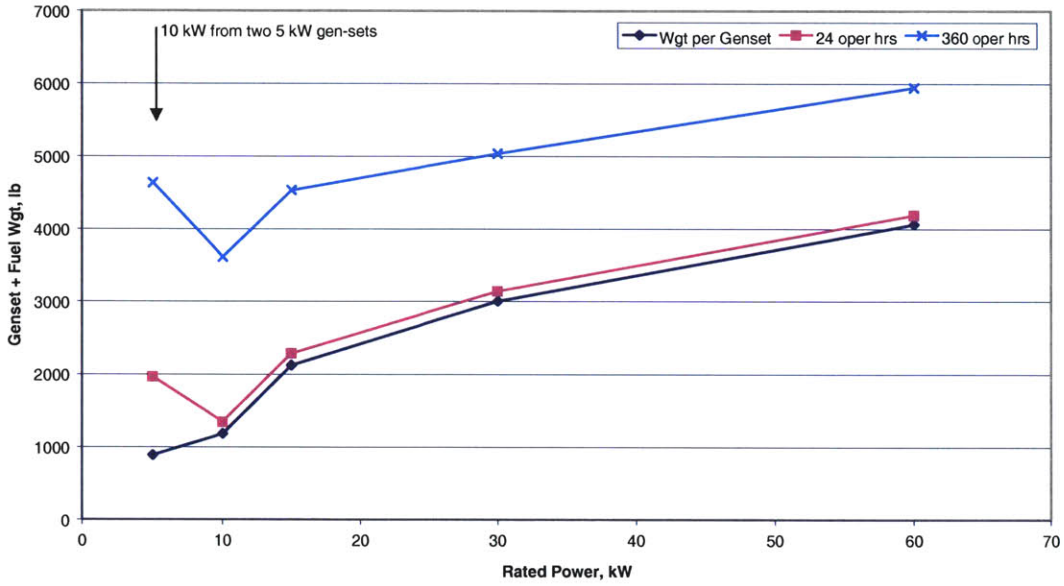

Figure 2-15: Mission weight for DoD mobile electric generators for 10 kW power demand and different mission durations [7].

Table 2.7: Approximate maintenance costs for Army TQGs (5-60 kW) [7].

Gen-set size (kW)	Annual maintenance cost per unit ($)	Number of Army TQGs	Total annual cost for this size class ($M)
5	504.31	4556	2.3
10	484.62	3916	1.9
15	591.13	1311	0.8
30	534.29	1285	0.7
60	638.45	898	0.6
Total			6.2

Properties of Current Small Military Generators [8]

Current Army procurement of generators up to 5 kW includes three major units: a 2 kW Military Tactical Generator (MTG), 3 kW Tactical Quiet Generator (TQG), and 5 kW Tactical Quiet Generator. Major properties of these generators are provided in Table 2.8 with Dynajet properties for comparison. Despite their relatively recent development and acquisition, user satisfaction with these units has been low.

Table 2.8: Military and Dynajet generator specifications.

		Engine Maker	Rated Output (kW)	Price (US Dollars)	Price per Kilowatt (US Dollars)	Fuel Type	Dry Mass (kg)	Fuel Consumption (liters/h)	PSFC (kg/kW-hr)	Noise (dB) from 7m	Volume (m^3)
IHI Aerospace Dynajet		IHI Aerospace	2.6	$9,000	$3,462	multiple	65	4.5	1.45	60	0.152
Military	**2kW Tactical Generator**	Yanmar L48AE-DEG, 4.2hp	2	$4,500	$2,250	diesel	66	1.94	0.81	79	0.168
	3kW Tactical Quiet Generator	Yanmar L70AE-DEGFR, 6.7hp	3	$9,000	$3,000	diesel	133	1.45	0.407	70	0.42
	5kW Tactical Quiet Generator	Onan DN2M, 11hp	5	$11,000	$2,200	diesel	386	2.51	0.42	70	0.95

The 2 kW MTG first entered service in 1997 to replace a gasoline generator set of the same output. The unit was intended to be lightweight and to operate reliably under demanding battlefield conditions. However, it has faced a number of problems, most notably "wet stacking" when operating at power levels below one-third rated power. This is a serious problem since many applications require only about 500 W. The problem was

"solved" by switching in a 600 W load resister at low power. Thus, the 2 kW unit consumes fuel at an 1100 W rate while delivering only 500 W to the load. This more than doubles the fuel consumption of the 2 kW generator at low power.

The 3 kW TQG is the newest addition to the U.S. supply, having been in the inventory since 1999. It is the first variable speed tactical generator and is therefore the first equipped with an inverter. Its nominal price under the current contract is reportedly $9,000 per unit. The unit has not been reliable to date, prompting the extension of the warranty to 18 months. A major problem has been inverter failures, at a replacement part cost of about $3,200.

Services at the bottom of the supply chain such as the National Guard and Reserves are faced with the problem of insufficient funding to purchase the expensive 3 kW TQG. As an interim solution, a kit was developed to retrofit old 3 kW gasoline generators with diesel engines. These retrofitted generators operate reliably but have no sound protection, making them very noisy. A better long-term solution is necessary.

The 5 kW TQG has been in service the longest and is considered reliable. However, it is very heavy. This is even the case when compared to other military generators. It weighs 190 percent more than the 3 kW TQG while producing only 67 percent more power.

Current Military Market Segmentation

The U.S. Military has many uses for mobile electric power sources. While now most generating units are not distinguished by the use to which their power is put, such distinctions may prove useful in assessing the demand for future products and identifying new market opportunities. Typical uses of electric power include:

- General lighting and domestic power
- Air-conditioning
- Sensitive electronics
- Battery charging
- Vehicular auxiliary power
- Construction and power tools

The military has established many formal technical and economic requirements for portable electric generators. These include such factors as:

- Acquisition cost
- Maintenance cost
- Fuel consumption
- Total cost of ownership
- Mean time before failure
- Weight
- Noise
- Electronic emissions
- Air quality emissions
- Ruggedness
- Power quality
- Load following
- Uses logistics fuel
- CBW compatibility

While requirements like the above are important to all military applications, their relative importance can vary greatly depending upon the specifics of particular uses. Therefore, the military market under 5 kW will herein be considered as divided into several sub-markets characterized by technical requirements, time scales, and market opportunities. These include:

- General purpose
- Shelter power
- Tent power
- Battery charging
- Silent watch
- Auxiliary Power Unit (APU)
- Autonomous vehicles and battle armor

Each of these applications or sub-markets is discussed below.

General Purpose

General purpose generators are purchased by PM-MEP, usually on 10-year cycles. These units are both purchased for inventory and approved for purchase by all DoD organizations.

The current 2 kW MTG and 3 kW TQG started their procurement cycle about 3-4 years ago, which would normally suggest that volume procurement of new designs (to be studied under the MP-2 program of PM-MEP) would be 5-7 years away. However shortcomings such as high noise and low reliability in the current units may open nearer term market opportunities. The current 2 kW MTG is quite noisy, has low reliability, and does not operate well below one-third load. The 3 kW TQG is also noisy, has reliability problems with its inverter, is heavy and is twice the price of the 2 kW MTG. Both units currently require considerable maintenance (for example, the oil must be changed every 100 hrs in the 2 kW MTG). The 5 kW generator has been in inventory longer and is considered reliable.

Shelter Power

A shelter is a small, portable room often used to house electronic equipment and its operators. A shelter may be on a truck or trailer or be pallet mounted and air transportable. Shelters are generally insulated and climate controlled, and many include their own power source. The U.S. military has on the order of 5000-6000 shelters in the field. The typical power requirement for a small communications shelter is 10 kW, about one-half of which is used for air-conditioning to meet an 18,000 BTU/hr (5.3 kW) thermal load. In the past, a 10 kW unit derived from the tactical quiet generator and modified to reduce noise and vibration has supplied power for such shelters. The 72-75 dBA noise requirement has consistently proven hard to meet. At this level, the noise and vibration is sufficiently objectionable that commanders reportedly prefer to power the shelter from larger, towed generators to reduce the operator fatigue and performance degradation associated with long-term exposure to high noise levels.

To meet future shelter power requirements with reduced weight, footprint, and power consumption, the Army has started an Integrated Power Unit Program. Integrated means that one power unit provides electric power, heating and cooling, and filtering for chemical protection. Projected demand is 750-1000 units over 5-6 years.

Tent Power

Most tents are not powered separately but run off base power due to the relatively high power requirements for air-conditioning due to the lack of insulation. Typically 54,000 BTU/hr (15.8 kW) of cooling is needed. A quiet integrated power unit with a large heating/cooling capacity but relatively modest electric power output (under 3 kW) could

provide an alternative to the current centralized approach with the usual gains associated with distributed power production.

Battery Charging

The current requirements for battery charging are in a state of flux and depend upon the deployment plan for the Land Warrior electronics system. If the first deployment is to light infantry then an engine driven charger is needed, mounted on a platform like an M-Gator. In this case about 400 generator sets would be needed. If the first deployment is with the Rangers, then primary batteries are sufficient. If the deployment is with the Interim Brigade Combat Teams, then the battery charging could be done with the light armored vehicle's APU (Stryker, see below), although the current 3.8 kW unit does not have the spare capacity needed to handle the charging load.

Silent Watch

This refers to the non-obtrusive powering of electronic equipment in remote locations. One long-term solution under study is to off-take power from future hybrid-electric vehicles, such as the Humvee under test or future combat vehicles. Another approach would be fuel cell based. The Army is funding research in fuel cells ranging in size from a few watts for a dismounted soldier to tens of kilowatts for base power. These are future technology options that cannot fill current needs. Silent watch applications now under study require relatively little power (1.5 kW). The options at this power level are really only small generators such as the 2 kW TQG. These are heavy however and are relatively noisy and are not considered a satisfactory solution.

Auxiliary Power Unit (APU)

An auxiliary power unit is a small generator mounted on a vehicle (usually an armored vehicle) to provide electrical and, in some cases, hydraulic power for either emergency situations or to permit electrical operations without operating the main vehicle propulsion engine. These range is size from the 1.5 kW electrical only unit on some versions of the M1 tank to the 10 kW electric plus 3 kW hydraulic unit for the U.S. Marines new Advanced Amphibious Attack Vehicle (AAAV) currently under development. The Marines plan to procure 800-1000 of these vehicles over the next 10 years.

The Army's Interim Brigade Combat Teams are being outfitted with a new, light armored combat vehicle known as the Stryker produced by General Motors Defense. In

addition to a 350 horsepower primary diesel engine, the Stryker is also outfitted with a 3.78 kW, liquid-cooled Kubota diesel APU costing $7700. This unit is contractor furnished equipment. The Army has issued a contract to buy 2131 Strykers from GM Defense over the next six years. Approximately 466 will be built this year, and 333 will be produced each year thereafter [9, 10].

Once they enter the inventory, APU's have historically been adapted to other portable power needs.

Small Autonomous Vehicles and Exoskeletons

The DoD is currently working on several small, autonomous land vehicles for a variety of special missions. These robotic craft are being developed for such applications as covert reconnaissance, mine clearing, exploring tunnels and caves, urban warfare, and the disposal of nuclear materials. Typically these vehicles are electrically powered with mass under 100 or even 50 kg. At this small size, vehicle power is a major concern. The prototypes and experimental units developed so far tend to use batteries (or even extension cords), but these solutions are very expensive and lead to very limited endurance. These vehicles really need a fuelled power generator to achieve the range-endurance needed for most missions. Commercial IC engine generator sets have been used on some of the larger units for demonstration purposes but these are very noisy and therefore undesirable for many military uses. Also, a gasoline-powered unit is not supportable in the field since gasoline is not a logistics fuel. A very quiet, compact JP-8 power source is needed for this emerging application.

The Defense Advanced Research Projects Agency (DARPA) Defense Sciences Office (DSO) has an exoskeleton program working on essentially self-powered body armor technology. From the point of view of the energy supply, this can be considered a walking, running 300-400 pound legged vehicle so that the energy supply is a major concern. At the moment, DARPA is supporting the development of a small gas turbine in the 500-1000 watt class. Many believe this is too small (unless several are used) and that the actual power requirements are closer to 2-3 kW.

2.1.4 Recreational

Recreational Vehicles

RV generators are a major and growing segment of the small generator market. Those currently on the market run on gasoline, diesel, or propane fuel and range in output from 3-12 kW. The two major producers include Cummins Corporation (Onan Generators) and Generac Power Systems. Specifications for three RV generators are summarized in Table 2.9.

According to the Recreational Vehicle Industry Association (RVIA), 311,000 RVs were shipped in 2002 [11]. Historical data shows that approximately 18 percent of RV's sold are Class A or C motorhomes, the types most commonly fitted with generators [12]. This suggests RV generator sales of 56,000 units. Assuming an average generator cost of $2,500, the market can be estimated at $140M per year.

Table 2.9: RV and Dynajet generator specifications.

		Engine Maker	Rated Output (kW)	Price (US Dollars)	Price per Unit Power ($US/kW)	Fuel Type	Dry Mass (kg)	Fuel Consumption (liters/h)	PSFC (kg/kW-hr)	Noise (dB) from 7m	Volume (m^3)
IHI Aerospace Dynajet		IHI Aerospace	2.6	$9,000	$3,462	multiple	65	4.5	1.45	60	0.152
Recreational Vehicle	**Onan Microlite 4.0KY/26100**	Onan, 9.5hp	4	$3,030	$758	unleaded regular	79	3.12	0.57	67	0.134
	Onan Marquis Gold 5.5HGJAB-901	Onan, 12.9hp	5.5	$3,560	$647	unleaded regular	126	4.18	0.55	68	0.326
	Generac Primepact 50G	Generac, 15hp	4.8	$2,140	$446	unleaded regular	90	3.35	0.51	68 (half load)	0.131
	Onan Microlite 3.6KY/26120	Onan, 8.6hp	3.6	$3,500	$972	LP vapor	79	2.7 lb/hr	0.34	67	0.134
	Onan Marquis Gold 5.5HGJAB-1119	Onan, 10.7hp	5.5	$2,795	$508	LP vapor	126	4.6 lb/hr	0.37	68	0.326
	Generac Primepact 50LP	Generac, 15hp	4.8	$2,490	$519	LPG	90	5.32 lb/hr	0.5	68 (half load)	0.131
	Onan Quiet Diesel 7.5HDKAJ/11451	Onan, 16.6hp	7.5	$8,500	$1,133	diesel	103	3.63	0.41	66 (3m)	0.313
	Generac Quietpact 7.5D	Generac, 13hp	7.5	$7,430	$991	diesel	219	2.8	0.31	73.6	0.308

Marine Generators

Marine generators are commonly installed on U.S. motor yachts. Carver Yachts is a representative example of the industry. Carver includes a generator set as standard

equipment on all of its 45- to 57-foot yachts, and approximately 75 percent of its yachts in the 35- to 44-foot range are sold with generators.

Carver's installed power outputs range between 7.3 and 21.5 kW, and sizing is driven almost entirely by air-conditioning. For example, their 44-foot motor yacht includes a 35,000 BTU/hr (10.3 kW_{th}) air conditioner that requires approximately 3.7 kW_e to run. This is more than one-third of power provided by the generators that Carver offers for installation on this yacht [13].

The National Marine Manufacturer's Association (NMMA) reported total U.S. production of 8,100 motor yachts in 2001 valued at $2.77B [14]. The average value was then $350,000 per unit, which is about the price of the aforementioned 44-foot Carver yacht. Carver sells approximately 600 yachts per year and is the largest producer in the Midwestern United States. Its parent company, Genmar Holdings Corporation, is the second largest motorboat producer in the United States and took in $92 million from luxury yacht sales in 1999 [15].

Unlike the case with motor yachts, marine generator sets are uncommon on sailing yachts. DC generators that take power off of the main engine provide for the electricity needs of sailboats in the 30 to 50 foot range. Generator sets are only occasionally installed on sailboats in tropical climates to power air conditioners.

Marine generators are subject to a number of specific requirements due to the environment in which they are used. Among these are ignition protection, corrosion resistance, and vibratory isolation. Other more standard requirements such as low weight, low noise, and durability are of course also important.

The installation of generators on new boats is formally regulated by the U.S. Coast Guard under the Code of Federal Regulations, Title 33, Part 183, Subparts I and J. The regulations require generator sets meet a number of requirements regarding ignition protection, batteries, overcurrent protection, fuel tanks, and others. The Coast Guard does not regulate generators installed on used boats; however, it does strongly encourage compliance with American Boat and Yacht Council (ABYC) AC generator set standards. Specifications for a number of marine generators in the 2-5 kW range are summarized in Table 2.10.

The average price per kilowatt of the marine generators in Table 2.10 is nearly 4 times that of portable generators in Table 2.1. This can be attributed to two factors:

requirements and demographics. The more demanding technical requirements of seagoing generators discussed above certainly contributes to higher prices. Additionally, the wealth associated with the market allows generator producers to fetch a premium.

Table 2.10: Marine and Dynajet generator specifications.

		Engine Maker	Rated Output (kW)	Price (US Dollars)	Price per Kilowatt (US Dollars)	Fuel Type	Dry Mass (kg)	Fuel Consumption (liters/h)	PSFC (kg/kW-hr)	Noise (dB) from 7m	Volume (m^3)
IHI Aerospace Dynajet		IHI Aerospace	2.6	$9,000	$3,462	multiple	65	4.5	1.45	60	0.152
Marine Generators	**Kohler 5E**	Kawasaki FD501D, 16hp	5	$5,900	$1,180	unleaded regular	99	2.88	0.42	65.1 (3m)	0.163
	Westerbeke 5.0BCG	Westerbeke 8hp	5	$6,500	$1,300	unleaded regular	162	3	0.44	65 (1m)	0.246
	Kohler 5EOZ	Yanmar 3TNE68	5	$8,700	$1,740	diesel	218	2.2	0.37	64 (3m)	0.276
	Northern Light M673D	Lugger L673, 9.25 hp	5	$6,000	$1,200	diesel	188	2.4	0.41	67 w/o SP, 34 w/ SP (1m)	0.185
	Onan MDKAU	Onan	5	$8,885	$1,777	diesel	159	2.3	0.39	71 (1m)	0.177
	Westerbeke 3.8BCDT	Westerbeke	3.8	$8,300	$2,184	diesel	83	1.76	0.39	70 (1m)	0.172
	Westerbeke 5.0BCDB	Westerbeke 9hp	5	$9,800	$1,960	diesel	198	2	0.34	68 (1m)	0.246
	Mase IS2500	Yanmar L48AE 4.7hp	1.9	$4,800	$2,526	diesel	65	0.93	0.41	54	0.094
	Mase IS3501	Yanmar, L70AE, 6.7hp	2.9	$5,600	$1,931	diesel	95	1.75	0.506	53	0.17
	Mase IS5501	Yanmar L100A, 10hp	4.8	$6,050	$1,260	diesel	130	2.91	0.51	53	0.23

2.2 Competing Market Solutions

2.2.1 Incumbents

The incumbent product for small-scale electric power generation is the internal combustion engine. Internal combustion engines benefit from being a century-old technology. They are well understood, and people are comfortable using them. IC engine manufacturers enjoy a near monopoly of the small power generation market that results in extremely large production volume. High volume means low prices for the consumer, which in turn further reinforces the competitive posture of the manufacturers.

IC engines can be categorized as either spark-ignition or compression-ignition. Though similar in many ways, each type has its own unique set of advantages and disadvantages. The greatest advantage of spark-ignition engines is cost. They are certainly the most inexpensive option for portable power generation. Another advantage is being lightweight. Major disadvantages include frequent, costly maintenance (see Section 2.4.1) and noisy operation. Compression-ignition engines offer high power specific fuel consumptions and durability for extended run time. Disadvantages include being heavy, high emissions, high maintenance costs, and noisy operation.

2.2.2 New Entrants

Fuel Cells

As discussed briefly in Section 2.1, there is currently a strong push in both the private and public sectors to make fuel cells a major competitor in the power generation market. Fuel cells offer many potential advantages, including efficiencies twice that of internal combustion engine generator sets, efficiency at all scales, and clean, quiet operation. However, fuel cells also face significant disadvantages that will hinder them from coming into common use. The primary hurdle is dependence on hydrogen (H_2) for fuel. This lack of flexibility is particularly damaging given the nonexistence of an H_2 infrastructure in the U.S. Only H_2 systems currently exist at small scales, and there is only a "potential" for alternative fuels. Fuel cells are also hampered by high development and manufacturing costs.

Recent news on the public front of fuel cell development was the creation of the Solid State Energy Conversion Alliance (SECA) in 1999 by U.S. Department of Energy (DoE). The SECA is currently working on 3-10 kW solid oxide systems for use with natural gas as fuel. Their goal is a price of $800 per kilowatt by 2005 and $400 per kilowatt by 2012.

A number of private companies are also earnestly developing fuel cells for the energy market. H Power Corporation is allied with General Electric in an effort to target the residential market with proton exchange membrane (PEM) fuel cells. Plug Power Corporation is following the same strategy. Coleman Powermate recently began selling its AirGen cooler-sized portable fuel cell to industrial customers with experience handling hydrogen. The unit sells for $6000 and produces 1 kW of continuous power, making it 73% more expensive than the Dynajet on a per kilowatt basis. Coleman expects to begin selling

to commercial and residential customers in the near future by offering small hydrogen fuel canisters.

Microturbines

Microturbines are small versions of the megawatt size gas turbine generators that provide power to entire cities. Their development was spurred by gas turbine research for the car industry that led to the invention of high-speed permanent magnet generators and reliable recuperators [16].

Advantages of microturbines include low maintenance costs, clean operation, and fuel flexibility. The disadvantages are high expense, low efficiency, and a lack of support infrastructure.

The best-known microturbine manufacturer is Capstone Turbine, which produces microturbines in the 30-60 kW range. Capstone had revenues of $19.5M in 2002 on sales of nearly 500 units [17]. However, the company has yet to achieve profitability. Other participants in this market are Emerson Electric and a division of Honeywell, the intellectual property of which was recently acquired by General Electric. In the larger size range, MTU has acquired the rights to the Honeywell LTS-101 helicopter engine (500kW) for ground based powergen applications.

IHI Aerospace is currently the only company that offers a microturbine producing power on the order of a few kilowatts. However, The Dutch Gas Turbine Manufacturers Association and a German consortium have both launched (independent) efforts aimed at developing units in the 3-5 kW range for residential cogeneration applications. This is seen as a "green" opportunity.

2.3 Regulatory Issues

2.3.1 Emission Standards

The emissions of hydrocarbon burning engines are becoming increasingly regulated due to growing concerns about global warming and air quality. What began as regulation of automobiles has now extended to standards for non-road engines across a range of power outputs, including the 2-5 kW range with which this study is concerned.

The regulations of two major environmental agencies are discussed in the following

subsections: the Environmental Protection Agency (EPA) and the California Air Resources Board (CARB). The EPA's standards are relevant to generators sold anywhere in the United States and are mandated by Section 213 of the Clean Air Act as amended in 1990. CARB standards are also discussed, as they are even more stringent than the EPA's. Furthermore, the size of California and the turbulence of its energy market in recent years make it particularly attractive for study.

Spark-Ignition Engines

Spark-ignition engine emission standards cover all types of engines for which combustion of the fuel-air mixture is triggered by an ignition source such as a spark plug. Standard gasoline reciprocating engines are the most common type of spark-ignition engines.

The EPA set standards for spark-ignition engines in Part 90 of the Code of Federal Regulations, "Control of Emissions from Nonroad Spark-Ignition Engines". The rulemaking divides nonroad spark-ignition engines into four separate classes. Class I engines have displacements less than 225cc, and Class II engines have displacements greater than 225cc. Classes III and IV are for handheld engines, meaning they are not important to generators.

Class I engines are currently regulated by Phase I requirements that limit emissions of hydrocarbons plus oxides of nitrogen (HC + NO_x) to 16.1 g/kW-hr and emissions of carbon monoxide (CO) to 519 g/kW-hr. Phase II requirements limit HC + NO_x to 16.1 g/kW-hr and CO to 610 g/kW-hr. Phase I requirements need only be met by new engines, while Phase II requirements must be met at the end of an engine's useful life. It is for this reason that CO requirements are actually less stringent for Phase II. Class I engines initially produced on or after August 1, 2003 must meet Phase II standards, and all Class I engines must meet Phase II requirements by August 1, 2007.

There is no expected improvement in CO emissions control, plus there is a factor added for performance degradation over the engine's life. Manufacturers of natural gas-fueled engines will also have the option under Phase II of meeting a requirement that non-methane hydrocarbon (NMHC) plus NO_x emissions are less than 14.8 g/kW-hr rather than meeting the HC+NO_x requirement. This option stems from the fact that HC emissions from natural gas-fueled engines have much higher methane content than emissions from engines run on other fuels. Methane's ozone-forming potential is significantly lower than

that of other hydrocarbons, so an alternative standard is appropriate.

Phase I requirements for Class II engines are already obsolete. Phase II requirements are summarized in Table 2.11 [18].

CARB standards for spark-ignition engines are part of Article 1, Chapter 9, Division 3, Title 13, of the California Code of Regulations. The standards again vary by engine displacement and model year. See Table 2.12 [19].

Table 2.11: EPA Class II spark-ignition engine emission standards in g/kW-hr [18].

Emission Requirement	Model Year				
	2001	2002	2003	2004	2005 and later
HC + NOx	18.0	16.6	15.0	13.6	12.1
NMHC + NOx	16.7	15.3	14.0	12.7	11.3
CO	610	610	610	610	610

Table 2.12: CARB spark-ignition emission standards in g/kW-hr [19].

Model Year	Displacement	HC + NOx	CO
2000-2001	>65cc - <225cc	16.1	467
	≥225cc	13.4	467
2002-2005	>65cc - <225cc*	16.1	549
	>65cc - <225cc**	16.1	467
	≥225cc	12.0	549
2006 and subsequent	>65cc - <225cc	16.1	549
	≥225cc	12.0	549

*Axis of crankshaft oriented horizontally, **Axis of crankshaft oriented vertically

Compression-Ignition Engines

Compression-ignition engine emission standards cover all types of engines for which combustion of a fuel-air mixture occurs spontaneously at high pressure. Diesel reciprocating engines are the most common type of compression-ignition engines.

The EPA set standards for compression-ignition engines in Part 89 of the Code of Federal Regulations, "Control of Emissions of Air Pollution from Nonroad Diesel Engines". The standards are specific to engine power output and model year and are summarized in Table 2.13 [20].

The EPA regulations also describe a voluntary low-emitting engine program. Engines meeting the somewhat stricter requirements of Table 2.14 receive a "Blue Sky Series" designation [21].

CARB standards for compression-ignition engines are part of Article 1, Chapter 9,

Division 3, Title 13, of the California Code of Regulations and are shown in Table 2.15. Like the EPA, the regulations are power and model year specific.

Table 2.13: EPA compression-ignition engine emission standards in g/kW-hr (g/hp-hr) [20].

Engine Power	Tier	Model Year	NMHC + NOx	CO	PM
kW < 8 (hp < 11)	Tier 1	2000	10.5 (7.8)	8.0 (6.0)	1.0 (0.75)
	Tier 2	2005	7.5 (5.6)	8.0 (6.0)	0.80 (0.60)
8 ≤ kW < 19 (11 ≤ hp < 25)	Tier 1	2000	9.5 (7.1)	6.6 (4.9)	0.80 (0.60)
	Tier 2	2005	7.5 (5.6)	6.6 (4.9)	0.80 (0.60)

Table 2.14: EPA Blue Sky Series emission standards in g/kW-hr [20].

Engine Power	NMHC + NOx	PM
KW < 8 (hp < 11)	4.6	0.48
8 ≤ kW < 19 (11 ≤ hp < 25)	4.5	0.48

Table 2.15: CARB compression-ignition emission standards in g/kW-hr [19].

Model Year	Engine Power	HC + NOx	CO	PM
2000-2004	<11hp	10.4	8.0	1.0
	≥11hp - <25hp	9.5	6.6	0.8
2005 and subsequent	<11hp	7.5	8.0	0.8
	≥11hp - <25hp	7.5	6.6	0.8

Microturbines

There are currently no EPA emission standards regulating microturbines specifically. The Clean Air Act directs the EPA to set standards for internal combustion engines, a category in which most would agree microturbines should be considered. However, the EPA states that regulations have not been created for a number of reasons. First, there are very few microturbines available on the market, suggesting the likelihood of people using them instead of reciprocating engines to avoid emission regulations is small. Second, microturbines in general have much better emission characteristics than diesels. Finally, the EPA has very little experience with turbines and therefore currently lacks the knowledge to develop a control program [22].

The California Air Resources Board also has not produced standards specifically applying to microturbines. However, CARB does regulate distributed generation, and this can have implications for microturbines under certain circumstances, as discussed in the following section on distributed generation.

Distributed Generation

The California Air Resources Board approved the first rulemaking on distributed generation in November 2001 [23]. The ruling regulates generators of all output ranges used for continuous power production. For example, a microturbine used for continuous power production in a single home has to meet the requirements, regardless of whether or not it is connected to the grid. The CARB distributed generation emission standards went into effect on January 1, 2003 and are summarized in Table 2.16.

Table 2.16: CARB distributed generation emission standards in g/kW-hr [23].

Pollutant	DG Unit NOT Integrated with Combined Heat and Power	DG Unit IS Integrated with Combined Heat and Power
NOx	0.23	0.32
CO	2.72	2.72
Volatile Organic Compounds (VOCs)	0.45	0.45
PM	An emission limit corresponding to natural gas with fuel sulfur content of no more than 1 grain/100 scf	An emission limit corresponding to natural gas with fuel sulfur content of no more than 1 grain/100 scf

Implications for the Dynajet

EPA and CARB emission standards are formulated to be met by engines with the best available control technologies (BACT) that are economically feasible. Manufactures rarely go beyond these standards because they have no economic incentives to do so. For example, there are no Blue Sky Series Engines available on the U.S. market yet "because isolated requests for especially clean-burning engines don't justify the expense of developing them" [21].

Though not yet available in the United States, the Dynajet is a product that meets Blue Sky Series requirements right now. In fact, its HC + NOx emissions of 3.5 g/kW-hr is well below the Blue Sky Series standard shown in Table 2.14. The Dynajet could conceivably become the standard against which other engines are measured, making it well positioned for sales in the United States market from an environmental perspective.

2.3.2 Grid Interconnection Standards

The possibility of connecting the Dynajet to the electrical power grid raises another set of regulatory issues concerned with safety and power quality. State public utilities commissions generally set regulations. The California Public Utilities Commission, for example, approved a regulatory document on December 21, 2000 known as Rule 21 [24]. One of the major requirements is a tripping mechanism to disconnect from the grid if frequency or voltage departs from specified limits. For small generators less than 11 kVA, the voltage must be maintained between 106 and 132 volts. Frequency must be maintained between 59.3 and 60.5 Hertz. The Institute of Electrical and Electronics Engineers (IEEE) is currently drafting Grid Interconnection Document P1547 in an effort to create one standard that all others can be modeled after nationwide. IEEE's standards are similar in nature to the State of California's.

Dynajet electricity quality must be evaluated carefully before it is considered for grid interconnection. However, a cursory first check indicates that it will most likely fare quite well against the requirements. For example, the Dynajet regulates voltage to within ±1 percent. For a base voltage of 120, this translates to voltages ranging from 118.8 to 121.2, thereby greatly exceeding the California operating window requirement of 106 to 132 volts.

2.4 Possible Dynajet Market Niches

As a prelude to considering the market position of the current Dynajet and any possible future derivatives, it is useful to compare, in general terms, the strengths and weaknesses of the Dynajet-type approach to the current competition (IC engines and solar), and potential new entrants such as fuel cells.

Micro Gas Turbine Strengths

- Low Weight
- Compact
- Low emissions
- Very low noise
- Multi fuel capability (potential)
- Long time between overhaul (potential)

- High thermodynamic quality (temperature) exhaust
- In production

Micro Gas Turbine Weaknesses

- Poor fuel consumption
- High (current) price

Several important implications can be drawn from these observations. First, the obvious way to make micro gas turbines more competitive is by reducing fuel consumption and price. However, a second and perhaps more valuable approach is to leverage the strengths that microturbines already have. This approach requires determining the applications that place high value on compactness, low weight, fuel flexibility, and maintainability. It also requires creatively formulating new applications that capitalize on strengths. Specifically, Section 2.4.2 discusses using the thermodynamically rich exhaust of microturbines for cogeneration.

Microturbines can benefit in a more general way from the fact that they are already in production and already meet next generation emission standards. Neither internal combustion engines nor fuel cells can claim to widely achieve both of these advantages.

2.4.1 Competitiveness in Established Market Segments

Civil Market Competitiveness

The competitiveness of the Dynajet can be evaluated according to a number of metrics. Many of the observed strengths and weaknesses of microturbines discussed in the previous section will appear again here in the context of established market segments.

Figure 2-16 shows price per kilowatt versus generator set power data for all applications. At its current price per kilowatt of nearly $3,500, the Dynajet is far more expensive than any of its competitors. This is particularly true for the price sensitive portable and recreational vehicle markets, which average $430 and $750 per kilowatt, respectively. Competing in these markets would require substantial price reductions. However, the Dynajet is closer in price to the more expensive marine generator set competitors. A price reduction or power increase by a factor of two would place the Dynajet on equal footing.

Generator set volume data (L×W×H) represented in Figure 2-17 is useful but can be

misleading. It truthfully suggests that the Dynajet is rather bulky in comparison to other generator sets of its size; however, the degree to which this is the case is skewed somewhat differently for each application. The dimensions of most recreational vehicle and portable generator sets are given without sound enclosures, so comparison to the Dynajet is not entirely fair. On the other hand, most marine generator set dimensions do include sound protection. But regardless of whether or not comparisons are fair, the same conclusion results – for existing applications, a modification of the Dynajet is necessary for it to be more competitive on the basis of compactness. Increasing the unit's power while holding volume constant is one potential avenue. Similar arguments can be made in the case of generator set mass (Figure 2-18).

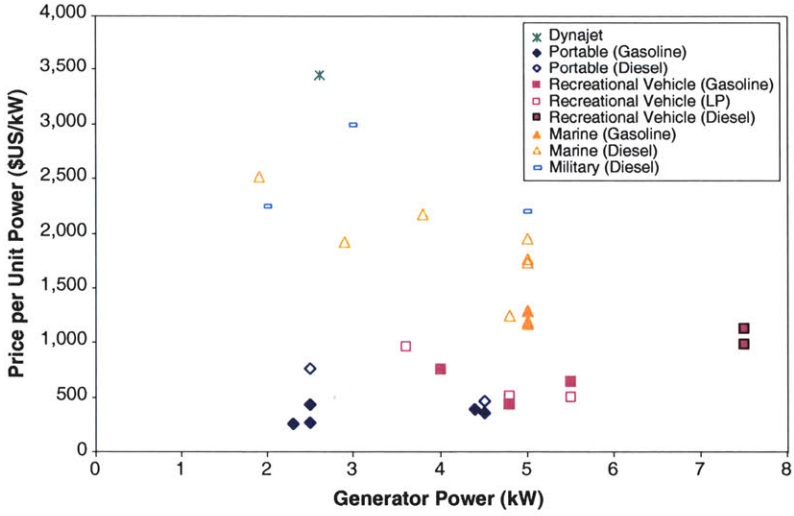

Figure 2-16: Generator purchase price vs. rated power output.

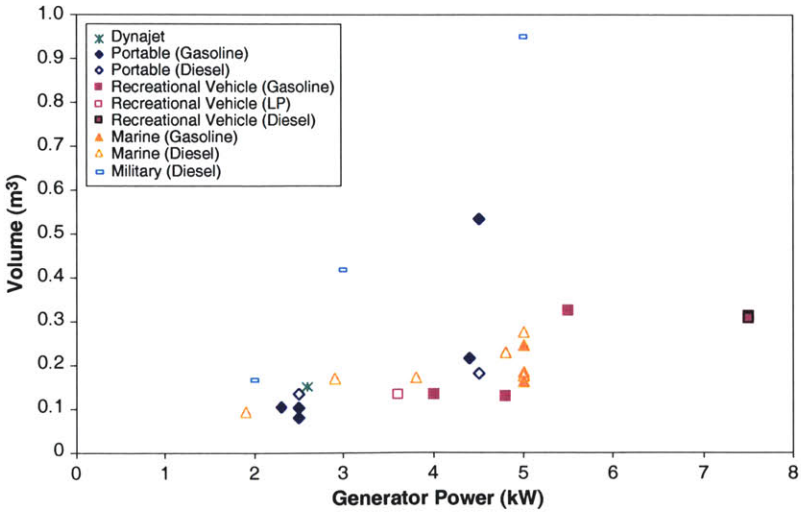

Figure 2-17: Generator volume vs. rated power output.

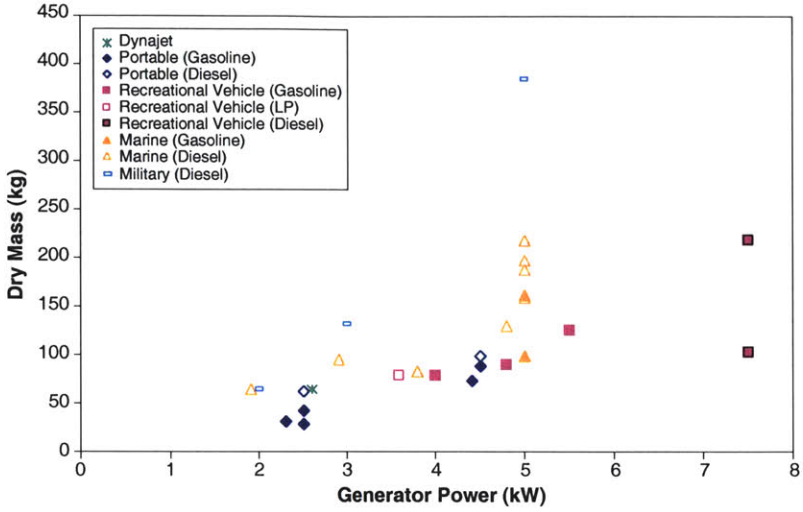

Figure 2-18: Generator mass vs. rated power output.

Poor fuel consumption is a weakness of gas turbines. Power specific fuel consumption (PSFC) versus generator set power data is shown in Figure 2-19. The PSFC's of existing generator sets fit into a band between 0.3 and 0.6 kg/kW-hr. The Dynajet uses roughly 2 to 5 times more fuel than potential competitors. This may not be a significant issue for the price insensitive marine market; however, it could be crippling in the RV and portable markets without somehow increasing the overall efficiency. Some potential ways to do this with the current engine are discussed in Section 2.4.2.

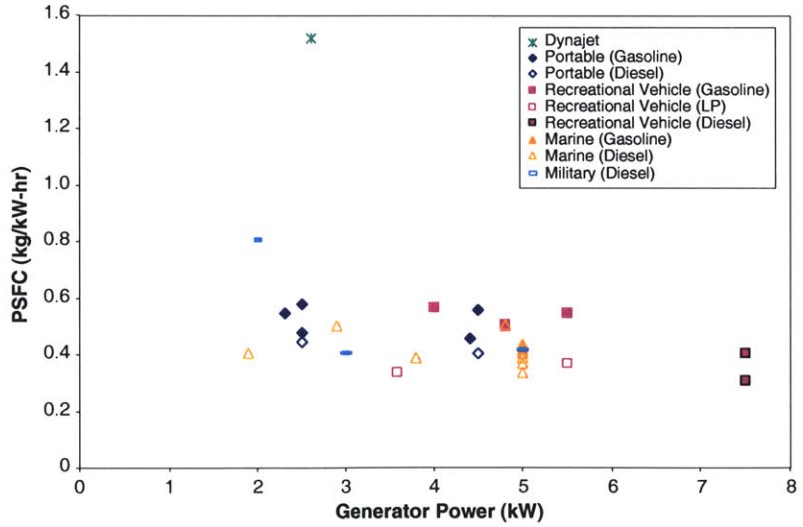

Figure 2-19: Power specific fuel consumption (PSFC) vs. rated power output.

Another major metric of performance is maintenance cost. The Dynajet requires maintenance at two major intervals. Every 250 hours the air filter and fuel filter must be

replaced at a cost of about $36 in parts and $160 in labor (2 hours). Every 500 hours the fuel injector must be replaced at a cost of about $100 in parts and $40 in labor (30 minutes). The total cost of maintenance then is $1064 per thousand hours, which equals $1.06 per hour or $0.41 per kilowatt-hour.

The Dyanjet maintenance cost is comparable to portable, marine, and RV generator sets that have maintenance costs on the order of $1 per hour and is far superior to standby generators with costs on the order of $10 per hour. Even so, it seems plausible that the Dynajet's maintenance costs could come down substantially. Capstone's 29 kW microturbine has a 40,000-hour design life and requires maintenance every 8,000 hours. Maintenance costs average $0.1375 per hour or $0.00474 per kilowatt-hour. For comparison, a 50 kW standby diesel generator set has maintenance costs of $0.60 per kilowatt-hour.

In addition to emissions, which were discussed in Section 2.3.1, a final metric of performance for many markets is noise. The Dynajet is 5 to 20 dB quieter than all but three of the generators against which it was compared, making it extremely competitive in this area.

Figure 2-20 through Figure 2-23 provide an overall comparison of the Dynajet's ownership costs against typical competitors in the various civil applications. The per hour ownership cost includes the purchase price and foregone interest amortized over 5 years, maintenance costs, and fuel costs. The following assumptions were made:

- Dynajet baseline values
  - Price = $9,000
  - Maintenance cost = $1.06/hr
  - Fuel consumption = 4.5 l/hr (at full power)
- Portable, marine, and RV generator set maintenance = $1.00/hr
- Standby generator set maintenance = $10.00/hr
- Published values used for price and fuel consumption of competitors
- Diesel/Gasoline price = $0.25/l
- Natural gas price = $0.006/ft^3
- Discount rate = 5%

The four figures show comparisons for cost of power ($/kWh) as a function of annual usage

between a Dynajet and civil competitors: Figure 2-20 for the current Dynajet costs; Figure 2-21 for variable Dynajet purchase price with fixed fuel and maintenance costs; Figure 2-22 for variable maintenance costs with fixed purchase and fuel prices; and Figure 2-23 for variable fuel consumption with fixed purchase and maintenance costs. The major point to take from these plots is that purchase price is the single greatest contributor to ownership cost. Figure 2-21 suggests that the Dynajet's price must be reduced by a factor of three to substantially improve competitiveness based on cost. Reductions in maintenance costs or fuel consumption show much less impact. This is mainly due to the low annual utilization rates of the applications characteristic of these markets.

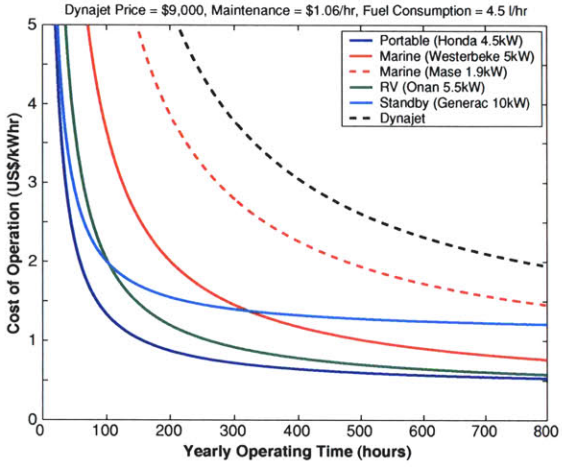

Figure 2-20: Baseline Dynajet cost of ownership comparison.

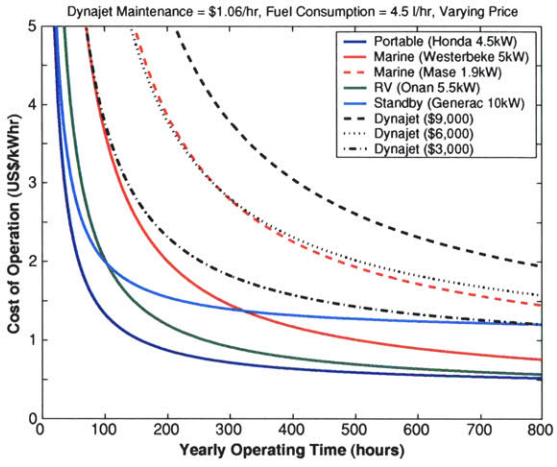

Figure 2-21: Cost of ownership comparison for various Dynajet prices.

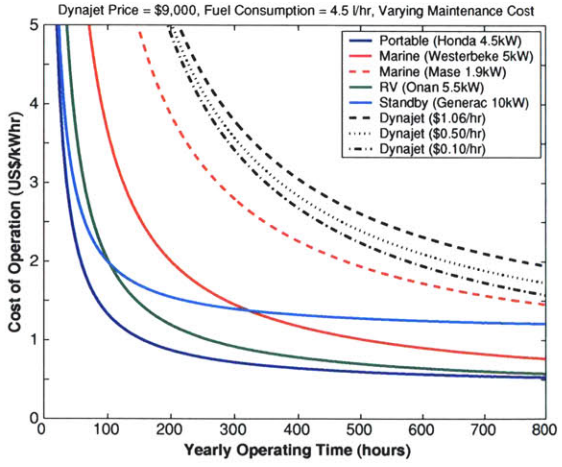

Figure 2-22: Cost of ownership comparison for varying Dynajet maintenance costs.

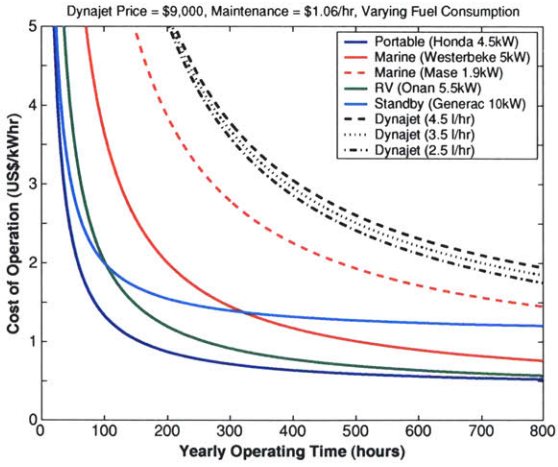

Figure 2-23: Cost of ownership comparison for varying Dynajet fuel consumptions.

Military Market Competitiveness

The U.S. military is a much more sophisticated customer than most in the civil marketplace. It gives greater weight to total cost of ownership rather than simple acquisition cost. Logistics burden (fuel, parts, maintenance) is another important consideration. Current military generators similar to the Dynajet were described in Section 2.1.3 and compared in Table 2.8.

Referring again to Figure 2-16 through Figure 2-19, the Dynajet is clearly superior to the military generators in terms of compactness and dry weight. At current prices, the Dynajet is 15-60% more expensive per kilowatt than inventory military generators. The Dynajet is much closer in price to military generators than it is to civil market generators simply because military generators are more expensive per unit power. The greater expense of military generators is a result of their specialized requirements and low production rates.

One weakness of the Dynajet is its relatively high fuel consumption, which leads to higher operational weight (generator plus fuel) for long missions. Figure 2-24 shows the operational weight for the Dynajet and various military generator weights for mission durations of 24 and 60 hours. As mission duration increases, fuel weight begins to dominate, so that the Dynajet's dry weight advantage is cancelled by its inferior fuel consumption.

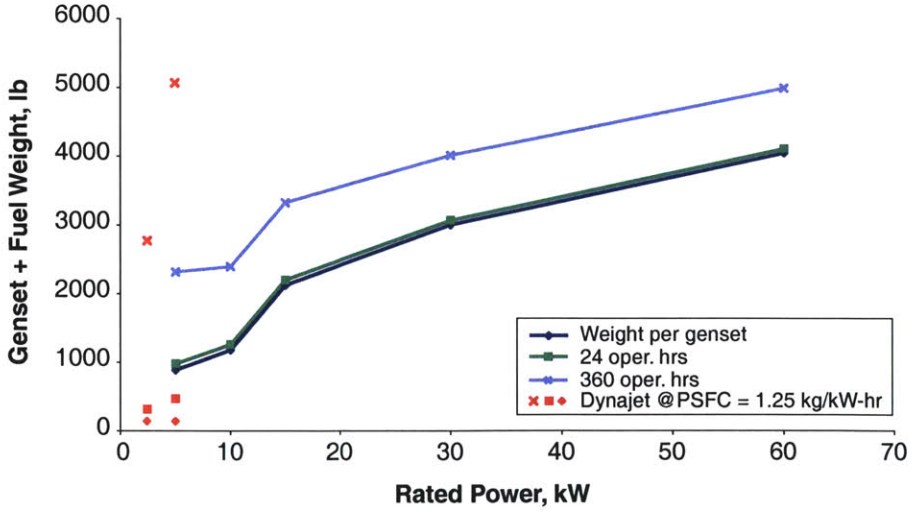

Figure 2-24: Military generator mission weights, including Dynajet.

As was the case for the civil market, an overall cost of ownership comparison of the Dynajet against military market competitors is instructive. Assumptions for this analysis include:

- Dynajet baseline
  - Price = $9,000
  - Maintenance cost = $1.06/hr
  - Fuel consumption = 4.5 l/hr
- Refer to Table 2.8 for military generator set cost and fuel consumption
- 2 kW MTG maintenance = $1.08/kW-hr = $2.16/hr
- 3 kW TQG maintenance = $0.36/kW-hr = $1.08/hr
- 5 kW TQG maintenance = $0.36/kW-hr = $1.80/hr
- Diesel price = $0.25/l
- Discount rate = 5%

Results are shown in Figure 2-25 through Figure 2-28. For reference, the plots also include a vertical line at 280 hours per year, the average peacetime utilization of the military's 5-60 kW tactical quiet generators.

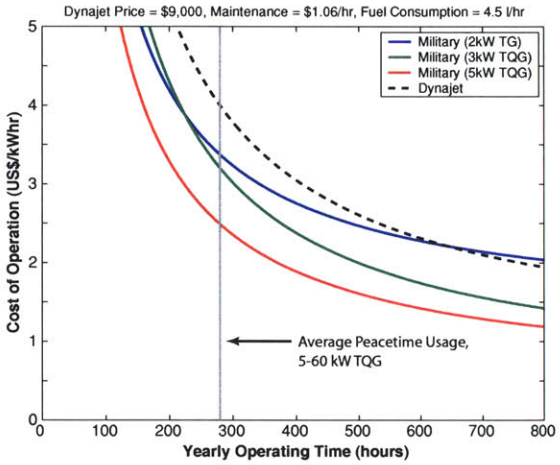

Figure 2-25: Baseline Dynajet cost of ownership comparison.

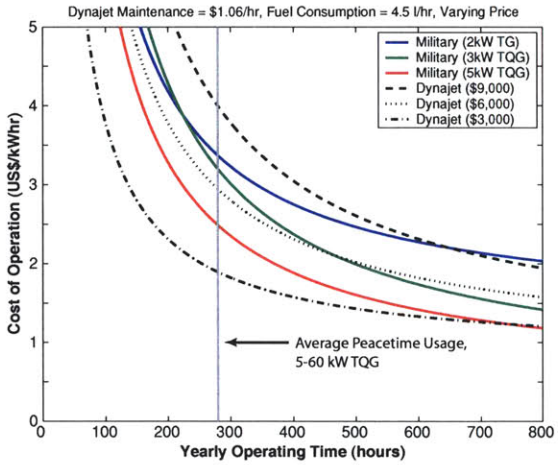

Figure 2-26: Cost of ownership comparison for varying Dynajet prices.

Again, varying price has the most powerful effect on Dynajet competitiveness. However, unlike the case for the civil market, in the military realm, a $9,000 Dynajet is closer to being priced competitively if total cost of ownership is the major concern. This is due to the fact that the Dynajet is relatively close in price to the military generators.

These figures were calculated using the average maintenance cost for small generators and the full power fuel consumption. However, the new 2 and 3 kW military generators have design problems that degrade their cost of ownership. This issue was first discussed in Section 2.1.3. In the case of the 3 kW TQG, lack of reliability (inverter failure is notable in this regard) has driven the mean time between failures (MTBF) down to about 300-400 hours (the requirement is 600 hours). In the case of the 2 kW MTG, "wet stacking" more than doubles the fuel consumption at low power.

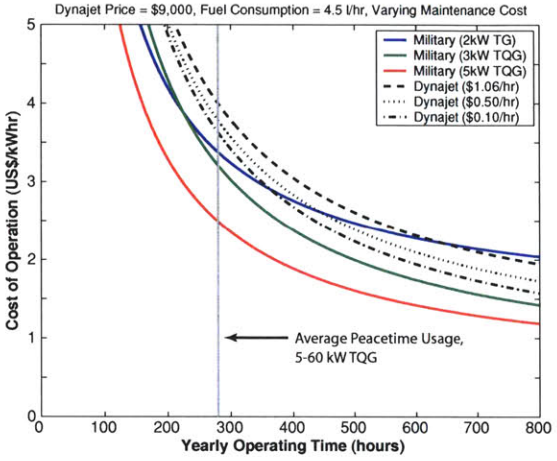

Figure 2-27: Cost of ownership comparison for varying Dynajet maintenance costs.

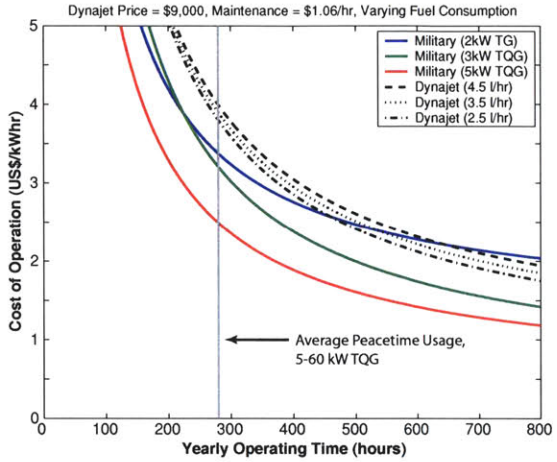

Figure 2-28: Cost of ownership for varying Dynajet fuel consumptions.

Since most military generators spend a significant fraction of their life operating considerably below rated power (Figure 2-7 and Figure 2-8), it is instructive to examine the competitive implications of part power operation. Figure 2-29 and Figure 2-30 compare the cost of ownership of Dynajet with that of the 2 kW MTG, both delivering power to net loads of 500 W and 1.5 kW, respectively.

At 500 W, the Dynajet at a $9000 unit price is 50% more expensive to operate than the current 2 kW generator. The unit price at which the costs of ownership are equal is $5380. At 1.5 kW, the comparison is closer with the Dynajet being 30% more expensive. The breakeven unit price at this power level is $6515.

To further illuminate the relative importance of the component costs that sum to the total cost of ownership, Figure 2-31 and Figure 2-32 breakdown the cost per kilowatt for several military generators and the Dynajet at rated power by cost component for two levels of annual usage: 280 and 560 hours. For all except the 2 kW MTG, the purchase price

dominates the ownership cost. The maintenance cost is a factor of 3-4 greater than the fuel cost for all cases except the Dynajet, for which the two are approximately equal.

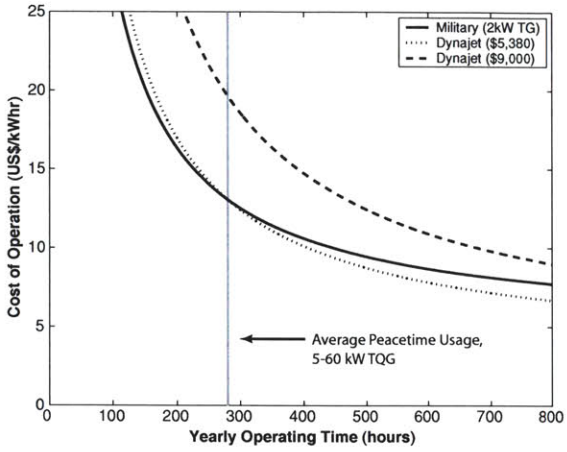

Figure 2-29: Dynajet comparison to 2 kW military TG at 0.5 kW net output.

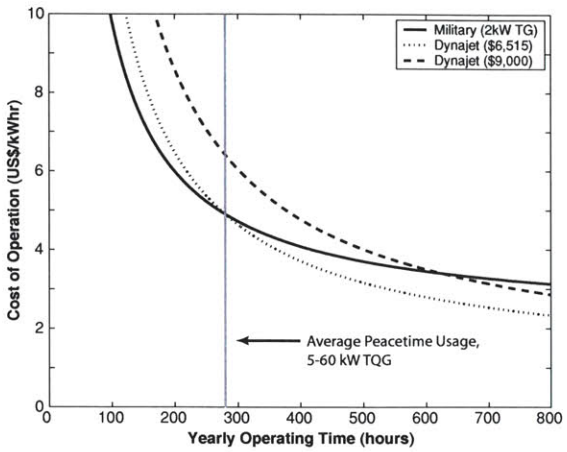

Figure 2-30: Dynajet comparison to 2 kW military TG at 1.5 kW net output.

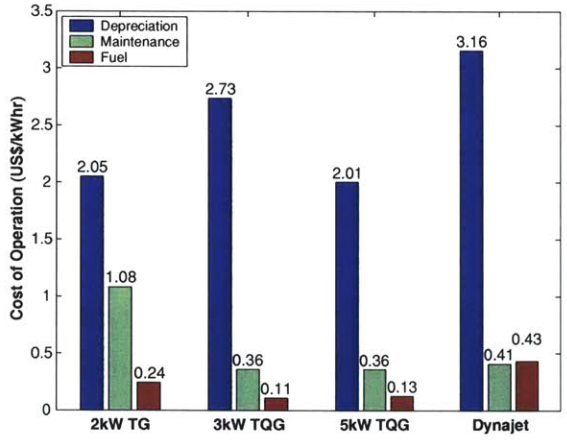

Figure 2-31: Cost components at 280 hrs/yr.

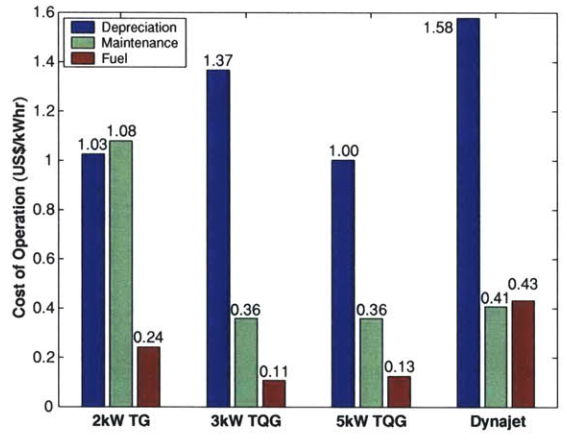

Figure 2-32: Cost components at 560 hrs/yr.

2.4.2 New Applications

New applications refer to uses for Dynajet-like power generators that are not covered by the concept of the current unit as a replacement for a conventional internal combustion engine-driven 2-5 kW generators. These applications exploit use of the technical characteristics of the Dynajet that distinguish it from the IC units in the marketplace. For example, the gas turbine is quieter and lighter and holds the potential for much longer life and therefore much lower maintenance costs. It also may be possible to transform the gas turbine's principal disadvantage compared to a diesel, much lower efficiency, into an advantage. Specifically,

the gas turbine rejects its waste heat at a significantly higher temperature than a small IC engine so that its exhaust is of a higher quality (in the thermodynamic sense). This means that more efficient use can be made of that exhaust in downstream thermodynamic cycles such as cooling or heating. Two examples are discussed below.

Dynajet for Cogeneration

Cogeneration applications may be a favorable market niche for a Dynajet-type product. The rationale here is that U.S. households that burn fossil fuels use more thermal energy than they do electric energy. A typical home in the U.S. is wired for 20-40 kW (the latter for air-conditioning), although the total monthly consumption is in the range of 500-1500 kW-hr, i.e. 1-2 kW on average. This large difference between the average and peak consumption implies that a generator sized for the peak will be greatly oversized on average.

There are several options for home-scale cogeneration. The first is that the unit is off-grid (i.e. not connected to the power grid). This approach has two disadvantages. The first is that the engine would be operating at relatively low power much of the time, which would reduce fuel efficiency (significantly for a gas turbine, less for a diesel, hardly at all for a fuel cell). The second disadvantage is that a considerable capital investment (the largely unused production capacity) would not be returning a benefit. The second option is to stay connected to the grid and sell the excess power back to the grid. The willingness of the power companies to buy power is currently in a state of flux in the U.S. due to ongoing deregulation (which means that the local power companies only distribute power, they do not produce it). Indeed, this is the strategy being pursued by some potential entrants such as the GE fuel cell business. The regulations at this time governing such sales vary greatly from locality to locality.

An Economic Analysis of Microturbines for Home Cogeneration Use

As an example of the role of economic and performance considerations important to cogeneration applications at this size scale, presented herein is a simple economic analysis of a typical Dynajet cogeneration application, specifically home heating, domestic, hot water, and electricity production. Such analysis can be further expanded to include cooling as well. The factors considered in the analysis include depreciation, maintenance, and fuel. Calculations were done for three levels of average power output: 1 kW, 2.6 kW, and 5 kW.

A typical wintertime household in New England burns 180 gallons of oil for heat and hot water each month. A microturbine cogeneration system producing electricity for domestic consumption or sale back to the grid power could be used to replace a furnace in this application.

To evaluate the economic viability of such a system, a cost/benefit analysis was performed. Costs include the system purchase price, opportunity cost, fuel, and maintenance. Purchase prices of $3,000, $6,000, and $9,000 were assumed in analysis and were amortized over 48 months in all cases (typical of the desired investment payback period in the U.S.). The opportunity cost is the interest forgone by purchasing the microturbine rather than investing the purchase amount at a rate of 5 percent over the amortization period. The total opportunity cost is also amortized. The cost of fuel is a function of the fuel consumed by the microturbine in a month less the amount that would have been consumed by a furnace (180 gallons). This difference is multiplied by an assumed oil cost of $1 per gallon. Finally, maintenance costs are assumed to be $0.001 per kilowatt-hour.
The benefit of cogeneration is electricity with an implicit emergency backup capability. Assuming the local utility charges $0.12 per kilowatt-hour, $108 is saved each month on 900 kilowatt-hours of household use. Energy produced beyond this amount can be sold back to the electric company at a rate of $0.06 per kilowatt-hour – approximately half of the electric company's service charges cover delivery costs.

Figure 2-33 shows the costs, earnings, and net return that will be realized for six combinations of microturbine price and power output at three conversion efficiencies (fuel energy to electric energy). While this study can be expanded by considering various fuel types and parametric variations of the fuel price, payback period, and discount rate, it is unlikely that the overall conclusions will change significantly. One conclusion is that at a price of $9,000 and efficiency near 5 percent, the Dynajet is not well suited for this application. However, an improved Dynajet with increased efficiency coupled with a significant price reduction could make this product an attractive home energy solution. For example, a $3,000 Dynajet continuously producing 1 kW of power at an efficiency of 11 percent could offer a return rate of approximately $28 per month. At this 11 percent efficiency, the breakeven price for the Dynajet is $4,100.

Another finding of the study is that at the retail price of fuel in the U.S. and the buyback price a utility might pay (assumed herein to be one-half of the retail price of

electricity), the cost of the fuel alone requires a 25-40% electric power conversion efficiency, considerably greater than that an evolved Dynajet is likely to achieve. This implies that the principal advantage to this scheme is the avoidance of the electricity purchase rather than its production and sales. Thus, a cogeneration unit for this application should be sized for the thermal load of the home rather than for its electricity consumption. It is assumed that a large part of the attractiveness of such an approach would be that an integrated backup power generation capability is integrated with the home thermal energy supply.

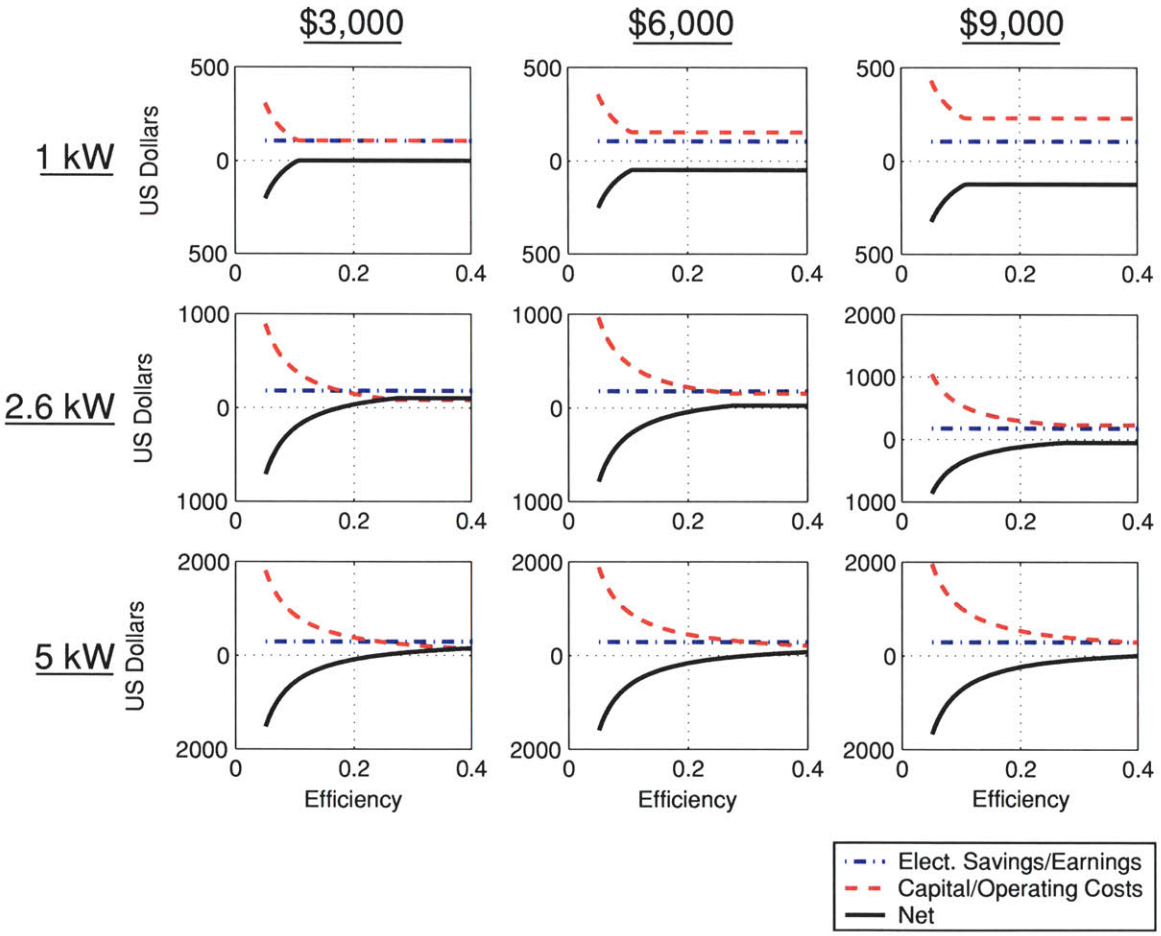

Figure 2-33: Microturbine monthly financials for differing purchase prices and outputs.

Cooling

Cooling is a major use of electric power in the U.S., even in many portable power applications - recreational vehicles, boats, and military shelters and tents, for example. Thus, for these applications, a cogeneration system that uses the exhaust heat of the gas turbine for cooling may be an attractive solution – attractive from the point of view of fuel

consumption and attractive because it increases the useful output of a gas turbine of a given size, making a small gas turbine generator equivalent to an IC engine unit several times its electric output.

There are many thermal cycles that use the enthalpy in a high temperature gas stream to cool a fluid. The engineering metrics for such cycles are Coefficient of Performance, COP (watts of heat pumped per unit of heat or of electric power input), size, weight, noise and vibration, and cost. Conventional small refrigerators and air conditioners with electrically powered compressors operate at COP's of 3-5. In general, adding complexity and cost to the cooler can increase COP. Commercial coolers based on absorption cycles (no compressor) run at COP's of about 0.6 at the 17 kW size. For these units, the energy input is a fuel burner generating heat. More sophisticated cycles can double or triple this COP, at the cost of additional heat exchangers and turbomachinery.

An Economic Analysis of the Dynajet for Residential Cooling

A typical U.S. home requires 10-30 kW of cooling. A case study of a 5 ton (17.5 kW) home cooling application is presented here to assess the economic feasibility of the Dynajet in this application.

For cooling analysis, the Dynajet can again be assumed to have maintenance costs of $1.06 per hour and fuel consumption of 4.5 liters per hour. Given its demonstrated impact, the Dynajet price should be varied. Also entering into the total per hour cost of the Dynajet is electricity savings/earnings. Based on average household power requirements, 1.25 kW of the 2.6 kW produced by the Dynajet are taken as electricity savings at a rate of $0.13 per kilowatt-hour. The other 1.35 kW are assumed to be sold back to the power company at a rate of $0.065 per kilowatt-hour.

The results of the analysis are shown in Figure 2-34. The Dynajet is always more expensive than the electric drive, even at very low Dynajet prices. The implication of the figure is that this is not an attractive Dynajet application.

An Economic Analysis of the Dynajet for Military Cooling

Cooling is a major driver for portable power generation in the U.S. military, often sizing the power generation requirements and consuming about one-half the power and an even greater fraction of the total fuel consumed (since the air-conditioning duty cycle is larger than the that of many other loads). At this time, the U.S. Army has about 10,000 portable air conditioners in the field ranging in size from 6,000-60,000 BTU/hr. The Air Force,

Navy, and Marines have many more. These units are expected to last 10-15 years on average (noting that the majority spend most of their peacetime lives in warehouses).

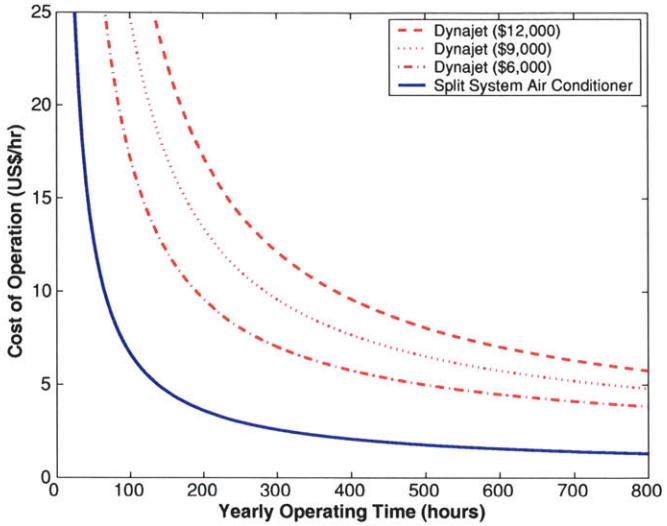

Figure 2-34: Dynajet home cooling cost comparison.

Military air conditioners are designed by the U.S. Army Communications-Electronics Command (CECOM) from commercially available components and then manufactured under contract (usually small) firms. Compactness is valued over efficiency for these applications, with the components tightly packed. The result is that these units operate at very low efficiency compared to commercial units, COP of 1 rather than 4-6 for energy efficient modern air conditioners. The units are also relatively expensive, $6,000-8000 per unit at the 18,000 BTU/hr size. The current procurement rate is 1000 per year at this size. Unlike generators, most air conditioners are centrally purchased and warehoused, with users drawing from stocks as needed.

Most applications for these military air conditioners are for portable shelters such as tents, vehicle mounted and transportable enclosures (buildings use the much more economical commercial units). These applications are mostly supplied by portable generators – either small generators integrated into the shelter or larger units connected externally. Given the current drive for fuel economy in the military, combined cycle machines are an obvious approach. Informally, it has been estimated that 50-75% of military air conditioner applications would opt for a combined cycle approach if one were available off the shelf. This would be about 500-750 units per year. However, the development of such technology has not been a sufficient priority to warrant Army funding in the past.

Recently, a Congressional set aside has started a small (in funding) environmental control unit (ECU) program at the Department of Energy Pacific Northwest Laboratory.

A typical (and high priority) example might be a small communications shelter such as the Standard Integrated Command Post (SICP), which has a 10 kW_e generator powering an 18,000 BTU/hr (5.3 kW) air conditioner. Operating with a COP of only 1, the air conditioner leaves less than 1/2 the generator output for other electrical needs. Thus, in this application, a cogeneration system with 5 kW_e output would suffice. A Dynajet (which generates 45 kW of waste heat) coupled to a commercial state of the art Serville cycle thermal air conditioner operating at COP of 0.63, would produce more than sufficient cooling (28 kW) but be low in electrical power output. The Dynajet has sufficient thermal output to support the much larger cooling requirements such as those for tents. This cooling capacity, far in excess of requirements, implies that cooling efficiency could be traded for cost or compactness in the design of a Dynajet based ECU.

Figure 2-35 shows a cost of ownership analysis for a Dynajet cogeneration system and military generator/air-conditioning package for shelter cooling. Assumptions for this analysis include:

- Dynajet cogeneration system baseline:
  - Price = $20,000
  - Maintenance cost = $1.06/hr
  - Fuel consumption = 4.5 l/hr
- Military 10 kW TQG price = $12,000
- Military 18,000 BTU/hr A/C price = $8,000
- Air conditioner maintenance = $100/yr
- Generator maintenance = $1.73/hr
- Military fuel consumption = 4.273 l/hr

The figure suggests that the Dynajet has promise for military shelter cooling applications. Even at equal acquisition costs, the Dynajet has an overall cost of ownership advantage due to fuel and maintenance cost savings.

2.5 Conclusions

In this section, market opportunities available for the Dynajet are summarized and various

strategies that might be adopted are discussed. The discussion is divided into subsections on the military and civil markets. For each, in so far as possible, an effort is made to identify the market niche, delineate the Dynajet strengths and weakness, and list the modifications needed to be successful in that niche. Finally, alternative market development strategies for a Dynajet type product are offered.

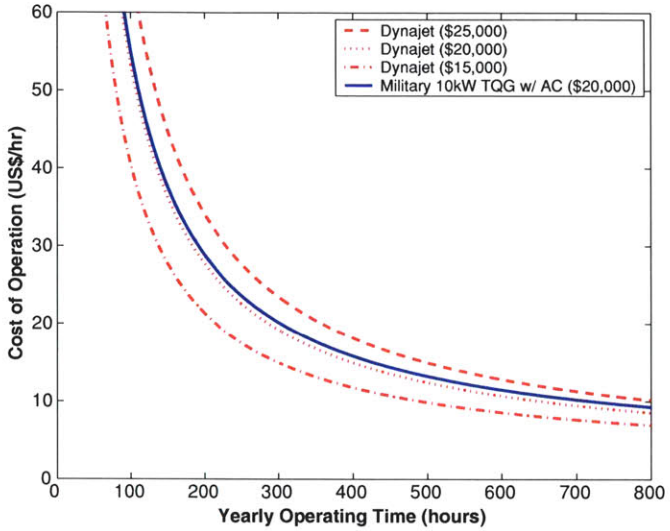

Figure 2-35: Dynajet military cooling cost comparison.

2.5.1 Military Applications

For military applications, the Dynajet's three primary advantages compared to current diesel approaches are lightweight (light enough to be carried by two people), very low noise (the only unit which meets military requirements), and superior maintenance costs. Compared to possible advanced technology solutions (such as fuel cells), the Dynajet has the advantage of being a developed product in production rather than a future promise. The Dynajet's primary disadvantages are very poor fuel economy (a factor of 3 worse than diesel generators) and its current high price for its size range. The relative importance of these factors, however, varies greatly with the application.

The near term military applications are summarized in Table 2.17 and discussed in the following paragraphs.

Battery Charging – for the new soldier system is an emerging requirement not currently met by any existing system. The Dynajet advantage here is that it is the lightest weight, lowest noise solution. Poor fuel consumption is a major detriment for longer missions because it increases the weight of the total system that must be transported. However, the

costs associated with the fuel consumption should be offset by superior MTBF and reduced maintenance costs compared to an IC engine. Little modification need be done to the Dynajet for this application, although it would benefit from reduced fuel consumption at part power and lower weight.

Table 2.17: Near term military applications.

	Power Needed	**Dynajet Mod's Needed**	**Price of Current Solution**	**US Market Potential**
Soldier Power Battery Charging	1.5 kW	Minor, (+improving eff. helps)	Emerging Application	400-800
Silent Watch	1.5 kw	Minor, (+improving eff. helps)	Emerging Application	In formulation
General purpose				
2 kW TQG	2kW	Lower price by 30-50%, improve efficiency	$4500	1000/yr
3 kW TQG	3 kW	Up output to 3 kW, improve efficiency	$9000	1000/yr
APU				
Stryker	4kW	Up output to 4 kW, adapt to vehicle	$7700	2100/6 yrs
Shelter Co-gen ECU	4-5 kW_e +5kW_{th}	Up output to 4-5kW Add thermal A/C	$20000	500-750/yr

Silent Watch – refers to the powering of electronic equipment in remote locations. Applications currently under study need less than 2 kW, well within the current capability of the Dynajet. The Dynajet advantages are low noise and lightweight. This may be a very real, target of opportunity, near term market but the number of units has been difficult to judge since the procurement requirements have not been formulated. Long-term, the Army talks about fuel cells and taking power from hybrid-electric vehicles, which implies that the long-term is many years away, suggesting that there is a shorter term opportunity for a Dynajet-type solution.

General Purpose – generators are purchased by PM-MEP, usually on 10 year cycles. The current 2 and 3 kW generators started their procurement cycle about 3 years ago, which would normally suggest that volume procurement of new designs (to be studied under the MP-2 program of PM-MEP) would be 5-7 years away. However shortcomings in the current units may open nearer term market opportunities. At the 2 kW size, the current generator is quite noisy, has low reliability, and doesn't operate well below one-third load.

The 3 kW unit is also noisy, has reliability problems with its inverter, and is twice the price of the 2 kW unit. This implies that a reliable, well-priced, quiet Dynajet may be able to penetrate an otherwise closed market. Increasing the Dynajet's output power to qualify as a 3 kW unit may be attractive because the current 3 kW TQG is twice the price of the 2 kW unit. However, note that the unit weight should not be allowed to grow much since the fact that the current Dynajet can be carried by only two people (unlike the 2 and3 kW military generators) is perceived as a significant advantage for many applications. To be competitive at the 2 kW size requires a Dynajet price reduction to the $4500-$6000 level.

APU – auxiliary power units are generally limited to armored vehicles and are purchased with the vehicle. The two new armored vehicle procurements at the moment are the Army Stryker and the Marine AAAV. The AAAV requirement at 13 kW (electric plus hydraulic) is too large for a Dynajet derivative and so is not included in Table 2.17. The Stryker, however, needs 4 kW electric. The Stryker is a weight-limited vehicle. Low noise, small size and low maintenance burden may make a Dynajet solution an attractive alternative to the current diesel. The APU is contractor furnished equipment so that sales would be made to the prime contractor (General Motors in the case of the Stryker) rather than the military. The principal modifications required for this application are an increase of power output to 4 kW and adaptation to the vehicle as needed.

Shelter Cogeneration – is a long recognized but unfulfilled need for the U.S. Military. The current approach of using an inventory TQG or APU to power the shelter and its air conditioner is poorly regarded by users because of high noise levels. The Dynajet offers significant improvements in noise and size but has too little output power for most applications. The coupling of a Dynajet to a thermal cycle air conditioner would largely solve the size problem since more than 50% of the electrical load is air-conditioning. It also addresses the Dynajet efficiency shortfall since the cogeneration effectively halves the net fuel consumption. This may also be an attractive application because it represents a high unit value market, with the current separate military air conditioner plus generator priced at more than $20,000 per unit. Also there is no direct competition at this time. The thermal output of the Dynajet is sufficient for larger tent cooling requirement. Cogeneration tent cooling is not a current requirement for the U.S. Army but may prove attractive. This application would require the development or adaptation of a suitable thermal cooler.

Table 2.18 summarizes the military applications identified and gives a qualitative assessment of the relative importance of the various engineering metrics.

Table 2.18: Summary of military application requirements.

		General Purpose	Shelter Power	Tent Power	Battery Charging	Silent Watch	APU	Auton. Vehicles	Battle Armor
Requirements	Total Power Range (kW)	3 - 60	10		2-Jan	1.5	3.8	0.5-3	2 - 3
	Electric Load (kW)	3 - 60	4.3			1.5	3.8		2 - 3
	A/C Load (kWe/kWth)	0	5.3/5.3	15.8		0	0		0
	Fuel Types	diesel	diesel	diesel	diesel	diesel	diesel	diesel	diesel
	Usage (hrs/yr)	280						small	
Performance Metrics	Fuel Consumption	medium	medium	medium	medium	high	high	high	high
	Price/kW	high	high	high	medium	medium	high	high	high
	Maintenance Cost	high	high	high	medium	high	high	low	low
	Life	high	high	high	medium	high	high	med	med
	Noise	medium	high	high	high	high	med	high	high
	Weight/Size	high	medium	medium	high	high	med	high	high

Strategic Considerations for the Military Market

In addition to the quantitative factors already discussed, there are several qualitative considerations that may influence marketing direction for the Dynajet. These include

- Reliability
- Total cost of ownership
- Timeliness

The military customer is very sophisticated when it comes to evaluating factors such as cost. Most military generators average only 200-300 operating hours per year, thus the Dynajet's relatively high fuel costs can be mitigated by lower maintenance and purchase price considerations. While the potential for reducing Dynajet costs are beyond the scope of this thesis, the importance that low maintenance cost can play should be emphasized. This is a natural advantage of well-engineered gas turbines.

Timeliness can be as important as technical performance and price. The Dynajet is in production. "Superior" solutions such as fuel cells are at this time only promises, but there are large resources invested in their R&D and strong advocates within the military. This implies that there is an advantage in pursuing near-term opportunities, getting a product into the military system, and incrementally improving the product. Thus, a Dynajet "interim solution" may have a quite long product life as the development cycles stretch and the actual performance degrades for the seemingly more attractive long-term solutions under development.

2.5.2 Civil Applications

For civil applications, the Dynajet's major advantages compared to current internal combustion engine competitors are very low noise and reduced emissions. As with the military market, the Dynajet's advantage compared to potential advanced technology solutions is its status as a developed, working product. The Dynajet's most significant disadvantage in the civil market is its extremely high price per unit power compared to existing alternatives and low efficiency compared to advanced technology such as fuel cells. Unfortunately, the civil market is much more sensitive to acquisition cost than cost of ownership. Other Dynajet disadvantages in the civil market include its relatively low output, high weight, and poor fuel consumption.

The near term civil applications are summarized in Table 2.19 and discussed in the following paragraphs.

Table 2.19: Near term civil applications.

	Power Needed	**Dynajet Modifications Needed**	**Price of Current Solution**	**US Market Potential (of order)**
General purpose				
Low output	2-3 kW	Large price reduction	$800	10,000/yr
High output	4-5 kW	Large price reduction, increased output	$1600	10,000/yr
Marine				
Standard generator	4-5 kW	Increased power and/or price reduction	$5,000 - $10,000	1,000/yr
Cooling and power, Combined cycle	4-5 kW_e + 2.5-32 kW_{th}	Increased power, thermal A/C added	$10,000 - $15,000	1,000/yr
RV				
Standard generator	2-5 kW	Increased power, price reduction	$2,500 - $4,500	10,000/yr
Cooling and power Combined cycle	2-5 kW_e + 0.5-3 kW_{th}	Price reduction, increased power, thermal A/C added	$3,000 - $5,000	10,000/yr

General Purpose – refers to portable generators used for residential and commercial applications. This is the least promising of the near term civil applications, the Dynajet's price being ten times that of current competitors. The Dynajet's advantages here are low noise and high reliability. These may make it attractive for noise sensitive or heavy use commercial applications.

Marine – generators can potentially be produced for electric power only or as part of cooling cogeneration systems. The marine application may be the most attractive near term civil application due to the relatively high prices of current generators and the relatively low sensitivity of the market to price and fuel consumption. The Dynajet's primary advantage for the marine application is low noise. The major disadvantage as a standalone is low power output, a problem that is mitigated to some extent when cogeneration is considered. Thus, the cogeneration option is the most promising. Investment required is adaptation to the marine environment and the addition of thermal air-conditioning at minimal additional cost and weight. The cycle should also be equipped for heating since many marine air conditioners have reverse cycle heating capability.

RV – generators, like marine generators, can also be configured as either standalones or cogeneration systems. However, it is unclear here whether cogeneration is necessarily a much better option since RV air conditioners are relatively inexpensive (a few hundred U.S. dollars). Adding a thermal air conditioner to the Dynajet may simply make its cost comparison to current RV generators even worse. Again, the major advantage of the Dynajet for this application is low noise.

U.S. residential cogeneration applications for the Dynajet are not listed here as a near term application because their attractiveness is less certain. First, the Dynajet is too small for residential use in the U.S. by factor of 2-4 (although it does seem to be well sized for Europe or Japan). Also, significant improvements in both price and efficiency are needed to compete with a large central powerplant. Section 2.4.2 showed that cost competitive cogeneration requires a factor of 3 improvement in fuel economy and a factor of 2 drop in price.

Table 2.20 summarizes the civil applications identified and gives a qualitative assessment of the relative importance of the various engineering metrics. Examples of typical competitors are also included.

Strategic Considerations for the Civil Market

Qualitative considerations that may influence civil marketing direction for the Dynajet include

- Environmental impact
- System integration

- Novelty

Environmental impact and regulation is an important marketing consideration that was alluded to briefly in Section 2.3.1. The Dynajet's extremely low emissions compared to IC engines may be attractive to environmentally conscious consumers. Perhaps more importantly, it may be attractive to environmental regulators. For example, state and national regulations mandated by the Clean Air Act set emissions requirements according to limits constrained by the "best available technology". Introducing the Dynajet to the generator market could conceivably result in tightened regulations, essentially mandating Dynajet levels of emissions for all portable generators. The Dynajet would be the reference for new standards. Similarly, although the emissions from standby generators are currently not regulated, it is clear from the California energy crises that the assumption of infrequent use upon which the exemption from regulation was based is not necessarily valid. Thus, California regulators are now examining the question of if and how standby and emergency generators should be treated. This may open an opportunity for the Dynajet in this price sensitive market.

Table 2.20: Summary of civil application requirements.

		Portable	Honda EN2500 AL	**Marine**	Westerbeke 5.0BCG	**RV**	Generac Primepact 50G
Requirements	Total Power Range (kW)	2.6	4.5	4 - 25	5	3 - 12	5.5
	Electric Load (kW)	2 - 6		3 - 20		2.5 - 9	
	A/C Load (kWe/kWth)			0.5/2.5 - 8/32		0.5/2 - 3/12	
	Heating Load (kWth)			3.5 - 32		5.5 - 16	
	Fuel Types	gasoline diesel	gasoline	gasoline diesel	diesel	gasoline LP	gasoline
	Usage (hrs/yr)						
Performance Metrics	Fuel Consumption	Low	0.56 kg/kW-hr	Medium	0.44 kg/kW-hr	Medium	0.55 kg/kW-hr
	Price/kW	High	$361	Low	$1,300	Medium	$446
	Maintenance Cost	Low		Medium		High	
	Life	Low		Medium		Medium	
	Noise	Medium	76 dB	High	65 dB	High	68 dB
	Weight/Size	High	32 kg	Medium	162 kg	High	90 kg
Units / Year		25000		8100		54000	

System integration refers to the possibility of using the Dynajet with thermal air-conditioning to replace separate generators and air conditioners. This can be attractive from a marketing standpoint both from the perspective of potential cost savings and reduced system complexity. However, the trade of added cost for added functionality must be considered carefully, particularly in the price sensitive RV market.

A final consideration for civil marketing of the Dynajet is its novelty. In a society that increasingly evaluates its self-worth by quantities of high technology gadgets, a gas turbine generator has something to offer.

Chapter 3

Engineering Study

The principal engineering objective of this study is to develop a cycle model of the Dynajet that accurately represents the engine's performance. The model must be consistent with measurements and provide a detailed accounting of all cycle nonidealities. The ultimate goal of the cycle model is utility as a guide to engine modifications for performance improvements. Together with the market study, the cycle model may be used to improve Dynajet competitiveness.

The engineering study brings to light a number of cycle characteristics that are not captured in the ideal Dynajet cycle model presented in Figure 1-2. These include heat leakage, flow distortion, and flow leakage. An alternative cycle model that includes these nonidealities is shown in Figure 3-1.

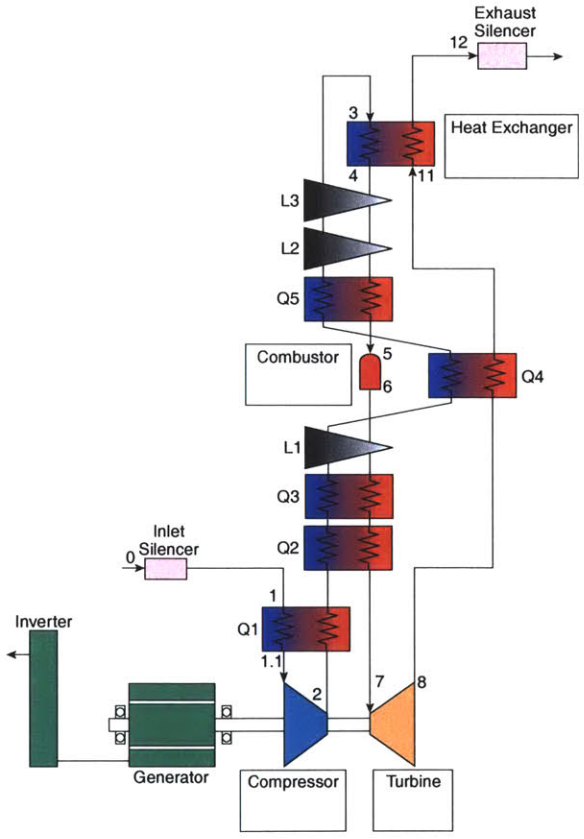

Figure 3-1: Dynajet cycle model with nonidealities.

At the outset of this research, the information available on the Dynajet included compressor rig and engine maps, component efficiencies determined from rig tests, limited temperature and pressure data collected in 1994 engine tests, and an IA cycle model. Using this information as a starting point, analysis was done to identify areas of concern and prompted new engine tests conducted in the spring of 2003. Data from these tests will be referred to throughout this thesis as "April '03" data. Furthermore, "reference values" referred to in the text and figures for quantities such as mass flow and pressure ratios refer to values from the April '03 data set. In the case of component efficiencies, "reference values" refer to those efficiencies calculated from rig tests.

3.1 Technical Approach

The first step in creating an accurate cycle model of the Dynajet was identifying inconsistencies in existing data. To begin this process, a simple cycle analysis was performed using the values of component efficiencies that defined the engine performance at the outset of the project. A major inconsistency discovered was the difference between the actual engine power output of 2.6 kW and expected output of 10.7 kW calculated from cycle analysis based on isolated component rig measurements. The task then became accounting for the lost 8 kW of power.

An incremental approach was taken to improve cycle model accuracy. Section 3.2 describes a simple adiabatic analysis of the Dynajet. This analysis offers insight but proved to be an inadequate match to test data and neglects several nonidealities that can adversely affect gas turbine performance. These nonidealities include heat leakage, flow nonuniformity, and flow leakage and are considered in Sections 3.3, 3.4, and 3.5, respectively. By adding the appropriate effect of nonidealities to the cycle model, a good match to Dynajet data was achieved and is presented in Section 3.6.

3.2 Adiabatic Cycle Analysis

The first Dynajet cycle analysis computations were based on a combination of data and modeling values provided by IA. Analysis assumed adiabatic components. Although this assumption was recognized as questionable for a small engine with many potential heat transfer paths, it offered the benefit of a basic starting point from which a great deal could

be learned and used as a foundation for more sophisticated analysis later. The goal of the adiabatic study was to determine a reasonable range of component efficiencies consistent with available data.

Cycle calculations were performed using an analysis program written in MATLAB. In its most basic form, this program mimics the commercially-available program GasTurb, taking inlet conditions, component efficiencies, compressor pressure ratio, and turbine inlet temperature as inputs to produce cycle power and efficiency as outputs. However, the MATLAB program offers the advantage of straightforward modification for other tasks. For example, for the current analysis under consideration, the interest was in component efficiencies as outputs, not inputs. The MATLAB program was tested against GasTurb and is described in greater detail in Appendix A.

Due to the greater accuracy of pressure measurements over temperature measurements, an initial aim of adiabatic analysis was to define the cycle using only inlet temperature, pressure ratios, mass flow, fuel flow, and power output. However, further consideration showed this objective to be impossible. Figure 3-2 shows a portion of the component efficiency solution space for fixed pressures, mass flow, fuel flow, and power output. The solution is not a point; it is a surface. One additional temperature, such as turbine inlet temperature, reduces the surface to a curve. Two additional station temperatures are needed for a unique solution.

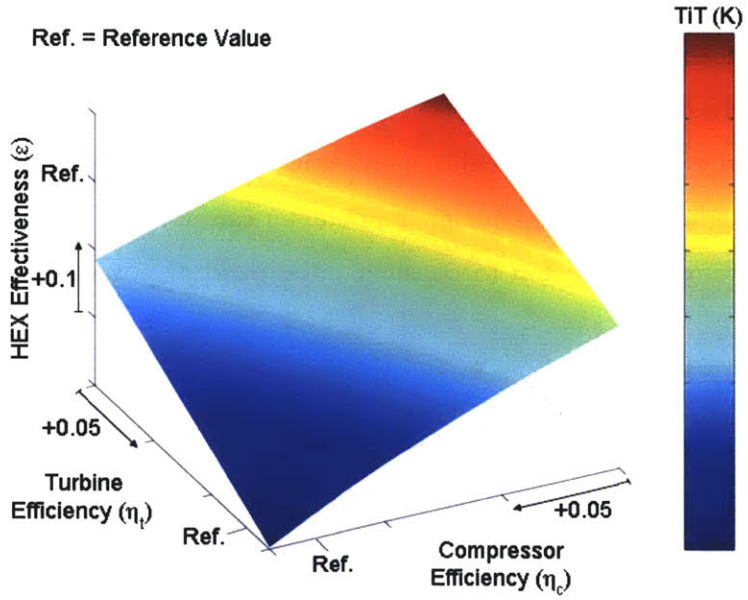

Figure 3-2: Efficiency solution space for fixed pressures, mass flow, and fuel flow.

Figure 3-3 shows the component efficiencies that result from cycle analysis for turbine exit temperature (T_{t8}) fixed at 884 K to match the engine data and a range of turbine inlet temperatures (T_{t4}). There are two curves shown for turbine efficiency. The solid curve represents results for the heat exchanger pressure ratios taken from the IA model, while the dashed curve represents lower heat exchanger pressure ratios. The pressure ratios were lowered in proportion to the increase in corrected mass flow of the data over the IA model.

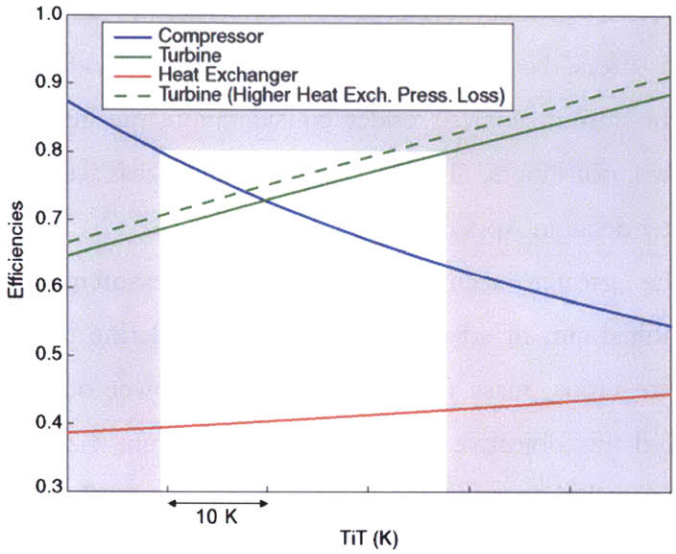

Figure 3-3: Efficiency solution space for fixed pressures, mass flow, fuel flow, and turbine exit temperature.

A 60 K spread in turbine inlet temperature translates to approximately 30 points in compressor efficiency range, 20 points in turbine efficiency range, and 5 points in heat exchanger effectiveness range. Eighty percent efficiency for turbomachinery of Dynajet size is near state of the art. Figure 3-3 also shows how the efficiency range can be reduced by assuming that neither the turbine nor the compressor can have efficiency above 80 percent, leaving only the unshaded region to consider. The band of possibilities is reduced to the following:

- $0.63 < \eta_c < 0.8$
- $0.69 < \eta_t < 0.8$
- $0.39 < \varepsilon < 0.42$

These ranges can be reduced more by further assuming that the compressor is less efficient than the turbine. This is typically the case, since compressors must deal with adverse

pressure gradients and their associated aerodynamic design difficulties, while pressure gradients are favorable through turbines.

The product of adiabatic cycle analysis is a set of component efficiency ranges consistent with Dynajet power output data. The ranges are inconsistent, however, with expected values from rig tests, suggesting the large impact of cycle nonidealities that must be considered in analysis. The first such nonideality considered was heat transfer.

3.3 Nonadiabatic Cycle Analysis

Small engines have more exposed surface area as a percentage of volume than geometrically similar large engines. This is due to the cube-square law: area scales with the square of length while volume scales with its cube, making volume decrease at a faster rate than area as length is decreased. The importance of this fact in reconciling Dynajet performance inconsistencies has to do with its effect on adiabatic behavior. More surface area per volume translates directly to greater heat transfer rates as a percentage of total system power and reduced validity of the widely applied assumption of adiabatic components in cycle analysis. Furthermore, the length scale across which conduction occurs is reduced while the boundary conditions (cycle temperatures) remain the same.

The first suggestion of a heat transfer effect on engine performance was the original cycle model provided to MIT by IA. This model included a 72 K temperature rise between the compressor exit and heat exchanger inlet that would not exist under adiabatic conditions. One potential source of this temperature rise is heat transfer from the combustor. This and other potential heat transfer paths are identified in Figure 3-4 and are listed below:

Q1. Compressor exhaust → Compressor inlet

Q2. Turbine scroll → Compressor exhaust

Q3. Combustor exhaust → Compressor exhaust

Q4. Turbine exhaust / heat exchanger → Compressor exhaust

Q5. Air-side heat exchanger exhaust → Compressor exhaust

Q6. Compressor exhaust → Ambient

From a modeling perspective, these paths can be considered as additional heat exchangers.

The April '03 data gives some insight to the magnitude of heat transfers Q1-Q6. The measured compressor scroll inlet and impeller inlet temperatures were 292.0 and 303.2

K, respectively. Based on the engine mass flow, this 11.2 K temperature rise corresponds to heat transfer that is 7.7 percent of the ideal Dynajet shaft power. Thus, the April '03 engine data indicates at least this amount of heat transfer for path Q1. More Q1 heat transfer occurs through the impeller, an issue addressed in Section 3.3.1. The April '03 data also indicates a 29.6 K temperature rise between the compressor exhaust and air-side heat exchanger inlet. Neglecting the flow leakage considered in Section 3.5, this corresponds to a heat transfer that is 22.3 percent of the ideal shaft power.

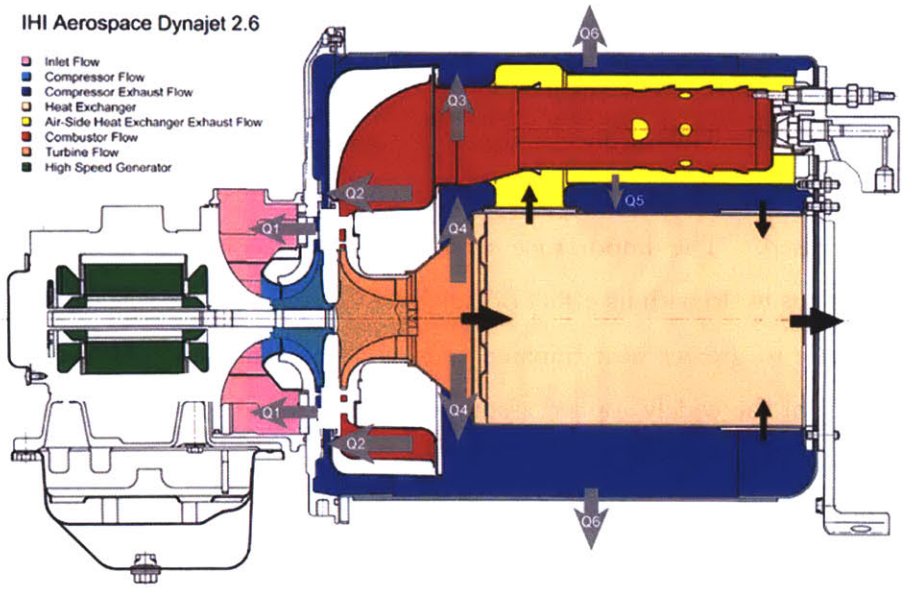

Figure 3-4: Dynajet heat transfer paths.

3.3.1 Compressor Heat Addition

Evidence of heat transfer to the compressor (Q1) was first seen in the disagreement between engine and rig compressor map data shown in Figure 3-5. Rig test corrected speed lines are at higher pressure ratios and corrected mass flows than corresponding engine test corrected speed lines. Compressor heat addition in the engine has this effect. Corrected flow in the engine data is lowered by failure to account for elevation in total temperature due to heat addition. Pressure ratio in the engine is lowered because more work is required to compress the high temperature (*e.g.* low density) flow.

A model of heat addition impact on compressor performance developed by Gong was used to reconcile rig data with engine data [25]. The assumptions of this model are best described with reference to Figure 3-6. Adiabatic compression from a pressure P_{t1} to P_{t3} is represented by A-D. Nonadiabatic compression from P_{t1} to P_{t2} is represented physically by

A-C. The model conceptually separates the nonadiabatic compression process into two steps. The first step is constant pressure heat addition from T_{t1} at A to $T_{t1.1}$ at B. This step is based on an assumption that all heat transfer can be modeled as temperature rise at the inlet. This approximation is reasonable because most heat addition occurs near the impeller entrance where the temperature differential is greatest, while most compression occurs near the exit where the tip speeds are highest. The second step is adiabatic compression along B-C. For this process, efficiency and work input per unit mass flow are assumed equivalent to those of the fully adiabatic process. The work input is approximately the same because it is proportional to wheel speed, which is constant, and not to temperature. The validity of the efficiency assumption depends upon the flatness of the efficiency curves in the region of the map under consideration. For the Dynajet, the efficiency curves are reasonably flat.

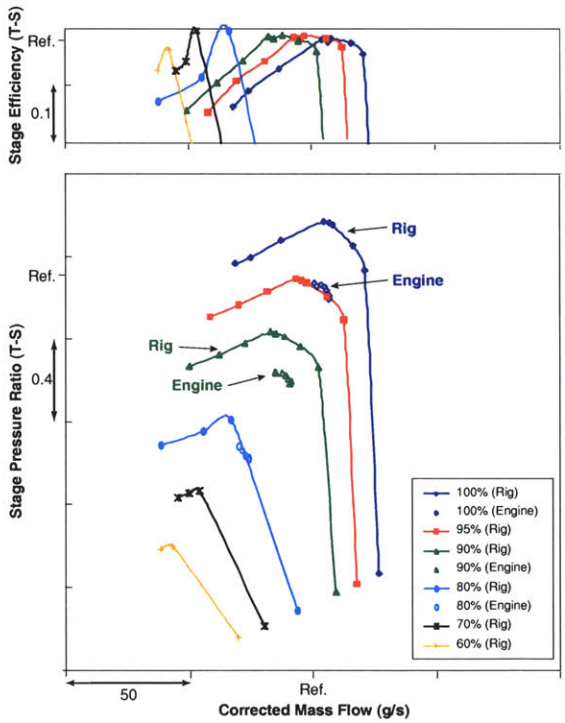

Figure 3-5: Engine and rig test compressor map disagreement.

The effect of heat addition on compressor pressure ratio can be derived from Euler's turbine equation:

$$\tau_c - 1 = \frac{\pi_c^{\frac{\gamma-1}{\gamma}} - 1}{\eta_c} = \frac{(\omega r_2)^2}{c_p T_{t1}} \left(1 - \frac{w_2}{\omega r_2} \tan \beta_2' \right) \tag{3.1}$$

where τ_c, π_c, T_{t1} and η_c are compressor temperature ratio, pressure ratio, inlet temperature, and efficiency, respectively. The value of these variables differs between adiabatic and

nonadiabatic operation. The variables ω, r_2, w_2, and β_2' are compressor rotational speed, exit radius, exit axial flow velocity, and exit metal angle, respectively. Due to fixed geometry and constant volume flow rate operation, these variables are equal for adiabatic and nonadiabatic compression. Thus, Eq. (3.1) can be rearranged as follows to give a relationship between adiabatic and nonadiabatic compression:

$$\left(\pi_{c,a}^{\frac{\gamma-1}{\gamma}}-1\right)T_{t1} = Constant = \left(\pi_{c,n}^{\frac{\gamma-1}{\gamma}}-1\right)T_{t1.1} \tag{3.2}$$

where the subscript a represents adiabatic compression with a corresponding inlet temperature T_{t1} and the subscript n represents nonadiabatic compression with a corresponding effective inlet temperature $T_{t1.1}$. From Eq. (3.2), the nonadiabatic pressure ratio is then:

$$\pi_{c,n} = \left[\frac{T_{t1}}{T_{t1.1}}\left(\pi_{c,a}^{\frac{\gamma-1}{\gamma}}-1\right)+1\right]^{\frac{\gamma}{\gamma-1}} \tag{3.3}$$

In addition to lowering pressure ratio, heat addition to the compressor also lowers mass flow. For a constant volume flow rate through the impeller, mass flow is proportional to the inlet density. This relationship leads to the following model for mass flow with heat addition:

$$\dot{m}_n = \dot{m}_a \frac{T_{t1}}{T_{t1.1}} \tag{3.4}$$

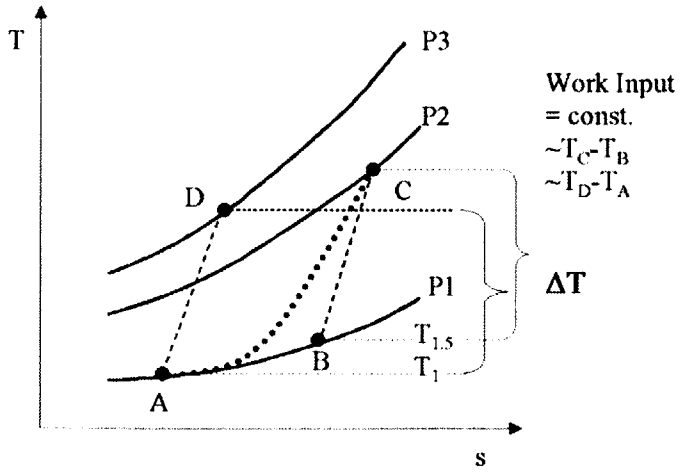

Figure 3-6: Temperature-entropy diagram for compression process with heat transfer [25].

For cycle modeling purposes, it is also important to understand the effect of the heat addition on efficiency. Impeller efficiency is defined as follows:

$$\eta = \frac{\left(\pi_c^{\frac{\gamma-1}{\gamma}} - 1\right) T_{t1}\, c_p\, \dot{m}}{W} \tag{3.5}$$

where W is the power of the rotor. By replacing the pressure ratio in Eq. (3.5) with the expression for nonadiabatic pressure ratio in Eq. (3.3), the following expression is attained:

$$\eta_n = \eta_a \frac{T_{t1}}{T_{t1.1}} \tag{3.6}$$

To verify the compressor heat addition model, Gong examined a number of test cases. The results were then compared to those from Fluent, a three-dimensional Navier-Stokes computational fluid dynamics (CFD) code. Figure 3-7, Figure 3-8, and Figure 3-9 compare results for pressure ratio, efficiency, and mass flow. The heat addition model shows good agreement with numerical solution.

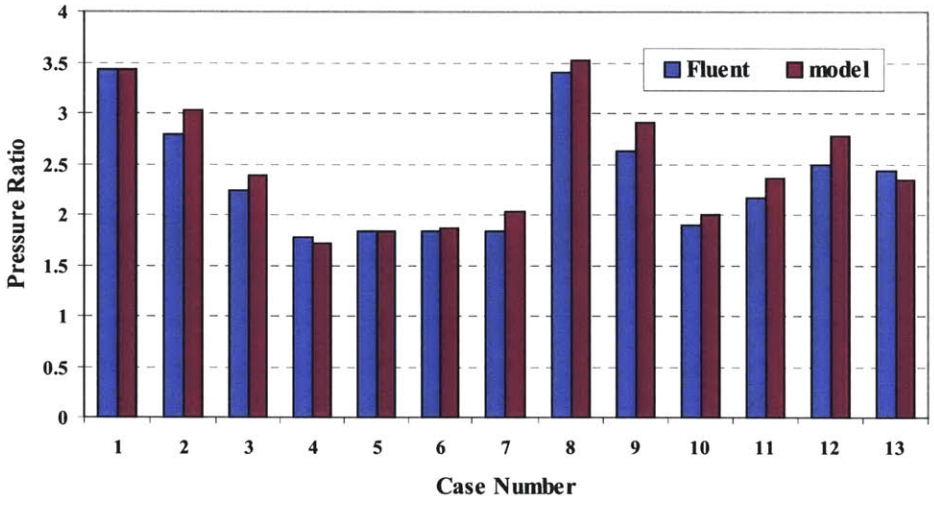

Figure 3-7: Compressor heat addition model pressure ratio results compared to Fluent [25].

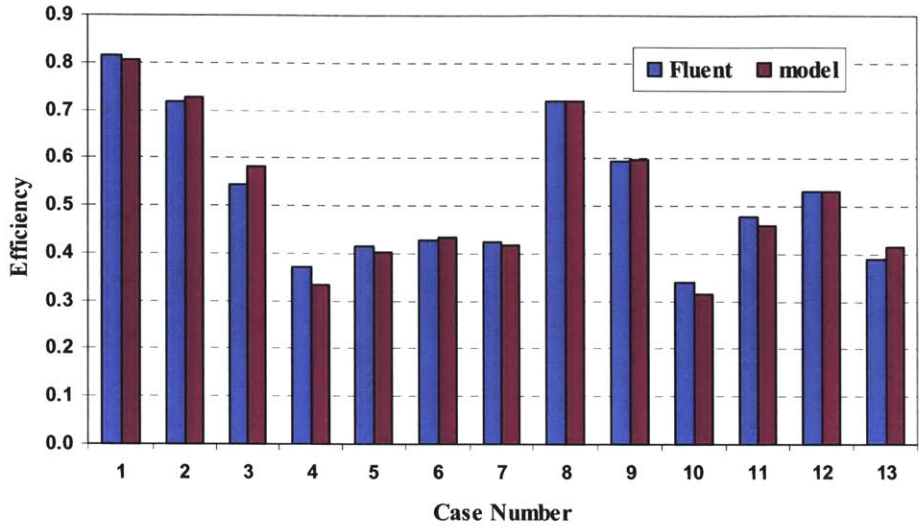

Figure 3-8: Compressor heat addition model efficiency results compared to Fluent [25].

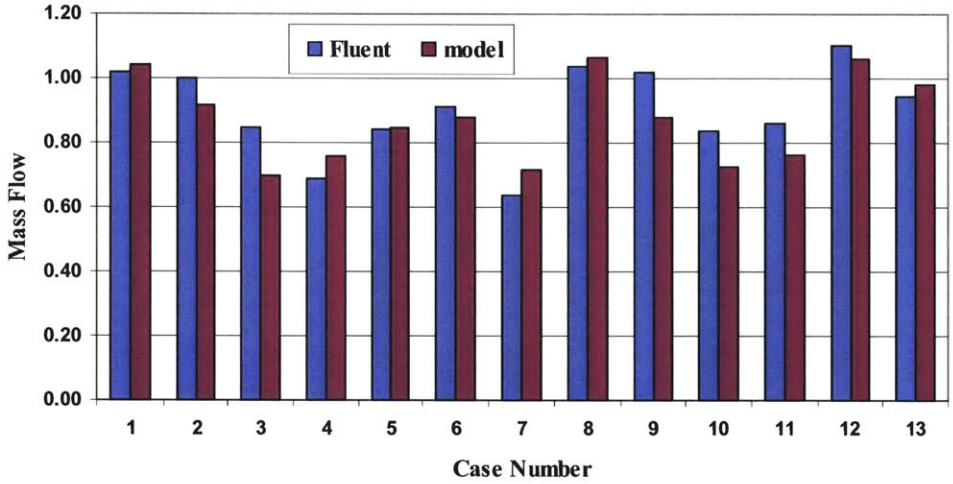

Figure 3-9: Compressor heat addition model mass flow results compared to Fluent [25].

Using this compressor heat addition model, it was possible to match the engine and rig compressor map data. Assuming a temperature ratio $T_{t1.1}/T_{t1}$ due to heat addition, the engine speed line is shifted to the right by the square root of the temperature ratio. This is the true speed line with heat addition and is shown in Figure 3-10. The true speed line is then shifted upward using Eq. (3.2) to see the pressure ratio that would be achieved without heat addition, as shown in Figure 3-11. By varying the temperature ratio until good agreement was found between the engine data and rig data, an estimate for the temperature rise due to heat addition to the compressor was generated.

A temperature ratio of 1.115 was found to give the best match. This corresponds to a temperature rise of 33.5 K, which requires heat addition equal to 25.4 percent of the ideal

shaft power. The effect of this heat addition on the engine's efficiency is calculated from Eq. (3.6). The rig compressor map indicates the adiabatic efficiency, which is defined as the reference efficiency. The engine's efficiency is determined by dividing the reference value by 1.115, which results in an 8 point reduction. The heat addition impacts on pressure ratio and mass flow are 14 and 5 percent drops, respectively.

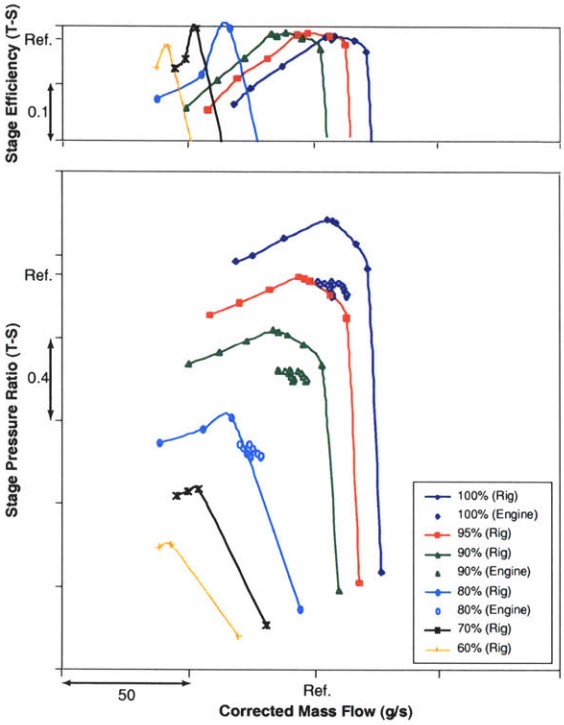

Figure 3-10: Adjustment to engine corrected flow for heat addition.

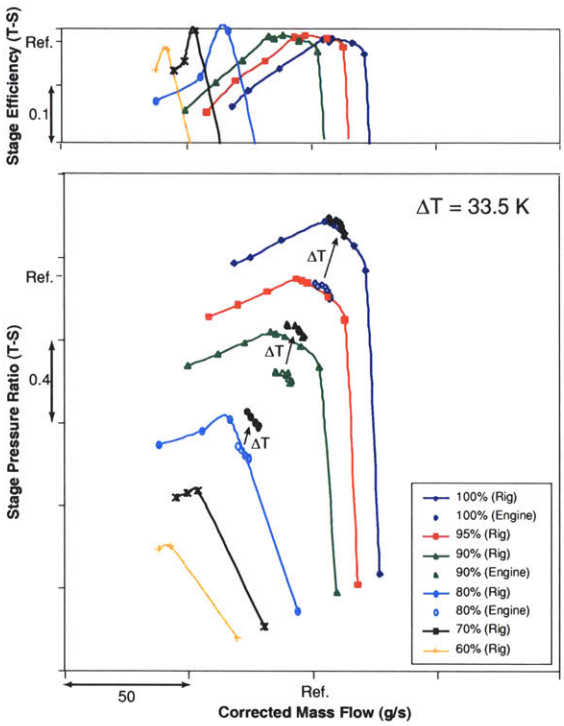

Figure 3-11: Heat addition match between rig and engine compressor maps.

It is possible to estimate the uniform heat transfer to the compressor in the April '03 data using the approach just described to match the engine and rig maps. In this case, a single point is matched to the rig map rather than an entire curve. The matching case shown in Figure 3-12 corresponds to a temperature increase of 26.3 K due to an overall heat transfer rate that is 19.2 percent of the ideal shaft power. Considering the aforementioned data indicating that the heat transfer to the scroll is 7.7 percent of the ideal shaft power, the heat transfer to the impeller must be 11.5 percent of the ideal shaft power. By Eq. (3.6), the effective compressor efficiency is reduced from by 6.4 points from the reference value.

3.3.2 Parametric Heat Transfer Analysis

Before attempting to create detailed models of all heat transfer paths Q1-Q6, an effort was

first made to identify their relative importance. The goal of this analysis was to identify paths that have little impact on cycle performance and neglect them in modeling. Figure 3-13 shows the sensitivity of power output to 1 kW of heat transfer across each of the six heat leakage paths.

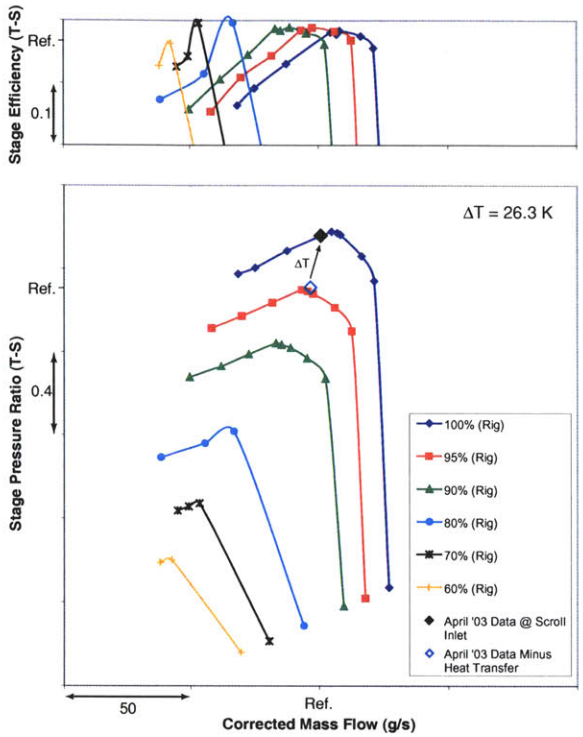

Figure 3-12: Uniform heat addition match of April '03 engine data to rig compressor map.

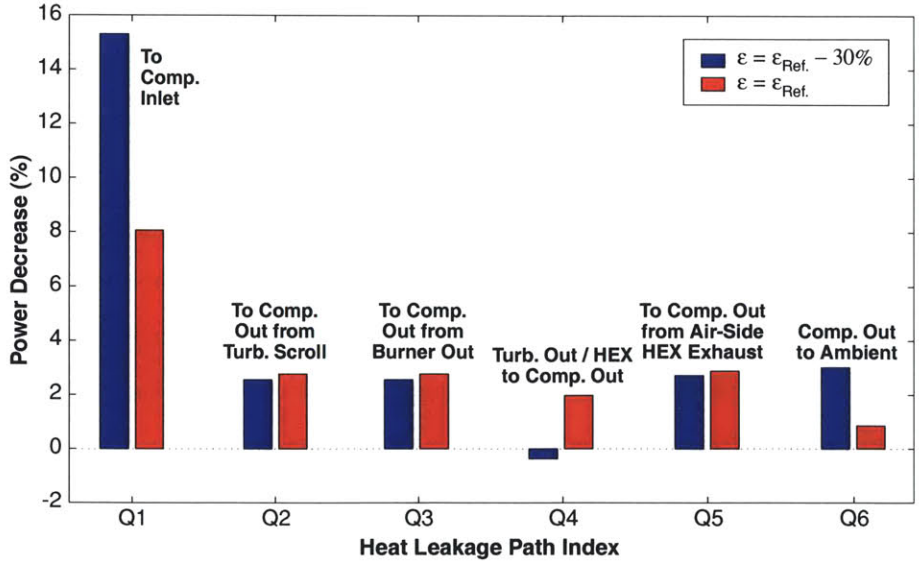

Figure 3-13: Cycle sensitivity to heat transfer.

The cycle is substantially more vulnerable to heat transfer to the compressor inlet from the compressor exhaust (Q1) than it is to heat transfer across any other path. This large impact is due to a combination of effects. As explained in the previous section, heat transfer to the compressor reduces the flow density, which lowers compressor pressure ratio for the same work input and also lowers mass flow capacity. Both of these effects adversely influence power output. Combined with this is the effect of reduced turbine inlet temperature, which also reduces power output.

Sensitivity to heat transfer across paths Q2-Q6 are similar in magnitude. Heat transfer from the turbine scroll (Q2) and combustor exhaust (Q3) to the compressor exhaust both reduce power through a reduction in turbine inlet temperature. Heat transfer from the heat exchanger air-side exhaust to the compressor exhaust (Q5) decreases the temperature differential from the heat exchanger air-side to gas-side. This reduction in temperature differential lowers the heat exchanger heat transfer potential, which in turn lowers power output. Heat transfer from the compressor exhaust to ambient (Q6) is a straightforward loss of enthalpy from the cycle.

The effect on power output of heat transfer from the turbine exhaust to the compressor exhaust (Q4) can be positive or negative, depending upon the heat exchanger effectiveness. If the heat exchanger is highly effective, the overall heat transfer from the gas-side to the air-side is reduced by leakage across Q4. However, if the heat exchanger effectiveness goes below a threshold, the overall heat transfer from the gas-side to the air-side is increased by leakage across Q4. In both cases, heat transfer across Q4 reduces the amount of heat transfer possible inside the heat exchanger itself because the air-side/gas-side temperature differential is reduced. If the reduction in exchanger heat transfer is more than 1 kW (the leakage path heat transfer), there is a net reduction in heat transfer from the air-side to the gas-side, and cycle power drops. If the reduction in exchanger heat transfer is less than 1 kW, there is a net increase in heat transfer from the air-side to the gas-side, and cycle power increases. This balance is controlled by the heat exchanger effectiveness. Figure 3-13 shows a sign change between the impact on power output of Path Q4 for the reference effectiveness and Path Q4 for the reference effectiveness less 30 points.

Although parametric analysis of Dynajet heat leakage paths offers valuable insight to the effect of each on cycle performance, none were identified as unimportant for

consideration. Section 3.3.1 provided an estimate of the total heat transfer across Q1. Section 3.3.3 will do the same for Q2-Q6.

3.3.3 Compressor Exhaust Heat Transfer

Heat transfer to ambient (Q6) was originally assumed to be small, but this hypothesis had to be proved analytically. Q6 can be estimated using an engine-level energy balance. Energy inputs to the system include fuel flow and airflow with specified enthalpy. Energy outputs include exhaust flow with specified enthalpy, electric power, heat from the generator, inverter, and bearings, and Q6. Only Q6 is unknown, so its value can be determined. By this analysis, Q6 is estimated to be less than 1 percent of the ideal shaft power, essentially zero compared to the scale of other heat transfer rates in the engine.

The conclusion that heat transfer to ambient is small was further supported by analysis of the engine case cooling flow shown in Figure 3-14. Data provided by IA suggests that the heat extracted by the cooling flow is 12.7 percent of the ideal shaft power. This value is within 1 point of the estimate for heat produced by the generator, inverter, and bearings, again suggesting that Q6 is negligible.

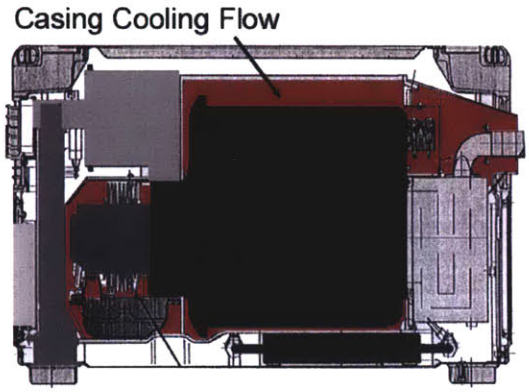

Figure 3-14: Engine case cooling air flow path.

Concern about heat transfer paths Q2-Q5 prompted engine tests with thermocouples reading metal temperatures in the compressor exhaust flow path. Data from these tests are summarized in Figure 3-15. The metal temperatures greatly exceed the compressor exit flow temperature of 491 K, meaning heat transfer must be present.

Using the metal temperature data, CFD was run on the compressor exhaust flow path geometry to estimate heat transfer from the various sources. A total of three viscous incompressible meshes were run in the Navier-Stokes solver Fluent. In all cases, heat

transfer was calculated by fixing the wall temperatures at the data values. Results are shown in Table 3.1. The heat transfer calculated varies between 22.2 percent of ideal shaft power for the small grid (0.3M elements) and 24.7 percent for the large grid (1.5M elements), indicating some grid dependence. However, this range agrees well with the 22.3 percent suggested by the flow temperature data.

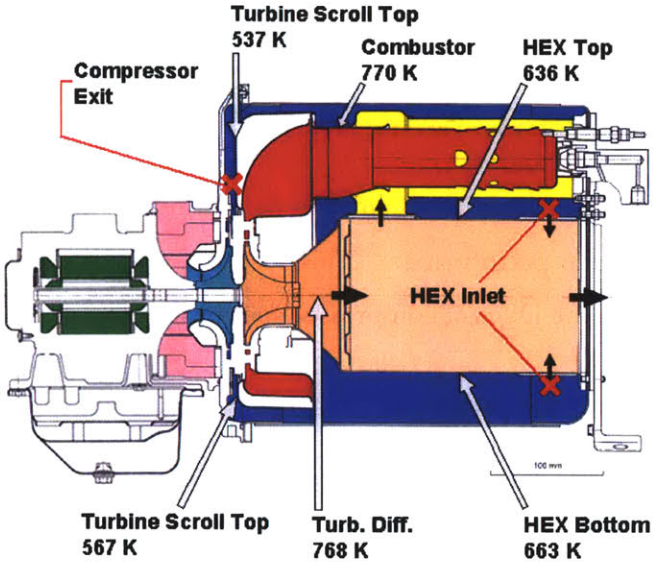

Figure 3-15: Exhaust flow path wall temperatures.

Table 3.1: Compressor exhaust flow CFD results.

	Mesh Elements (Millions)		
	0.3	1	1.5
Inlet Total Temperature (K)	492.5	493.8	493.7
Exit Total Temperature (K)	518.9	520.1	522.5
Delta T (K)	26.4	26.3	28.8
Pressure Ratio (P_{t3}/P_{t2})	0.9974	0.9972	0.9970
Heat Transfer (% of ideal shaft power)			
Combustor Exhaust	1.3	1.4	1.0
Heat Exchanger Air-Side Exhaust	4.6	5.2	5.6
Turbine Exhaust	2.6	2.6	2.9
Turbine Shroud	4.3	4.4	4.3
Heat Exchanger	9.3	9.7	10.9
TOTAL	22.2	23.3	24.7

The CFD results are a valuable source of information for cycle modeling because they set the heat transfer percentages from the various paths:

- Q2: Turbine scroll (17.6% of total heat transfer to comp. exhaust)
- Q3: Combustor exhaust (3.9% of total heat transfer to comp. exhaust)
- Q4: Turbine exhaust / HEX (55.9% of total heat transfer to comp. exhaust)
- Q5: Air-side HEX exhaust (22.6% of total heat transfer to comp. exhaust)

Adjustments to the total compressor exhaust heat transfer can be made while holding these percentages fixed.

3.4 Effects of Flow Nonuniformity

An abundance of gas turbine research has demonstrated an adverse impact of flow nonuniformity on engine performance. This section presents analysis that quantifies the effects of distortion on the Dynajet compressor and turbine.

3.4.1 Compressor Distortion

In Section 3.3.1, uniform heat transfer to the compressor was offered as one possible explanation for the disagreement between rig and engine maps shown in Figure 3-5. However, limiting analysis to the simple case of uniform temperature rise at the inlet requires heat transfer to the compressor that is approximately 25.3 percent of the ideal shaft power. This number is substantial and may not exist in the engine. For this reason, and also because it is good engineering practice to look at multiple alternatives, other explanations were sought. The alternative discussed here is non-uniform heat transfer resulting in thermal inlet distortion. It is first considered to explain the disagreement between the compressor rig and engine maps. Next, it is applied to the April '03 data to provide an alternative to the 19.2 percent of ideal shaft power calculated for uniform heat transfer.

The presence of Dynajet compressor distortion is certain. Figure 3-16 shows the evolution of April '03 thermocouple measurements from the scroll inlet to the impeller inlet. As discussed in Section 3.3, the mean temperature increases by 11.2 K, suggesting heat transfer that is 7.7 percent of the ideal shaft power. What was not discussed is the extent to which the temperature rises nonuniformly. Flow at the top of the impeller inlet that has the shortest scroll residence time is approximately 296 K, or 14 K cooler than the longer residence time flow at the bottom of the impeller inlet. The variation in corrected speed through the compressor inlet is as follows:

- Ambient: 291 K → N_C = 99.5%
- Scroll inlet: 292 K → N_C = 99.3%
- Impeller inlet top: 296 K → N_C = 98.6%
- Impeller inlet bottom: 310 K → N_C = 96.4%

It should be noted that the impeller inlet flow temperatures do not accurately represent the effective compressor corrected speeds. Additional heat addition occurs through the impeller flow path. Through parallel compressor theory, it is possible to estimate this effect.

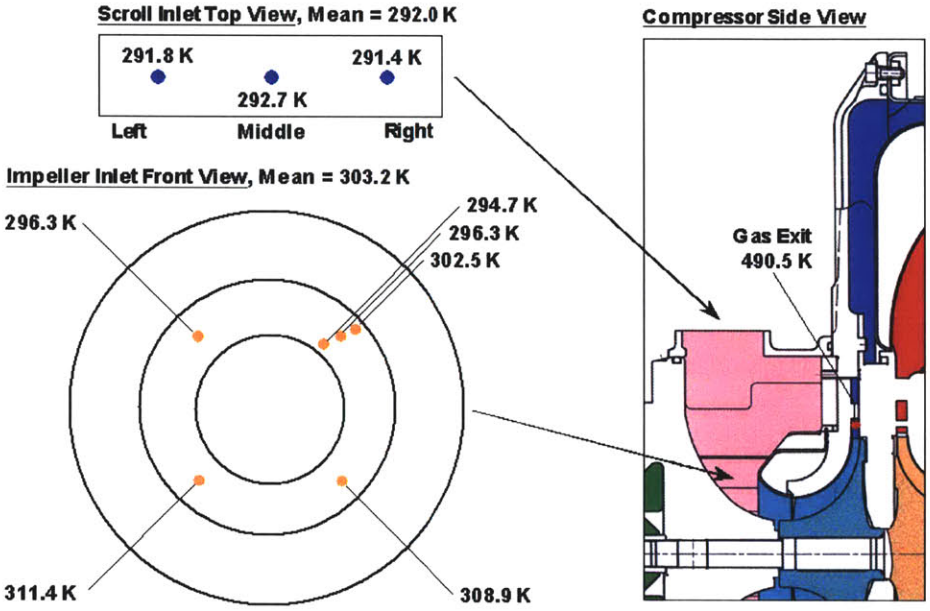

Figure 3-16: Evolution of temperature through the compressor inlet scroll.

Parallel Compressor Theory

Parallel compressor theory is a commonly used analysis tool for compressor inlet distortion [26]. Its application essentially treats a distorted compressor as two compressors operating in parallel with different inlet flow conditions. In the case of the Dynajet, for which thermal distortion is the primary concern, the two compressors operate at different inlet stagnation temperatures.

In its simplest form, parallel compressor theory relies on three assumptions:

1. Static pressure is uniform at the diffuser exit.
2. Circumferential cross-flow within the compressor can be neglected.
3. Distorted and undistorted sectors both operate on the uniform flow performance curve.

Although these assumptions are reasonable approximations of the many flow conditions, they are imperfect and cannot be relied upon to give a highly accurate solution. However, they are sufficient for predicting trends.

Figure 3-17 compares an undistorted compressor to the particular type of distorted compressor under consideration. The undistorted compressor operates at a uniform inlet temperature, but the distorted compressor does not. While the majority of the distorted compressor flow is at the same temperature as the undistorted compressor flow, an arc of specified circumferential extent operates at an elevated temperature. Parallel compressors represent these two sectors of differing temperature.

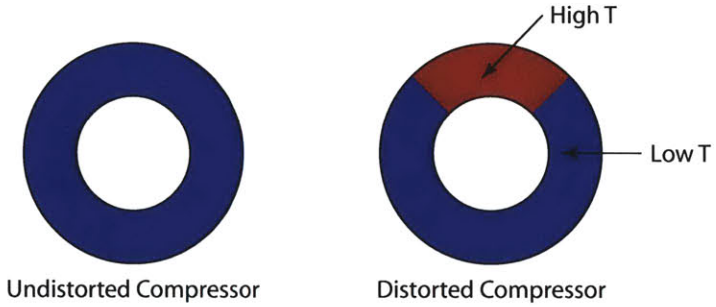

Figure 3-17: Distorted compressor conceptual model for parallel compressor theory.

Applying parallel compressor theory relies on the assumption that the static pressure is uniform at the diffuser exit. Therefore, it was necessary to generate a total-to-static compressor map for the Dynajet. The data shown in Figure 3-5 takes this form; however, the static pressure in this case is well beyond the diffuser exit, and can essentially be considered total pressure. This data was converted to static pressure at the diffuser exit by assuming a diffuser exit swirl angle equal to the metal angle (~30 degrees) and calculating velocity and Mach number from mass conservation and the known stagnation exit conditions.

To perform analysis, assumptions must be made about the inlet conditions. Total pressure at the inlet is assumed uniform and the total temperature of each sector is specified. To fully define the distortion, the circumferential extent of the distortion is specified by a given arc angle.

The general case approach to generating a distorted speed line is demonstrated by Figure 3-18. An initial exit static pressure is selected and the corrected mass flows of the hot and cold sectors are read from the compressor map. Using the specified hot and cold sector areas and temperatures, their respective mass flow rates are determined by Eqs. (3.7) and

(3.8):

$$\dot{m}_H = \dot{m}_{H,Corr} A_H \sqrt{\frac{T_0}{T_H}} \tag{3.7}$$

$$\dot{m}_C = \dot{m}_{C,Corr} A_C \sqrt{\frac{T_0}{T_C}} \tag{3.8}$$

where $\dot{m}_{H,Corr}$ and $\dot{m}_{C,Corr}$ are the hot and cold sector corrected flow rates, A_H and A_C are the hot and cold sector areas, T_H and T_C are the hot and cold flow temperatures, and T_0 is a reference temperature, 288 K. A mass weighted average corrected flow rate is calculated as follows:

$$\dot{m}_{Corr,Mean} = \frac{\dot{m}_C \dot{m}_{C,Corr} + \dot{m}_H \dot{m}_{H,Corr}}{\dot{m}_C + \dot{m}_H} \tag{3.9}$$

The total pressure ratio for each sector is determined from the known static conditions and geometry at the exit of the diffuser. Using continuity and the isentropic relations relating total pressure to static pressure through the Mach number, exit total pressures are determined. The total pressure ratio for the distorted speed line is again a mass weighted average:

$$\pi_{Mean} = \frac{\dot{m}_C \pi_C + \dot{m}_H \pi_H}{\dot{m}_C + \dot{m}_H} \tag{3.10}$$

where π_H and π_C are the hot and cold flow total pressure ratios. By performing these calculations for a range of total to static pressure ratios, a complete distorted speed line is generated. Figure 3-18 shows this progression.

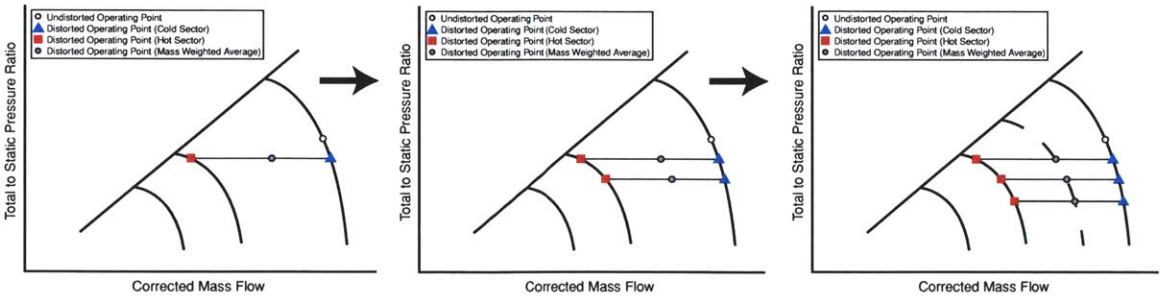

Figure 3-18: Application of parallel compressor theory (adapted from [26]).

Information about heat transfer and efficiency is also an important element of distortion analysis. The heat transfer necessary to provide a specified amount of distortion is given by the steady flow energy equation:

$$\dot{Q} = \dot{m}_H c_p (T_H - T_0) + \dot{m}_C c_p (T_C - T_0) \tag{3.11}$$

To calculate the overall efficiency, the efficiency of each sector must first be determined:

$$\eta_H = \frac{\left(\pi_H^{\frac{\gamma-1}{\gamma}} - 1\right) T_0}{T_{2H} - T_H} \tag{3.12}$$

$$\eta_C = \frac{\left(\pi_C^{\frac{\gamma-1}{\gamma}} - 1\right) T_0}{T_{2C} - T_C} \tag{3.13}$$

where T_{2H} and T_{2C} are the hot and cold flow exit temperatures. The overall efficiency is then calculated as a mass weighted average similarly to Eqs. (3.9) and (3.10).

Applying Parallel Compressor Theory to the Dynajet

In an effort to match the rig and engine maps, 319 K was chosen for the hot sector temperature, which corresponds to 95 percent corrected speed. The reasoning for this choice can be explained with reference to Figure 3-5. To capture the engine data in a distorted speed line, the hot sector speed line must lie at lower mass flows than the engine data. Due to the assumption of matched static pressure at the diffuser exit, the maximum pressure ratio of the hot sector speed line limits the maximum pressure ratio of the distorted speed line. Thus, the hot sector speed line must also lie at or above the level of the engine data. This rules out speed lines much below 95 percent, and the constraint that mass flows be lower than that of the engine data does not offer a choice of higher speed lines, particularly if there is to be much undistorted flow.

One obvious choice for the cold sector temperature is 288 K, or 100 percent corrected speed. As an alternative, 303 K (97.5 percent corrected speed) was also considered. The latter choice requires more heat transfer for equal distortion areas because the cold flow also requires heating.

To justly compare the results of the parallel compressor analysis to the engine speed line, it was necessary to adjust the engine speed line to reflect conditions at the impeller face.

This was done by taking the engine's upstream corrected flow and raising its temperature, and therefore its corrected mass flow, by the appropriate amount determined from the heat transfer of the distorted speed line to which it was compared.

Figure 3-19 shows total-to-total pressure ratio curves for a range of distorted sector fractions as well as the heat transfer necessary for each. The cold sector is at a temperature of 288 K, while the hot sector is at 319 K. The best match between the engine and rig data is achieved by a distortion area of approximately 60 percent, which corresponds to heat transfer that is 13.8 percent of the ideal shaft power. At the total pressure ratio matching data from the engine, distortion reduces the compressor efficiency by 6 points relative to the rig value.

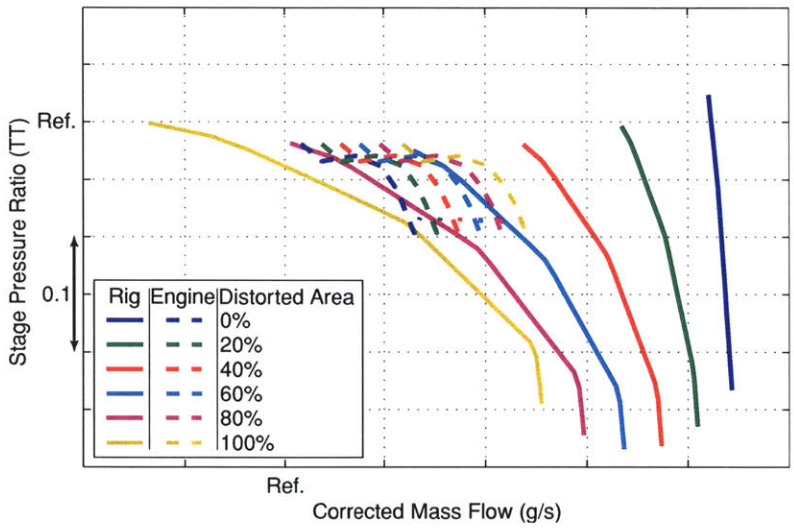

Figure 3-19: Distorted speed lines for a range of distorted areas.

Figure 3-21 and Figure 3-22 show the case of distortion with an elevated cold sector temperature. The cold sector is at a temperature of 303 K, while the hot sector is again at 319 K. The matching case for this distortion variation is a distorted area of approximately 40 percent, which corresponds to heat transfer that is 16.9 percent of the ideal shaft power. This heat flux is slightly higher than the unheated cold flow result of 13.8 percent. Thus, there appears to be more performance penalty per unit of heat transfer if the heat is concentrated within a small circumferential area.

An estimate of the nonuniform heat transfer necessary to reconcile the April '03 engine data with rig data can also be achieved with parallel compressor theory. Figure 3-23 shows the April '03 compressor operating point overlaid on the compressor rig map with

speed lines interpolated in one-half percent increments between 95 percent and 100 percent. The best matches of April '03 data to distorted rig data are achieved with a hot sector corrected speed of 95.8 percent. Figure 3-24 shows distorted results with this hot sector corrected speed against a range of cold sector corrected speeds. The upper left plot shows the percent difference between the distorted solution and engine data, and the upper right plot compares the distorted solution pressure ratio to the reference pressure ratio from engine data. Both plots indicate a decent match of the distorted solution to engine data over the entire range. The corresponding effective distorted efficiency is approximately 5.7 points below the rig value, while the heat transfer is 16.9 percent of the ideal shaft power.

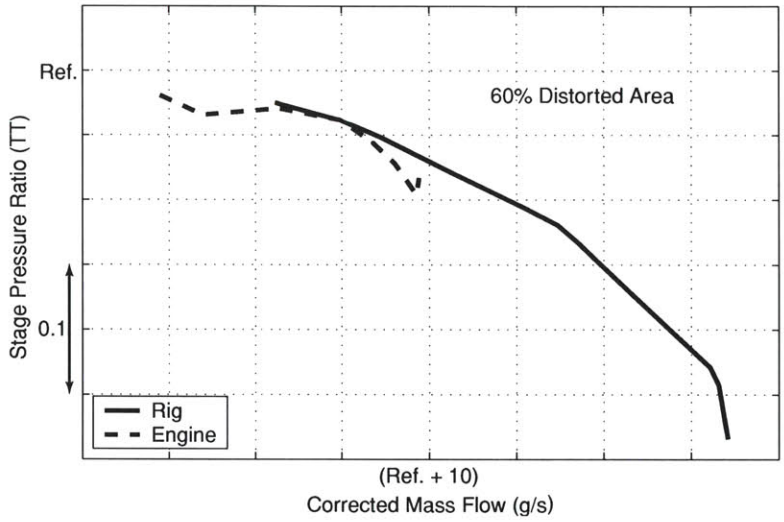

Figure 3-20: Sixty-percent distorted area speed line with matching engine data.

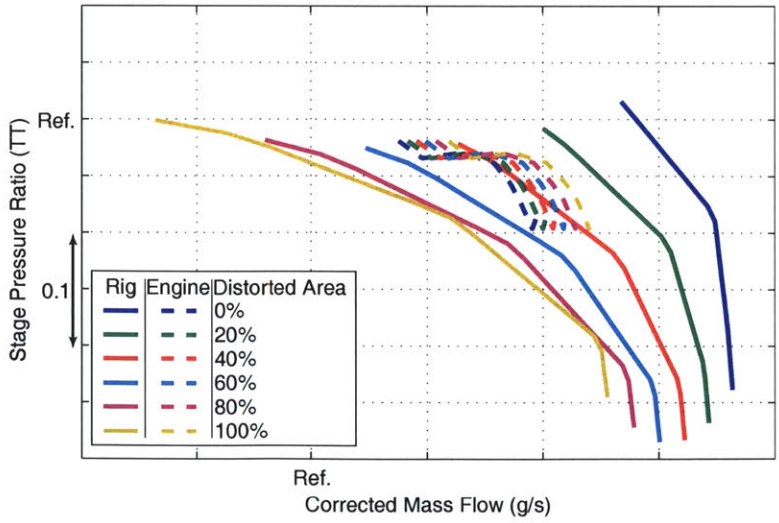

Figure 3-21: Distorted speed lines for a range of distorted areas at an elevated cold sector temperature.

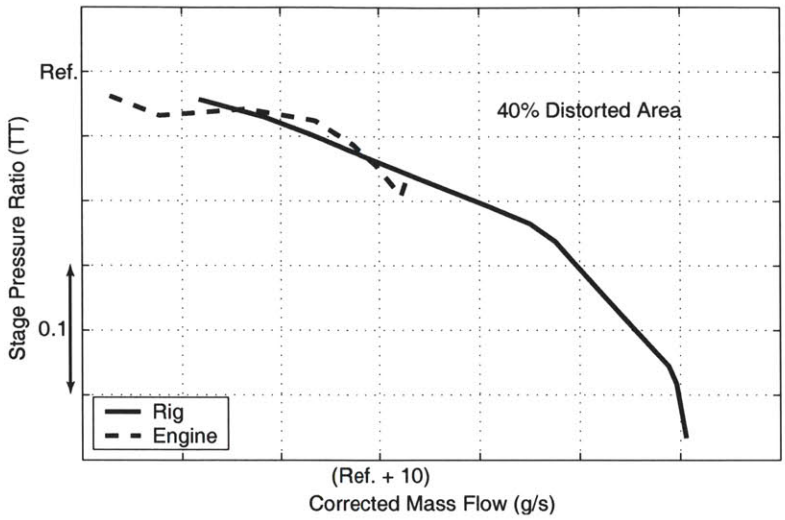

Figure 3-22: Forty-percent distorted area speed line for elevated cold sector temperature with matching engine data.

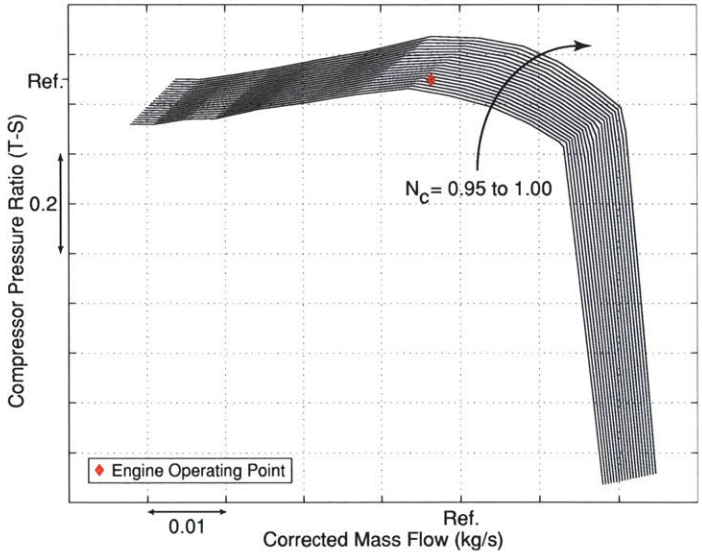

Figure 3-23: Dynajet compressor rig map with engine operating point.

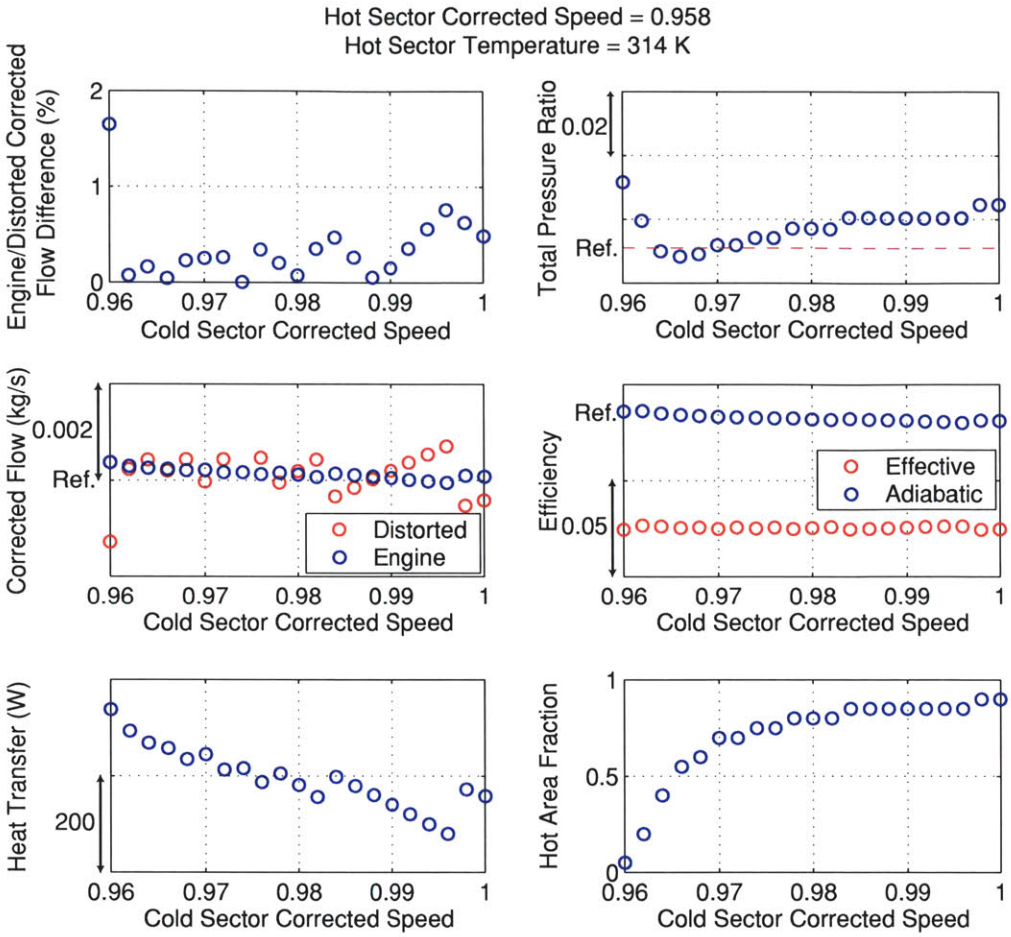

Figure 3-24: Distorted compressor analysis match to engine data for a hot sector corrected speed of 0.958 and a range of cold sector corrected speeds.

Model Consistency Check

A number of checks were carried out to verify that the parallel compressor analysis performed was self-consistent. For the 0 and 100 percent distorted area cases, the operating curves produced should exactly overlap the 100 percent (or 97.5 percent speed line for the elevated cold flow temperature case) and 95 percent rig speed lines, respectively. Figure 3-25 and Figure 3-26 show this to be true.

Compressor Distortion Summary

Uniform heat transfer to the Dynajet compressor equal to 25.4 percent of the ideal shaft power is necessary to reconcile the rig and engine maps. However, simple analysis of thermal inlet distortion using parallel compressor theory suggests that the heat required can be as little as 13.8 percent of the ideal shaft power if it is applied non-uniformly. Thus, inlet

distortion does in fact lower the required heat addition compared to the uniform flow case. The exact amount of heat transfer required is influenced by the distortion pattern. Performance penalty is inversely proportional to the area over which the heat is applied.

A similar relationship was found in reconciling the April '03 data with rig data. Applied uniformly, heat transfer equal to 19.2 percent of the ideal shaft power is required to attain a match. With distortion, the required heat transfer is 16.9 percent of the ideal shaft power.

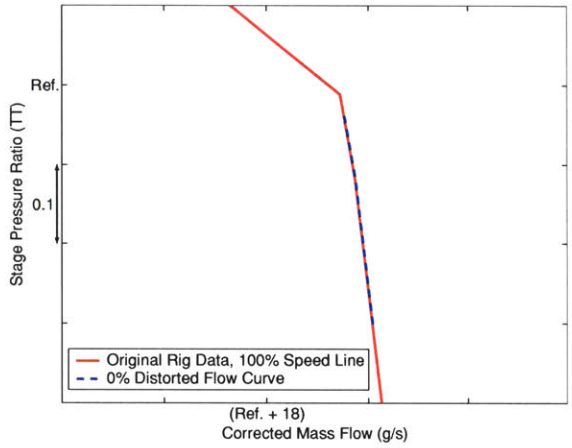

Figure 3-25: Parallel compressor model consistency check at 0% distorted area.

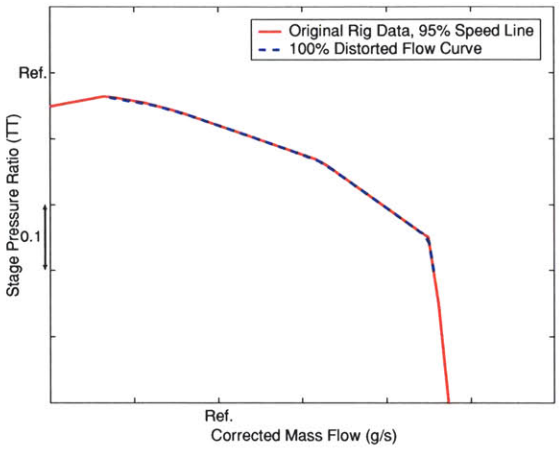

Figure 3-26: Parallel compressor model consistency check at 100% distorted area.

3.4.2 Turbine Distortion

Like flow into the compressor, flow into the turbine is three-dimensional in nature. Figure 3-27 shows isometric and side views of the turbine impeller and inlet scroll. At the scroll inlet, the flow has a temperature distribution given by the combustor exit pattern factor. This temperature nonuniformity is carried by complex three-dimensional flow to the impeller inlet guide vanes.

The goal of turbine distortion analysis is to determine the importance of flow nonuniformity. Does distorted inflow to the turbine cause a performance penalty relative to operation with the same mass-averaged uniform flow? If so, what level of distortion is necessary for this effect to become important? This section will show that the answers to both questions depend significantly upon the turbine map and level of distortion under consideration. However, distortion is likely to have at least some negative impact on performance.

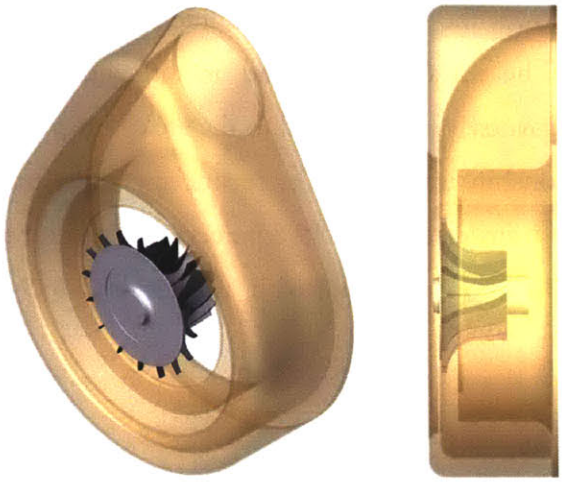

Figure 3-27: Isometric and side views of turbine inlet scroll and impeller.

Degree and Cause of Dynajet Turbine Distortion

April '03 distortion data recorded by thermocouples on the turbine nozzle guide vane (NGV) leading edges is shown in Figure 3-28. The temperature range is quite large, extending 50 K above and below the mean, reference value.

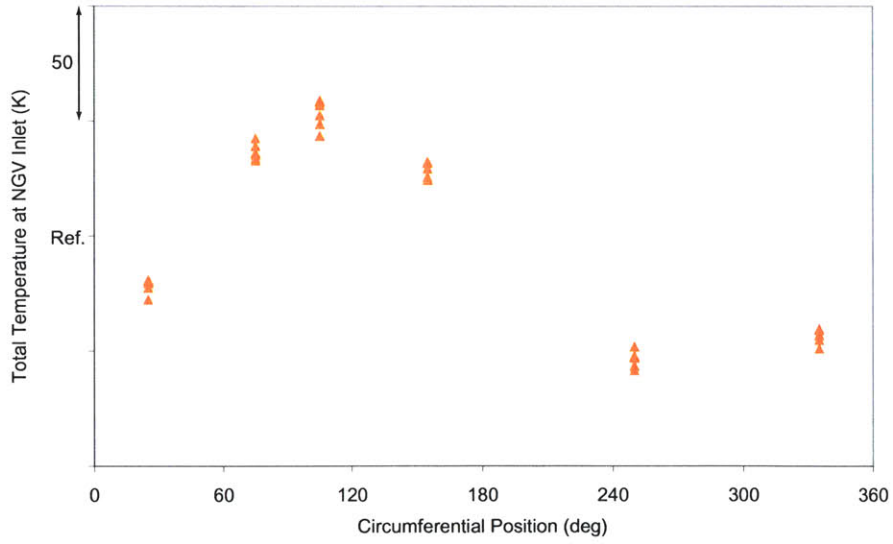

Figure 3-28: Nozzle guide vane temperature measurements showing distortion.

The engine data is useful for demonstrating the thermal distortion at the inlet to the turbine; however, it offers no insight regarding how this distortion appears. To establish this understanding, CFD analysis of the turbine scroll was performed.

A geometric model of the turbine scroll was created in SolidWorks and exported to Gambit for mesh generation. To reduce the required mesh size, the geometry's vertical

symmetry was used to allow consideration of only half the volume. An unstructured mesh was created using tetrahedral/hybrid elements defined in two zones as shown in Figure 3-29. A dense mesh was imposed in the narrow passage that contains the NGVs, while a coarser mesh was imposed in the remaining volume.

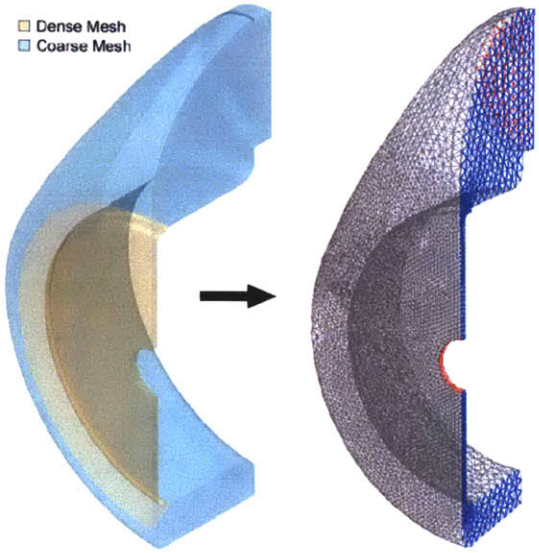

Figure 3-29: Turbine scroll mesh zones.

Fluent was used to execute the computational analysis. Boundary conditions were set to model the true operating conditions. At the inlet to the scroll, a "pressure inlet" boundary condition was imposed and used with a varied set of parabolic total temperature profiles (temperature varying with the square of the passage radius). Such profiles are typically assumed at combustor exits.

At the scroll exit, a "pressure outlet" boundary condition was set. Static pressure was specified to give the appropriate mass flow. Due to streamline curvature in the scroll, the static pressure is not uniform at the NGV inlet. Thus, to allow nonuniformity at the NGV while still using the pressure outlet, the exit boundary was artificially moved radially inward as shown in Figure 3-30.

In Fluent, a fully three-dimensional, double precision, coupled explicit solver was used. Flow compressibility and viscosity were accounted for using ideal gas and k-ε turbulence models, respectively. Results for a baseline geometry mesh are shown in Figure 3-31 through Figure 3-34. The characteristics of this baseline are summarized under Test Case 1 in Table 3.2. The test case uses a parabolic temperature profile at the inlet with a

mean temperature 100 K above the reference turbine inlet temperature and amplitude of 100 K.

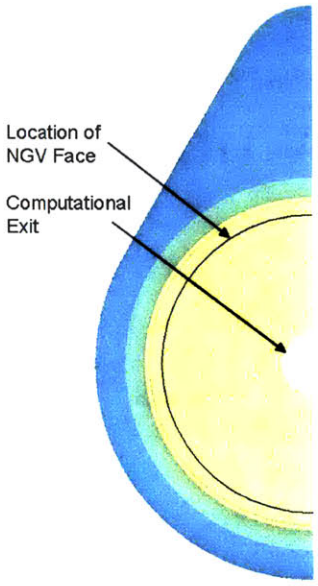

Figure 3-30: Physical and computational boundaries of turbine scroll.

Figure 3-31 shows velocity vectors for the full geometry colored by total temperature. From the coloring, it is evident that the hot core flow follows a path out of the scroll through the upper half of the exit, while the cool outer flow leaves through the lower half of the exit. Figure 3-32 zooms in on a recirculation zone past the lip of the scroll inlet duct. The Fluent calculations were initially run inviscidly, but numeric instability in the separation zone led to the use of a viscous model. Figure 3-33 shows how the temperature profile at the scroll inlet develops along the geometry midplane. There is some mixing, but not enough to eliminate the temperature nonuniformity before the NGV inlet. This is reflected in Figure 3-34. A 200 K temperature spread at the scroll inlet is reduced to 100 K at the NGV inlet.

There was difficulty encountered converging the governing equation residuals. Figure 3-35 shows, for example, that the continuity and energy residuals only dropped by one order of magnitude. This poor convergence may be due to the complexity of the flow. Despite weak residual convergence, mass flow calculations at the inlet and exit agreed within 1.7 percent and converged to the expected value (see Figure 3-36 and Figure 3-37). The CFD results are sufficient to discern fundamental flow physics and the temperature profile shape at the NGV inlet. A highly accurate solution is not necessary for this problem.

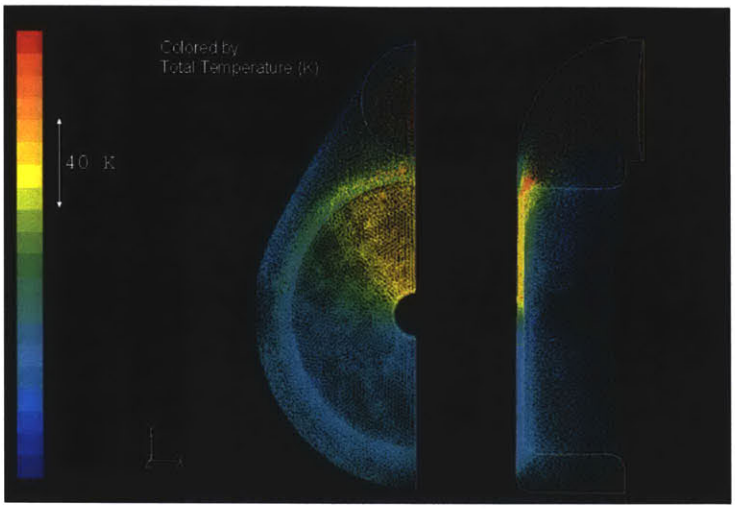

Figure 3-31: Turbine scroll velocities colored by total temperature.

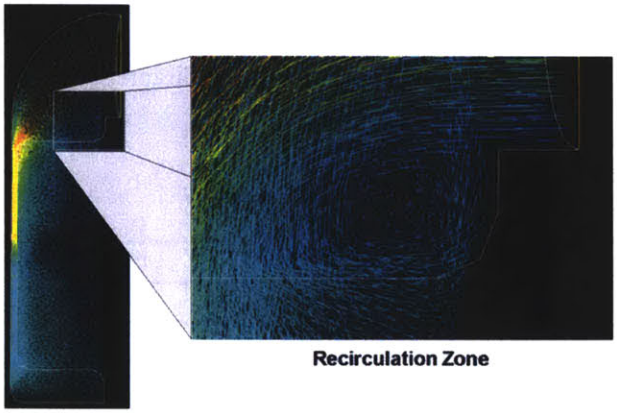

Figure 3-32: Turbine scroll recirculation zone.

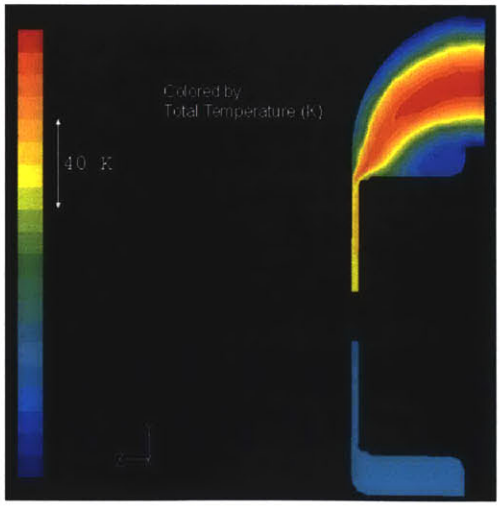

Figure 3-33: Turbine scroll total temperature profile.

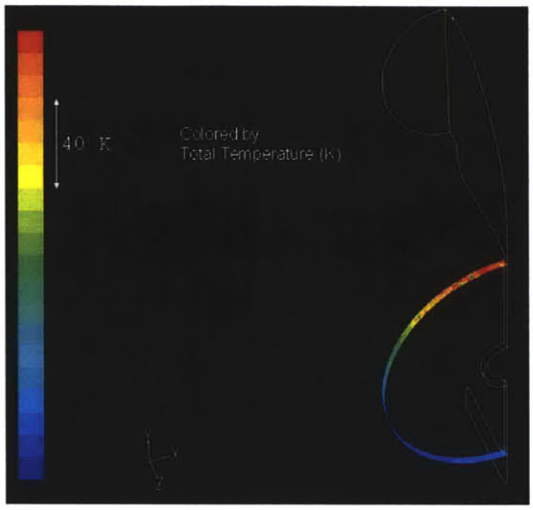

Figure 3-34: Total temperature profile at NGV inlet face.

Table 3.2: CFD test case characteristics.

Test Case	Number of Elements	Exit Radius (mm)	Mean Inlet Temperature (K)	Inlet Temperature Amplitude (K)
1	64712	12.28	Ref. + 100	100
2	64712	12.28	Ref. + 100	50
3	64712	12.28	Ref.	100
4	382171	12.28	Ref. + 100	100
5	67207	12.18	Ref. + 100	100

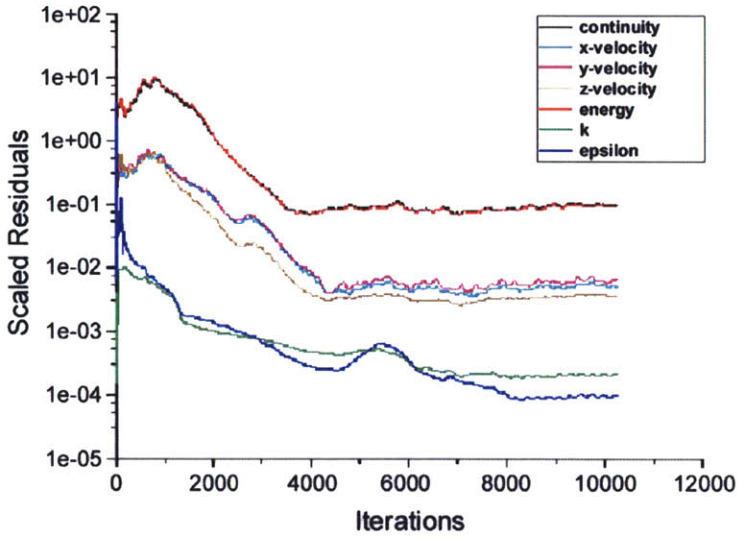

Figure 3-35: Test Case 1 scaled residuals.

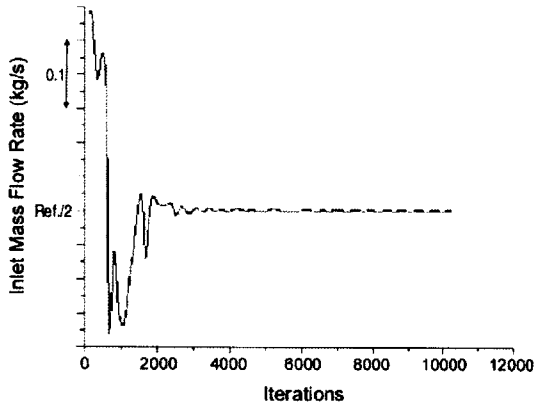

Figure 3-36: Test Case 1 inlet mass flow convergence.

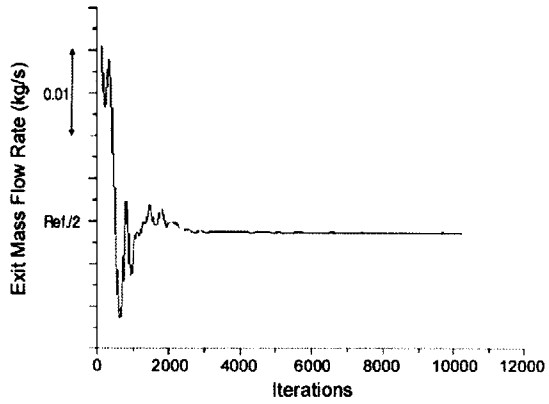

Figure 3-37: Test Case 1 exit mass flow convergence.

The temperature profile at the NGV inlet for the baseline Fluent case (Test Case 1) is shown in Figure 3-38. The figure graphically shows the aforementioned observation that the core flow from the combustor feeds the upper half of the NGV, while the outlying flow feeds the lower half. This leads to a temperature peak at the top of the NGV (90 degrees) and considerably cooler temperatures on the opposite side.

Figure 3-38 also shows four other Fluent cases, the parameters for which are summarized in Table 3.2. From these additional cases, the effects of inlet temperature amplitude (2), mean inlet temperature (3), mesh density (4), and exit radius (5) can be observed. The Case 2 temperature amplitude at the scroll inlet is half that of Case 1, and this factor appears to remain the same at the NGV inlet: Case 1 has a temperature range of approximately 100 K at the NGV inlet, while Case 2 has range of approximately 50 K. The mean temperature at the scroll inlet is roughly the same as that at the NGV inlet. This is shown by all five cases. Test Case 4 shows that mesh density changes have a slight effect the temperature profile magnitudes, but the overall trend remains unchanged. Finally, Test Case 5 shows that the radius of the exit does not have a significant impact on the solution.

The static pressure profile at the NGV inlet is shown in Figure 3-39 normalized by the turbine exit dynamic pressure based on the wheel tip speed. The static pressure nonuniformity is small. This plot also shows reasonable agreement between the five test cases. Cases 1, 2, 4 and 5 should and do lie very close to each other. For the same total pressure and mass flow, Case 3 must have higher static pressures since its total temperature is lower. This is also reflected in the plot.

Case 3 was chosen to closely agree with the Dynajet data, and it does so. Exclusive consideration of this result leads to the conclusion that the combustor exit profile has amplitude of 100 K.

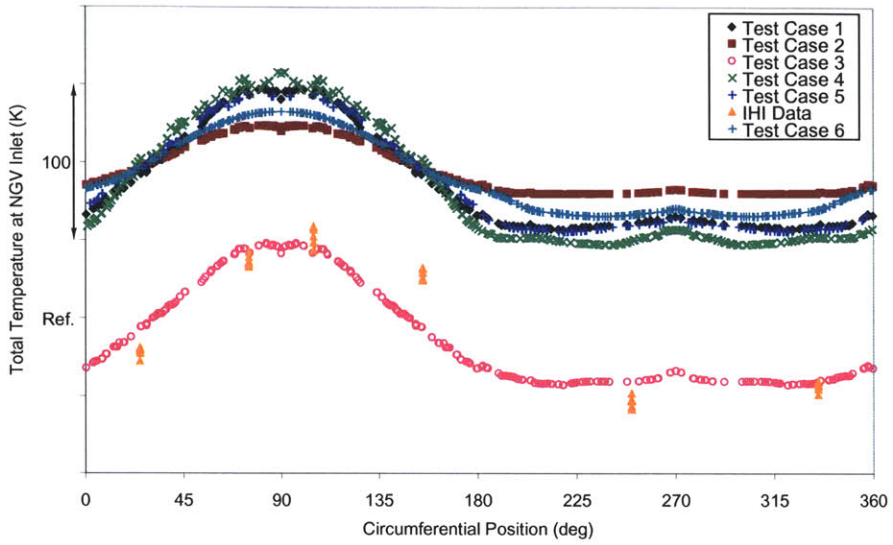

Figure 3-38: CFD test case temperature profiles at NGV inlet.

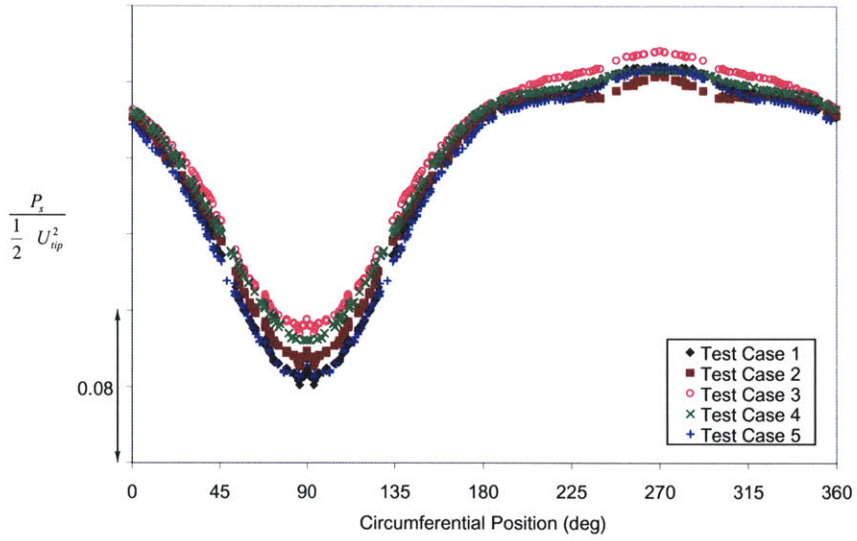

Figure 3-39: CFD test case static pressure profiles at NGV inlet.

Parallel Turbine Model

To the best of the author's knowledge, there is no formally published parallel turbine theory. The model used here is an adaptation of parallel compressor theory. The same three assumptions are made:

1. Static pressure is uniform at the impeller exit.

2. Circumferential cross flow within the turbine can be neglected.
3. Distorted and undistorted sectors both operate on the uniform flow performance curve.

However, unlike the compressor, the turbine does not terminate with a vaned diffuser and large plenum. Rather, it terminates with rotating impeller blades that create an unsteady, nonuniform pressure field. Thus, a more detailed argument for assuming uniformity in analysis is required.

Greitzer performed analysis of the effect of asymmetric flow on turbomachinery exit static pressure distributions [27] that is useful to review here. He found the pressure and velocity perturbations at the impeller exit due to a nonuniform upstream distribution are given by:

$$P' = -\rho i U \xi e^{\left[-\frac{nx}{r}+i(n\theta-\sigma t)\right]} \tag{3.14}$$

$$C_x'\big|_{x=0} = \xi e^{[i(n\theta-\sigma t)]} \tag{3.15}$$

where ρ is the upstream mean density, U is the disturbance propagation speed, ξ is magnitude of the axial velocity maldistribution at the exit, n is the harmonic number of the Fourier component of the maldistribution, σ is the circular frequency of the nonuniformity, r is the mean annulus radius, x is the axial coordinate, θ is the circumferential coordinate, and t is time.

In the impeller reference frame, a steady circumferential pressure distribution in the absolute frame is seen as an unsteady disturbance that propagates at the impeller speed. As applied to Eq. (3.14), this means U equals the impeller speed. Given that the impeller speed is of the same order of magnitude as the axial flow velocity, a simple Bernoulli argument shows that the pressure distribution downstream of the impeller is the same order of magnitude of that upstream. The relevance of this fact to the parallel turbine model is in deciding whether the static pressure nonuniformity downstream can be neglected. The upstream static pressure perturbation calculated for the turbine distortion discussed in the previous section is negligible compared to the mean static pressure. This suggests that the pressure perturbation downstream is small.

Additional support for neglecting downstream pressure distribution can be found in comparing it to the velocity distribution. The relationship of streamline curvature to

pressure causes the velocity perturbation to be 90 degrees out of phase with the pressure perturbation. This fact is captured in Eqs. (3.14) and (3.15) and is shown graphically in Figure 3-40. Due to the phase lag, the mean pressure perturbation for each peak and trough of the velocity perturbation curve is the same, zero. The velocity perturbation curve peaks and troughs represent the different distortion sectors. Thus, each distortion sector has the same mean static pressure at the impeller exit.

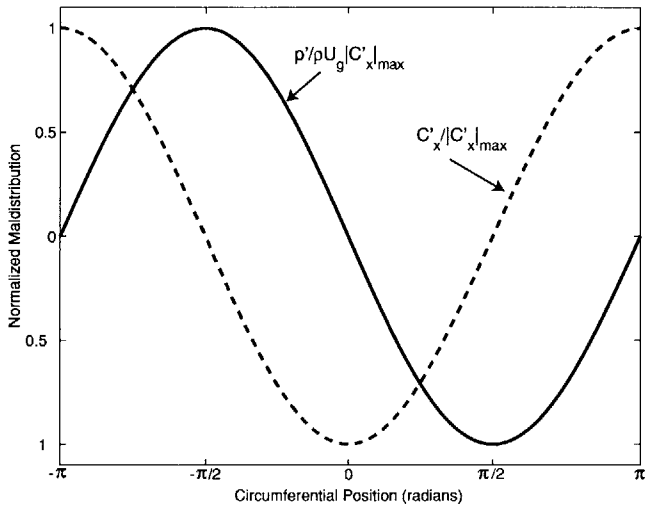

Figure 3-40: Static pressure and axial velocity nonuniformity at compressor exit (normalized) [27].

The static pressure at the impeller exit can be reasonably approximated as uniform for application of a turbine distortion model. Two arguments support this assertion. First, the magnitude of distribution nonuniformity is small. Second, the mean pressure distribution for each sector of distortion is the same due to a phase lag between pressure and velocity disturbances.

Applying the Parallel Turbine Model

When this research began, a turbine map for the Dynajet did not exist. To determine the value of attempting to generate one, the impact of distortion on other turbines was considered first.

The map for a small radial turbine provided by IA is shown in Figure 3-41. The approach taken to determine its susceptibility to distortion was to compare uniform flow performance on the 100 percent corrected speed line with performance of parallel turbines operating on two different speed lines, one hot and one cold. The 90 percent and 120

percent speed lines were chosen for hot and cold, respectively. Since most turbine rig tests are run at room temperature, a temperature of 288 K was assumed for the 100 percent speed line. This places the hot and cold speed lines at 356 K and 200 K.

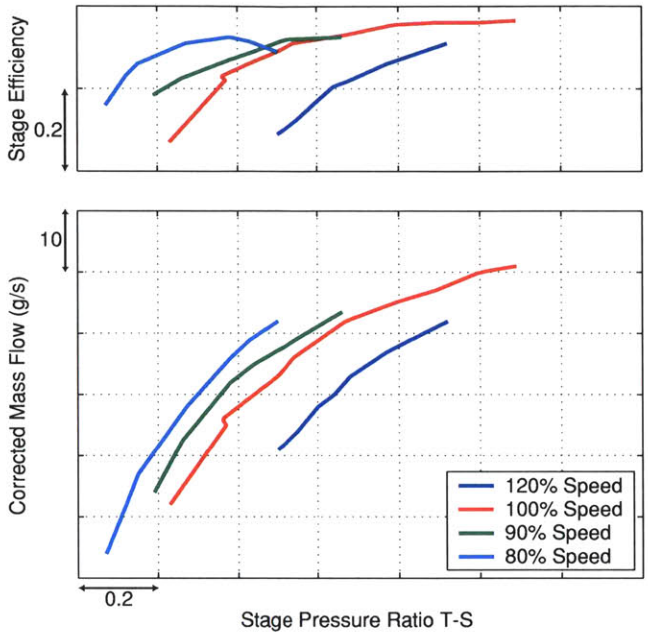

Figure 3-41: Small radial turbine map example.

The driving constraint on the distorted speed line is that its mass-averaged temperature equal that of the 100 percent speed line, 288 K. Energy must be conserved by any distortion present. Eq. (3.16) expresses this requirement:

$$T_0 = \frac{\dot{m}_H T_H + \dot{m}_C T_C}{\dot{m}_H + \dot{m}_C} \tag{3.16}$$

The distorted flow must also conserve mass:

$$\dot{m}_{Total} = \dot{m}_H + \dot{m}_C \tag{3.17}$$

Three additional equations express the corrected flow rates of the hot and cold sectors and their contributions to the total flow area:

$$\dot{m}_{H,Corr} = \frac{\dot{m}_H \sqrt{T_H / T_0}}{A_H} \tag{3.18}$$

$$\dot{m}_{C,Corr} = \frac{\dot{m}_C \sqrt{T_C / T_0}}{A_C} \tag{3.19}$$

$$A_H + A_C = 1 \tag{3.20}$$

Of the variables, A_H, A_C, $\dot{m}_H$, $\dot{m}_C$, and $\dot{m}_{Total}$ are unknown. There are five equations and five unknowns, so the system can be solved to fully define the circumferential areas and flow rates of the hot and cold sectors.

To determine the effect of distortion on power, it is necessary to determine its effect on efficiency. The exit temperatures of the hot and cold sectors are given by:

$$T_{2,H} = T_H\left[1-\eta_H\left(1-\pi^{\frac{\gamma-1}{\gamma}}\right)\right] \tag{3.21}$$

$$T_{2,C} = T_C\left[1-\eta_C\left(1-\pi^{\frac{\gamma-1}{\gamma}}\right)\right] \tag{3.22}$$

By taking their mass-average and calculating a mean temperature ratio, a mean efficiency can be determined:

$$T_{2,Mean} = \frac{\dot{m}_H T_{2,H} + \dot{m}_C T_{2,C}}{\dot{m}_H + \dot{m}_C} \tag{3.23}$$

$$\tau_{Mean} = \frac{T_{2,Mean}}{T_0} \tag{3.24}$$

$$\eta_{Mean} = \frac{1-\tau_{Mean}}{1-\pi^{\frac{\gamma-1}{\gamma}}} \tag{3.25}$$

Figure 3-42 shows the impact of turbine distortion on efficiency. The distorted efficiency is approximately 5 points less than the undistorted. Figure 3-43 shows the impact of turbine distortion on flow rate. For equal pressure ratios, the distorted turbine passes less flow than the undistorted turbine. Reductions in efficiency and mass flow both contribute negatively to turbine power. Figure 3-44 shows that the distorted turbine produces approximately 250 W less power than the undistorted turbine. Note, however, that combining reductions in efficiency and mass flow to determine a power reduction is purely academic. In an engine, matching would have to be considered.

For comparison, parallel turbine analysis was also performed on a Cummins turbine map found in Japikse [28] and shown in Figure 3-45. Figure 3-46, Figure 3-47, and Figure 3-48 show this turbine's distorted performance under one particular operating condition.

The solid black lines are at a corrected speed of 35,000 RPM, while the dashed red lines are for the same mass-averaged total temperature at distorted corrected speeds of 30,000 RPM and 40,000 RPM. Similarly to the IA turbine, Figure 3-46 shows that the Cummins turbine efficiency is reduced by distortion. However, Figure 3-47 shows that the turbine's mass flow is actually increased by distortion. The combined effects of efficiency and mass flow lead to essentially zero difference in turbine power output between the distorted and undistorted cases. Figure 3-48 demonstrates this result.

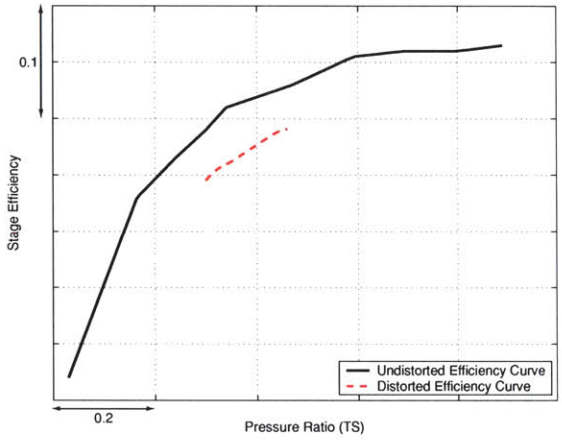

Figure 3-42: Comparison of distorted flow efficiency to uniform flow efficiency for small IA radial turbine.

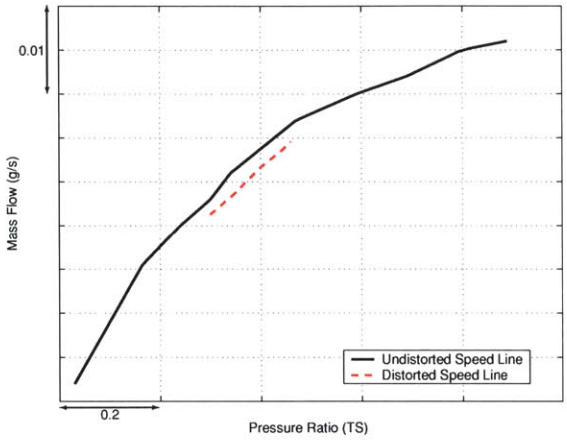

Figure 3-43: Comparison of distorted mass flow to uniform mass flow for small IA radial turbine.

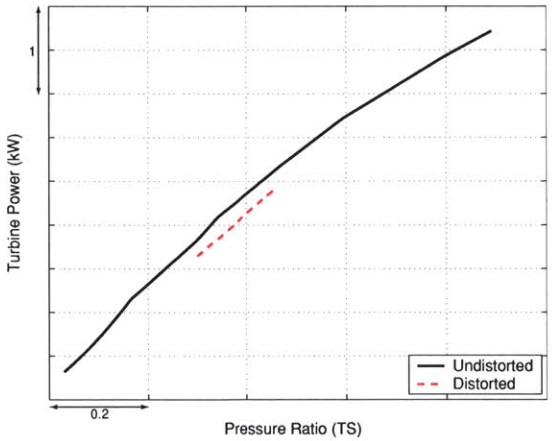

Figure 3-44: Comparison of distorted flow efficiency to uniform flow efficiency for small IA radial turbine.

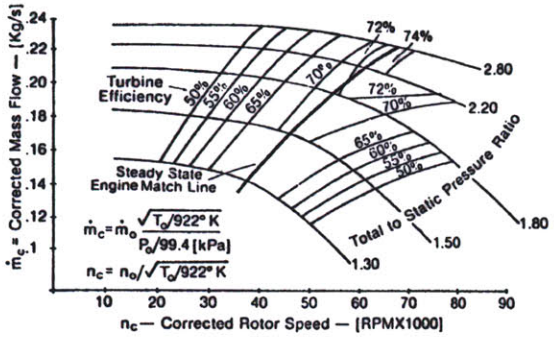

Figure 3-45: Cummins radial turbine map [28].

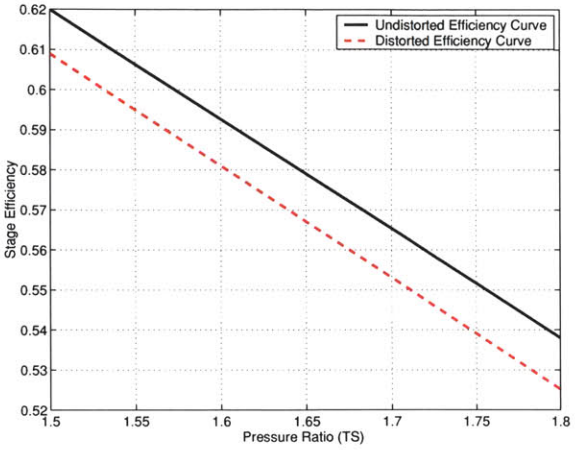

Figure 3-46: Comparison of distorted flow efficiency to uniform flow efficiency for Cummins radial turbine.

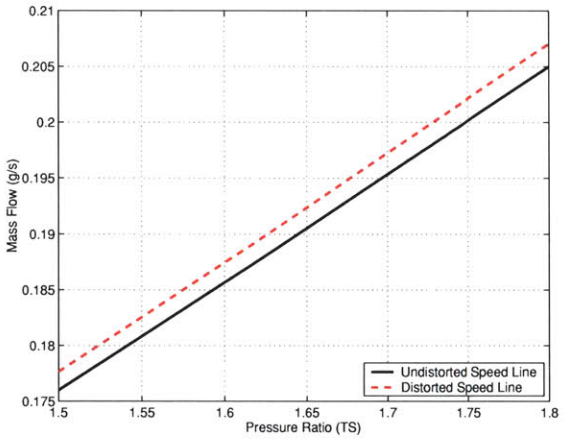

Figure 3-47: Comparison of distorted mass flow to uniform mass flow for Cummins radial turbine.

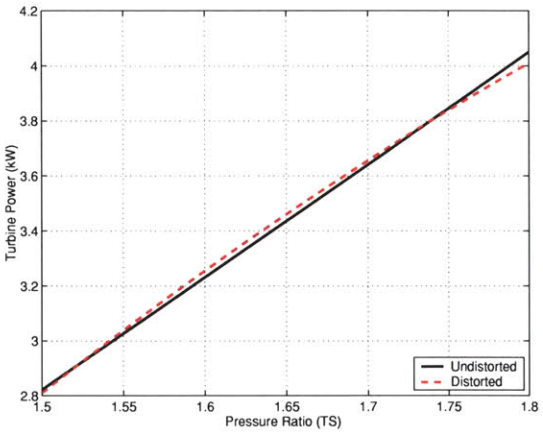

Figure 3-48: Comparison of distorted flow efficiency to uniform flow efficiency for Cummins radial turbine.

The turbine map under consideration strongly influences the result of distortion analysis. While both the IA turbine and the Cummins turbine show reduced efficiency with distortion, they show opposite trends in mass flow adjustment. Thus, the impact of distortion on their overall power output is quite different.

Dynajet Turbine Distortion Analysis

As a result of showing that distortion can negatively impact turbine performance and, further, that the impact is largely dependent on the map under consideration, engineers at IA generated an approximate map for the Dynajet based on available data to test its unique susceptibility to distortion. The map is shown in Figure 3-49. Red circles indicate existing

IA turbine performance data, while the solid black lines are IA speed line estimates. The blue square represents the design point.

The approach taken to locating the April '03 operating point on the map was to interpolate speed lines and find the one that gave the best match to the data mass flow rate and pressure ratio. The result was a corrected speed of 101 percent relative to the design corrected speed, which corresponds to efficiency 2.5 points below the reference (design and rig) value.

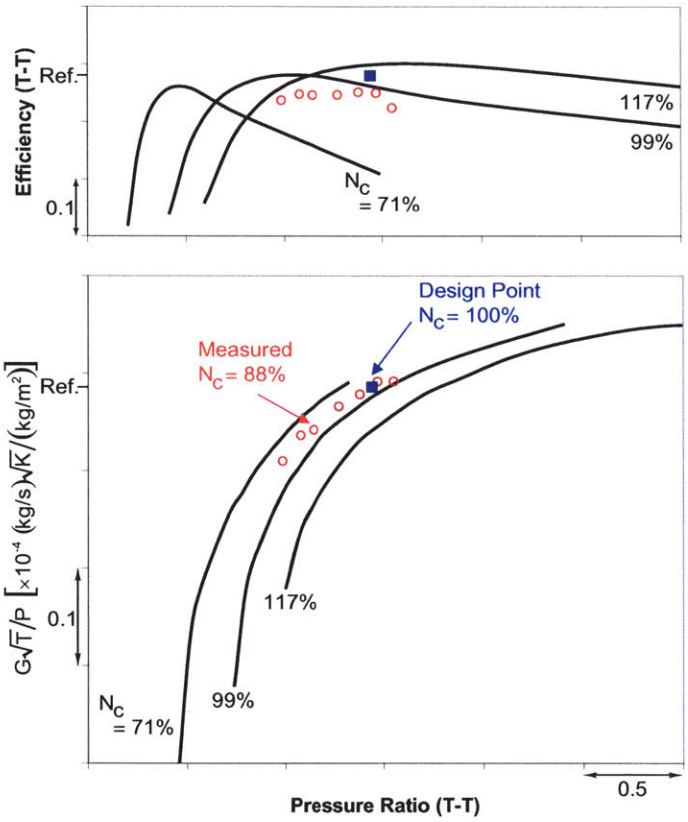

Figure 3-49: Dynajet turbine map estimated from data.

For distortion analysis, speed lines 50 K above and below the 101 percent speed line were chosen to simulate the distortion indicated by data. The distortion lowers efficiency by one-half point relative to the aforementioned undistorted estimate from the map. Thus, the distorted turbine efficiency is a total of 3 points below the reference efficiency.

Turbine Distortion Summary

Through the development of a parallel turbine model, an understanding of the thermal flow distortion impact on turbine performance was sought. The goal was to determine whether

distorted flow performance is the same as performance under the equivalent mass-averaged uniform flow.

For the cases studied, analysis determined that distorted performance is in fact worse than the mass-averaged uniform flow performance. However, the extent of the performance penalty depends greatly on the particular turbine map under consideration. It was further determined by CFD analysis and experimental data that the Dynajet does have turbine thermal distortion of approximately 50 K above and below the mean temperature. Parallel turbine analysis of an approximate Dynajet turbine map provided by IA found that this distortion reduces efficiency by one-half point.

3.5 Flow Leakage

Flow leakage was the last nonideality considered in the course of Dynajet cycle research. Despite late consideration, this section will show that the magnitude of flow leakage is great, and Section 3.7.1 will show that its impact on performance is significant.

Leakage is known to exist in the Dynajet at three locations shown in Figure 3-50. Leakage 1 (L1) occurs between the compressor exhaust and the slip fit that joins the combustor exhaust pipe to the turbine scroll. Leakage 2 (L2) occurs between the compressor exhaust and the air-side heat exchanger exhaust through the flange connecting it to the heat exchanger. Leakage 3 (L3) occurs between the compressor exhaust and the air-side heat exchanger exhaust through another slip fit piping attachment.

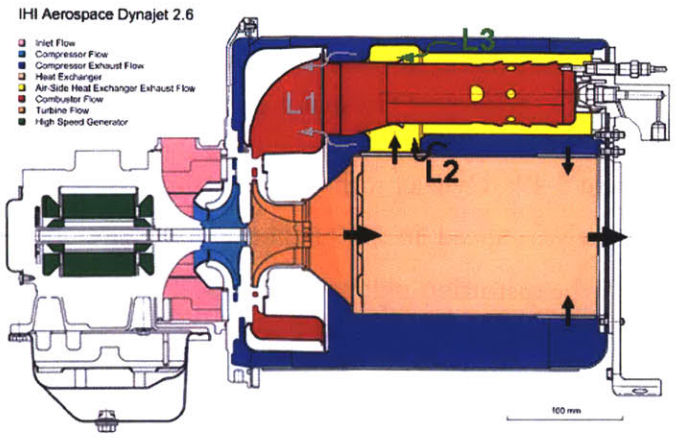

Figure 3-50: Dynajet flow leakage paths.

IA conducted tests to quantify leakage at off-design conditions. To estimate the operating leakage from test leakage, a seal leakage calculation method outlined by Meyer and Lowrie [29] was applied and is described here. Seal mass flow is calculated as follows:

$$\dot{m} = \left(\frac{\dot{m}_i}{\dot{m}_c}\right)(\dot{m}_c)C_D \tag{3.26}$$

where m_i is the ideal flow, m_c is the ideal critical flow, and C_D is the seal discharge coefficient. The ratio of ideal flow to ideal critical flow can be expressed in terms of ideal and critical ideal velocities and specific volumes, which can in turn be expressed in terms of ideal Mach number:

$$\frac{\dot{m}_i}{\dot{m}_c} = \frac{V}{V_c}\frac{v_c}{v} \tag{3.27}$$

$$\frac{\dot{m}_i}{\dot{m}_c} = M_i\left(\frac{1+\frac{\gamma-1}{2}M_i^2}{1+\frac{\gamma-1}{2}}\right)^{\frac{1}{\gamma-1}} \tag{3.28}$$

The critical ideal mass flow can be alternatively expressed as follows:

$$\dot{m}_c = AP_{t1}K \tag{3.29}$$

where A is the seal area, P_{t1} is the seal inlet total pressure, and K is a tabulated value that varies with the fluid type and temperature. Combining Eqs. (3.26), (3.28), and (3.29), it is possible to express the seal mass flow as follows:

$$\dot{m} = M_i\left(\frac{1+\frac{\gamma-1}{2}M_i^2}{1+\frac{\gamma-1}{2}}\right)^{\frac{1}{\gamma-1}} P_{t1}K\underbrace{AC_D}_{Constant} \tag{3.30}$$

Using Eq. (3.30), test data may be used to solve for AC_D, a constant. Knowing this, it then becomes possible to solve for the leakage at any operating condition knowing only the seal inlet total temperature, seal inlet total pressure, and seal pressure ratio.

Using this method, IA off-design leakage data for L1 and L2 were used to estimate corresponding leakage at engine operating conditions. The estimated L1 leakage is 14 percent of the total engine mass flow. For L2, it is 4 percent. No testing was done to quantify L3. However, it is similar to L1 in pressure ratio and geometry, so they are assumed to be of equal magnitude. Despite the rather large magnitudes of these leakages, cycle analysis in Section 3.6 will show that they agree well with other cycle and component data.

3.6 Creating a Dynajet Cycle Model with Nonidealities

The cycle model first introduced in Figure 3-1 was developed to fully represent the Dynajet nonidealities identified thus far. Included are:

- Flow leakages L1-L3
- Heat leakages Q1-Q5
- Effects of compressor heat transfer and distortion reflected in effective efficiency
- Effects of turbine distortion reflected in efficiency

The remainder of this section discusses finding the best model parameter match to Dynajet data.

3.6.1 Initial Unmatched Cycle Model

Sections 3.3-3.5 focused on using appropriate physical models to estimate the effects of nonidealities on the Dynajet. Thus, in attempting to find the best model parameter match to Dynajet data, a baseline model using the original nonideality estimates was chosen as a starting point. Major parameters include:

- Q1 = Comp. Inlet Net = 16.9% of ideal shaft power
- Q2+Q3+Q4+Q5-Q1 = Comp. Exhaust Net = 18.1% of ideal shaft power
- Q2 = 17.6% of total
- Q3 = 3.9% of total
- Q4 = 55.9% of total
- Q5 = 22.6% of total

  } 100% of heat transfer to comp. exhaust

- L1 = 14% of total engine mass flow
- L2 = 4% of total engine mass flow
- L3 = 14% of total engine mass flow
- $\eta_{c,adiabatic}$ = Ref. Value
- $\eta_{c,effective}$ = Ref. Value – 5.7 points
- η_t = Ref. Value – 3 points
- Fuel Flow = 0.961 g/s

The compressor inlet heat transfer (Q1) and compressor effective efficiency listed are the estimates made by distortion analysis in Section 3.4.1, the flow leakages are exactly those found in Section 3.5, and the turbine efficiency listed results from Section 3.4.2 analysis. The only variation from original estimates is the net heat transfer to the compressor exhaust. Rather than the 22.3 percent of ideal shaft power found in Section 3.3, 18.1 percent was chosen to maintain a 26 K temperature rise with reduced flow due to

leakage. Note, however, that the relative contributions of Q2-Q5 to this total are held constant.

In all prior analysis, the heat exchanger was modeled by an effectiveness and pressure ratios. However, an alternative approach was chosen for this modeling effort. Rather than fix heat exchanger effectiveness, the gas-side temperature drop was instead fixed to match April '03 engine data. This data is expected to be very accurate due to thermocouple immersion in a relatively uniform temperature field with little opportunity for error. Thus, heat exchanger effectiveness was calculated as an output rather than being used as an input.

The cycle outputs that result from modeling estimates are shown in Figure 3-51. The calculated power output is 2.9 kW, only 0.37 kW higher than the 2.53 kW required to match the April '03 data. Though still unmatched, this difference is substantially less than the 8.1 kW inconsistency found using simple adiabatic analysis in Section 3.1, reflecting progress made in closing the cycle.

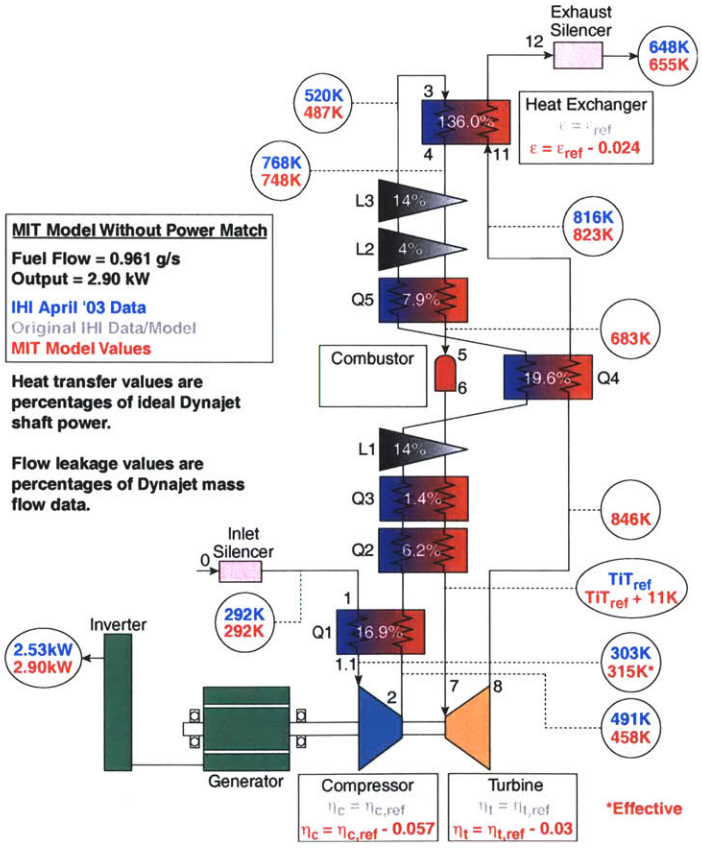

Figure 3-51: Dynajet cycle model without power match.

The unmatched cycle has a number of positive attributes. Most notable is the small 2.4 point differential between the calculated heat exchanger effectiveness and the reference value from rig data. This near match can be attributed to the flow leakage. By reducing air-side mass flow, the leakage allows greater air-side temperature rise for the same gas-side heat transfer. Without flow leakage, the calculated heat exchanger effectiveness would be about 20 points lower. Other noteworthy characteristics of the unmatched cycle are compressor and turbine efficiencies close to reference (rig) values. Adiabatically, the compressor operates at its reference efficiency, while the turbine is only 3 points below its reference efficiency. Finally, half of the cycle temperatures match April '03 data within 1 percent or less.

Ways to improve the cycle model include power matching, increasing heat exchanger effectiveness, and improving temperature matches to April '03 data between the compressor exhaust and combustor inlet. Improving temperature matches between the compressor exhaust and combustor exhaust requires raising the model temperatures, which are between 3 and 7 percent too low.

3.6.2 Best Cycle Model

The approach taken to achieving the best cycle match to April '03 data was to match the engine power output of 2.53 kW and reference heat exchanger effectiveness while reducing model/data temperature differences between the compressor exhaust and combustor inlet. A number of cycle parameters can be adjusted to accomplish these goals in whole or in part. Compressor performance and compressor exhaust heat transfer were chosen for adjustment because they have the greatest influence over the matching objectives. Reducing compressor efficiency lowers output and increasing compressor exhaust heat transfer lowers the model/data temperature differences. Adjusted cycle parameters are as follows:

- Q1 = Comp. Inlet Net = 18.1% of ideal shaft power
- Q2 = 17.0% of total
- Q3 = 5.1% of total
- Q4 = 46.8% of total
- Q5 = 31.2% of total

} 100% of heat transfer to comp. exhaust

- Q2+Q3+Q4+Q5-Q1 = Comp. Exhaust Net = 22.8% of ideal shaft power
- $\eta_{c,adiabatic}$ = Ref. Value – 2.5 points
- $\eta_{c,effective}$ = Ref. Value – 8.4 points

The heat transfer was increased from 16.9 to 18.1 percent of the ideal shaft power, the average of the heat transfers calculated uniformly and nonuniformly (16.9 and 19.2 percent, respectively). The net heat transfer to the compressor exhaust was increased from 18.1 to 22.8 percent of the ideal shaft power. Furthermore, the relative contributions from Q2-Q5 were changed slightly to increase the share from the air-side heat exchanger exhaust (Q5). Finally, the adiabatic compressor efficiency was reduced 2.5 points relative to the reference value, which corresponds to an effective efficiency of 8.4 points below the reference value when accounting for the compressor inlet heat transfer.

The final cycle match shown in Figure 3-52 achieves the goals of 2.53 kW power output and heat exchanger effectiveness matched to the reference value. Model/data temperature differences in the compressor exhaust are significantly reduced. While the deltas for T_{t3} and T_{t4} were 33 and 20 K for the unmatched model, the matched model reduces these differences to 18 and 6 K.

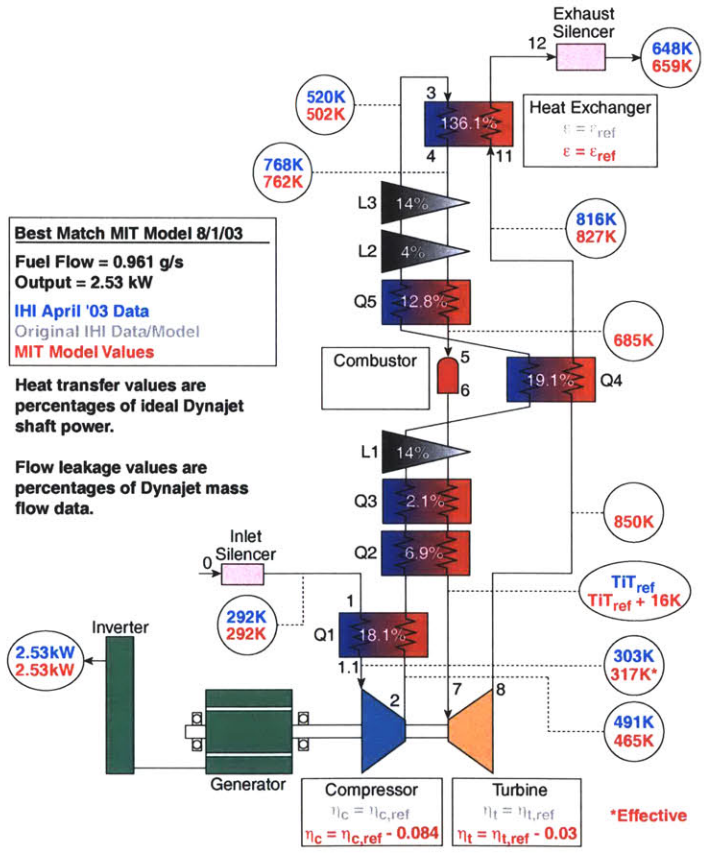

Figure 3-52: Dynajet cycle model with best match to IA April '03 data.

The final cycle match shows only minor disagreement between model and rig temperature measurements. The disagreement percentages are summarized in Table 3.3.

The largest disagreement is 5 percent, a fairly small number given the number of variables involved in the analysis. This and other disagreements can be attributed to measurement error or modeling inaccuracy. The measurement errors can be significant. For example, a conduction error estimate made for the NGV thermocouples found that they read at least 6.8 K low. If this is the case, the difference between model and engine (reference) conditions is not 16 K but rather 9 K or less. The NGV thermocouple conduction error analysis is described in Appendix B.

Table 3.3: Difference between IA April '03 data and best match cycle model.

	IA Data	MIT Best Match Model, 8/1/03	Percent Difference
T_{t1} (K)	292	292	0.00
$T_{t1.1}$ (K)	303	317	4.62
T_{t2} (K)	491	465	5.30
T_{t3} (K)	520	502	3.46
T_{t4} (K)	768	762	0.78
T_{t5} (K)		685	
T_{t7} (K)	Ref.	Ref. + 16	
T_{t8} (K)		850	
T_{t11} (K)	816	827	1.35
T_{t12} (K)	648	659	1.70

3.7 Dynajet Cycle Model Analysis

For this research, accurately modeling the Dynajet cycle is a means to an end, not the goal. The goal is to determine how to best change the Dynajet cycle for improved performance. This section looks at the Dynajet model with the intent of pinpointing sources of Dynajet performance penalties and considering the ramifications of their removal.

It is a valuable exercise to first look at the Dynajet cycle from the perspective of its temperature-entropy diagram shown in Figure 3-53. From the diagram, it is straightforward to discern the effects of cycle nonidealities. A description of each leg of the cycle follows:

1-1.1) Heat transfer to the compressor inlet (Q1) is evidenced by an increase in temperature and entropy.

1.1-2) Flow is compressed at an adiabatic efficiency 2.5 points below the reference value (8.4 points below the reference value, effective) with associated entropy increase.

2-3) Heat transfer to the compressor exhaust (Q2-Q5) is responsible for the lack of coincidence between stations 2 and 3.

3-4) Temperature and entropy increase through air-side of heat exchanger.

4-5) Heat exchanger exhaust mixing with low temperature leakages L2 and L3 cause a reduction in temperature and entropy, as does heat leakage through Q5.

5-6) Heat is added by combustor.

6-7) Combustor exhaust mixing with low temperature leakage L1 causes a reduction in temperature and entropy, as does heat leakage through Q2 and Q3.

7-8) Work is extracted from flow by turbine at efficiency 3 points below the reference value. Temperature decreases and entropy increases.

8-11) Heat leakage through Q4 decreases turbine exhaust temperature.

11-12) Temperature and entropy drop through gas-side of heat exchanger.

The effect of flow leakage L1 is most dramatic, reducing the turbine inlet temperature by 100 K and severely decreasing the enthalpy available to the turbine.

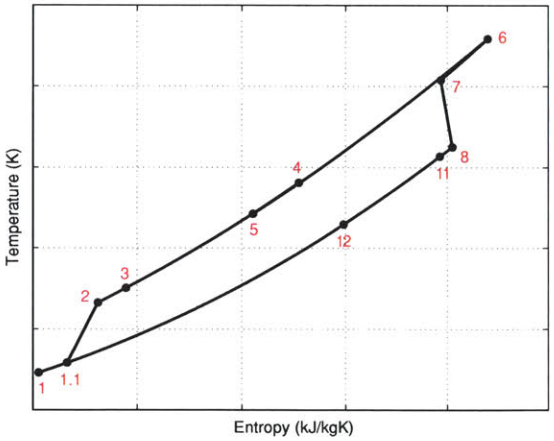

Figure 3-53: Dynajet T-S diagram.

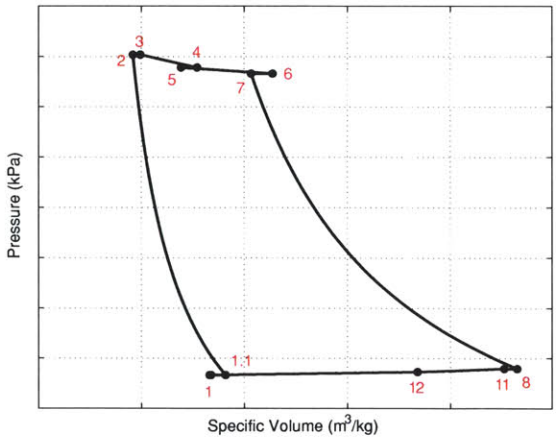

Figure 3-54: Dynajet P-V diagram.

3.7.1 Impact of Nonidealities on Dynajet Performance

The effects of various secondary nonidealities on power output at fixed fuel flow are shown graphically in Figure 3-55. "Secondary nonidealities" refer to heat leakage, flow leakage, and turbomachinery adiabatic efficiencies below design levels. Thus, the bar above Q1 on the plot represents the amount of additional electric output that could be recovered from the cycle with the removal of heat transfer to the compressor, while the η_t bar represents that amount of electric output that could be recovered by increasing the turbine efficiency by 3 points to its reference (rig) value.

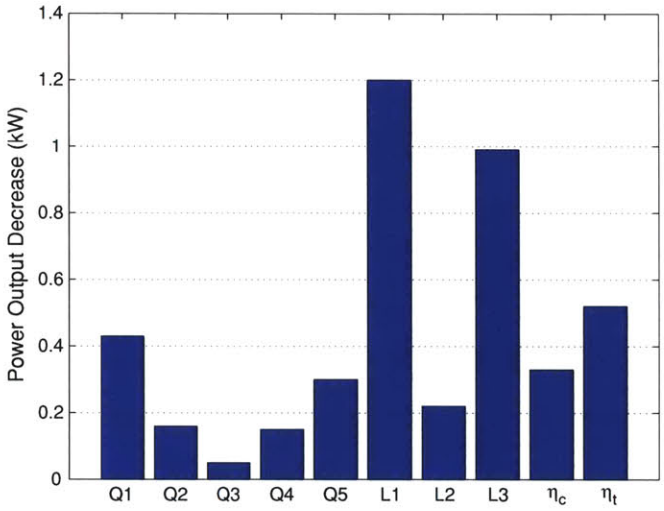

Figure 3-55: Power output debit due to nonidealities at constant fuel flow = 0.961 g/s.

Leakage L1 has the greatest impact on performance, debiting the cycle 1.2 kW. L3 is a close second at 1 kW, while L2's debit is only 0.2 kW due to the small magnitude of leakage. Among the heat leakages, Q1 has the greatest impact at over 0.4 kW. Q3 debits the cycle about 0.3 kW, and the remaining heat transfer paths all have impacts of less than 0.2 kW. The effects of compressor and turbine efficiencies below design levels are approximately 0.3 and 0.5 kW, respectively. Alternatively, Figure 3-56 shows the fuel flow increase due to secondary nonidealities at constant power output.

Flow Leakage Impact

The modes by which heat transfer and thermal distortion effect Dynajet performance were carefully considered in their respective sections of this thesis. What has not been considered is the impact of flow leakage. Figure 3-55 and Figure 3-56 show that flow leakage has the

greatest effect of all nonidealities on Dynajet performance. The reasons for this warrant analysis.

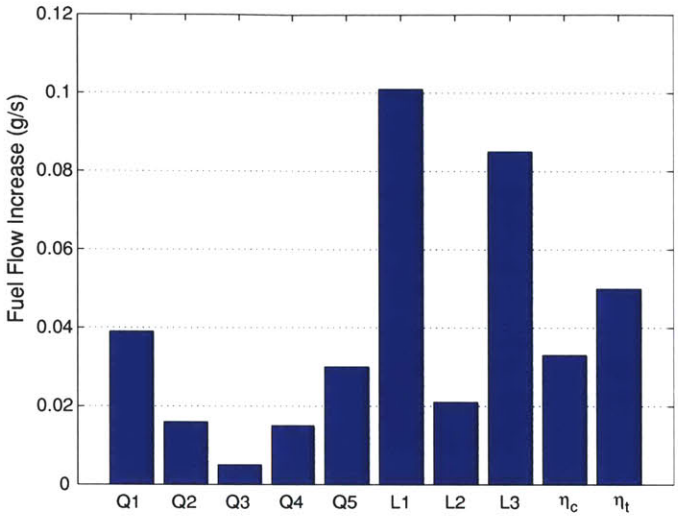

Figure 3-56: Fuel flow increase due to nonidealities at constant power output = 2.53 kW.

Figure 3-57 shows the variation of power output, overall efficiency, turbine inlet temperature, and heat exchanger heat transfer as the leakages L1-L3 are uniformly varied from 0 to 100 percent of their nominal value at constant fuel flow. The primary effect of flow leakage is to reduce the amount of heat transferred in the heat exchanger by limiting the air-side capacity for it. In doing so, turbine inlet temperature, overall efficiency, and power output are limited as well. The total effect of all flow leakage at constant fuel flow is a power reduction of 3.5 kW. Heat exchanger heat transfer without leakage is more than 20 kW larger than it is with leakage. Figure 3-58 and Figure 3-59 show the same effects in light of T-S and P-V diagrams.

Leakage has an important effect on turbine pressure ratio that can be seen best in the Figure 3-59 P-V diagram. The turbine inlet pressure with leakage is higher than it is without it. This is due to the fact that the mass flow through the air-side of the heat exchanger is higher without leakage, which increases its pressure loss. Off-design pressure ratio is a function of corrected mass flow [30]:

$$\frac{P_2}{P_1} = 1 - \left(\frac{\dot{m}\frac{\sqrt{RT}}{P}}{\left(\dot{m}\frac{\sqrt{RT}}{P}\right)_{des}} \right)^2 \left(1 - \frac{P_2}{P_1}\right)_{des} \tag{3.31}$$

This effect is included in modeling of Dynajet performance. Thus, the power output and overall efficiency benefits of reducing leakage are partially diminished by reduced turbine pressure ratio.

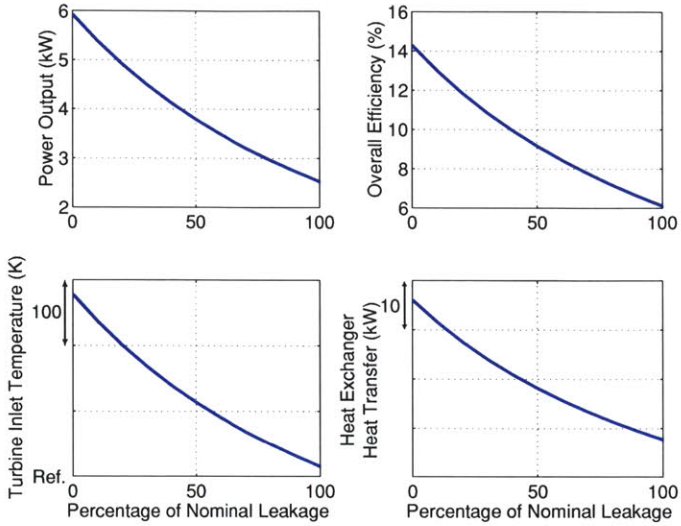

Figure 3-57: Impact of flow leakage on performance at constant fuel flow = 0.961 g/s.

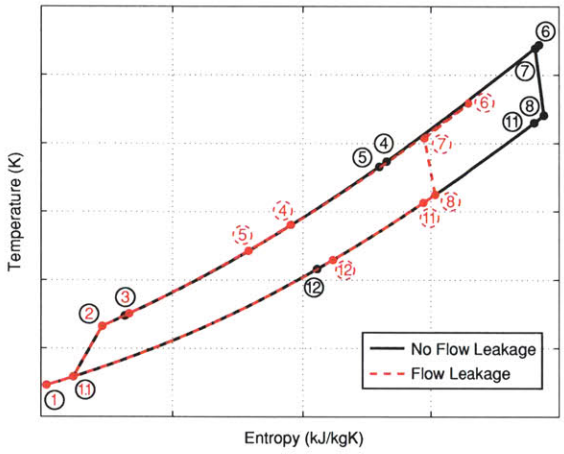

Figure 3-58: Dynajet T-S diagrams with and without flow leakage at constant fuel flow = 0.961 g/s.

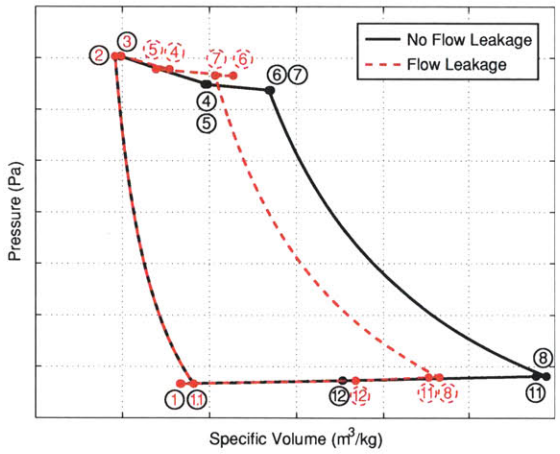

Figure 3-59: Dynajet P-V diagrams with and without flow leakage at constant fuel flow = 0.961 g/s.

Figure 3-60 shows the effects of various degrees of flow leakage at constant power output. The total impact of flow leakage is approximately 0.2 g/s of fuel flow. Again, the cause is reduced capacity of the heat exchanger to transfer heat with leakage.

The T-S and P-V diagrams for performance with and without leakage at constant power are shown in Figure 3-61 and Figure 3-62. It is worth noting that the air-side heat exchanger temperature rise is about the same with and without leakage because this is

controlled by effectiveness, which is the same for both. The effect of leakage can be seen on the gas-side where the temperature drop is much larger without leakage because the air-side can accept more heat transfer. Effectiveness is a useful parameter, but it does not fully capture the influence of heat exchanger heat transfer on performance.

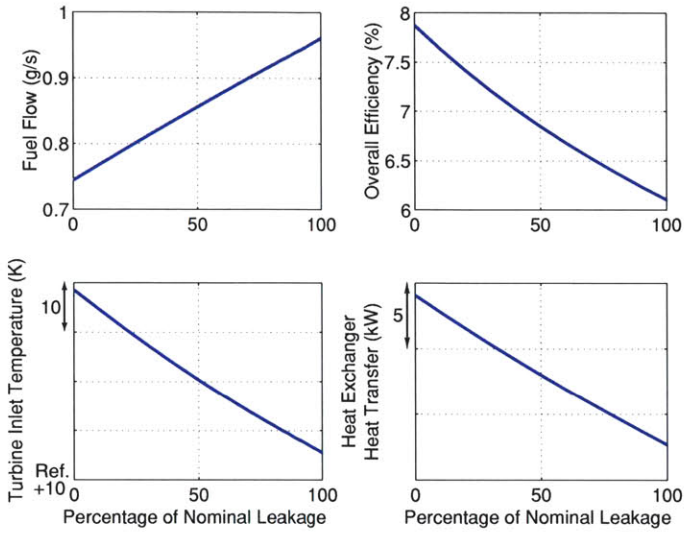

Figure 3-60: Impact of flow leakage on performance at constant power output = 2.53 kW.

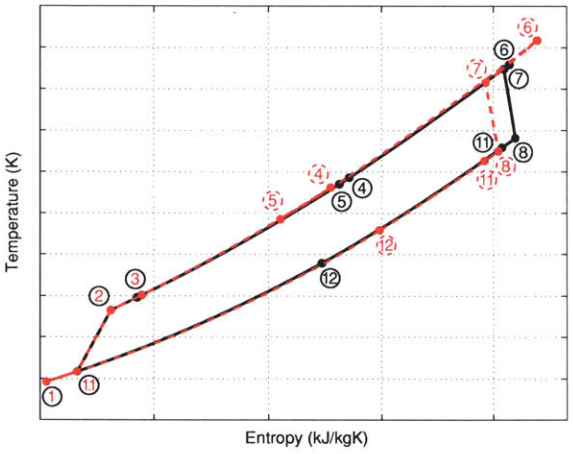

Figure 3-61: Dynajet T-S diagrams with and without flow leakage at constant power output = 2.53 kW.

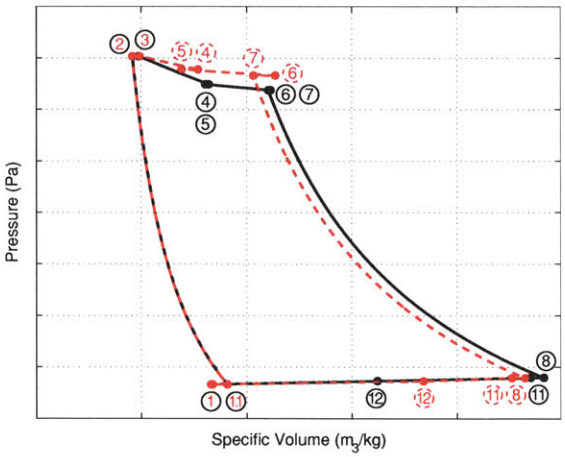

Figure 3-62: Dynajet P-V diagrams with and without flow leakage at constant power output = 2.53 kW.

3.7.2 Potential for Dynajet Performance Improvement

This section considers two major improvement possibilities for the Dynajet. The first is removal of all secondary nonidealities. Dynajet operation under this condition can be considered an upper limit on performance. The second improvement possibility is removal

of those nonidealities that are straightforward to fix, a more practical and expedient option. Relatively straightforward improvements include reducing heat transfer to the compressor exhaust and reducing flow leakage. In addition to improving overall efficiency, reducing flow leakage also has the effect of reducing turbine distortion by decreasing thermal nonuniformity at the combustor exit. Difficult engine improvements include reducing heat transfer to the compressor inlet, reducing compressor distortion, and improving component efficiencies. These improvements would require significant redesign.

Upper Performance Limit

Dynajet performance with all secondary nonidealities removed was calculated to determine its upper performance limit. All heat and flow leakages were removed, and the compressor and turbine efficiencies were restored to their design values. To give some idea of the range of improvement possibilities, two extreme cases were considered: fixed power output and maximum power output. The cycle limit imposed to define maximum power output was a turbine exit temperature of 923 K. This is the same fuel flow limiter used by the BOM Dynajet.

At constant power output, removal of all secondary nonidealities makes it possible to reduce fuel flow to 0.611 g/s. This is a 36 percent reduction relative to the BOM Dynajet. Overall efficiency at this output and fuel flow is 9.6 percent, a 3.5 point increase. As a consequence, the turbine exit temperature is reduced from 850 K to 737 K.

At a maximum turbine exit temperature of 923 K, the Dynajet with no secondary nonidealities produces 6.43 kW, 154 percent more than the BOM Dynajet. At this much higher output, the fuel flow is 0.835 g/s, still 13 percent less than the current Dynajet. The overall efficiency is 17.9 percent, 11.8 points higher than the current Dynajet and 8.3 points higher than the constant power output improvement case. This overall efficiency approaches that of small diesels, between 20 and 25 percent. The overall efficiency is higher at higher output because the turbine inlet temperature is greater. This trend is a characteristic of regenerated gas turbines. At constant compressor pressure ratio, cycle efficiency increases with increasing turbine inlet temperature.

Expedient Performance Limit

Before calculating the "expedient" performance limit for Dynajet improvement, it is first necessary to determine what is "expedient." It is expected that eliminating flow leakage is possible through the use of bellows. Heat leakage, conversely, can be reduced but never completely eliminated.

To quantify the potential for heat leakage reduction, an engine test was performed with insulation over the outside of the turbine exhaust, combustor, and heat exchanger. Figure 3-63 compares wall temperatures measured in this test to those measured without insulation. The wall temperatures with insulation were as much as 26 percent higher, indicating much lower heat transfer. This was reflected in the temperature rise through the compressor exhaust, which insulation reduced from 26 K to 7 K. As a result of insulating, the Dynajet corrected fuel flow was reduced from 0.965 g/s to 0.935 g/s.

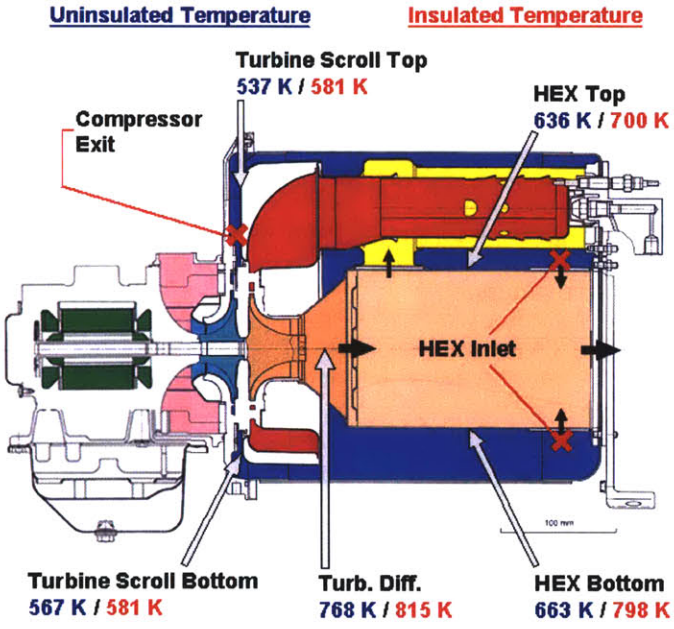

Figure 3-63: Compressor exhaust wall temperatures with and without insulation.

The results of insulation testing are useful for modeling potential improvements to the Dynajet. The insulated data can be loosely matched to the engine model by reducing net heat transfer to the compressor exhaust by 80 percent. This results in a compressor exhaust temperature rise of 7 K, a power output match, and fuel flow of 0.935 g/s. At a fuel flow of 0.961 g/s, the same reduction in compressor exhaust heat transfer results in a power output

of 2.82 kW. An 80 percent reduction in compressor exhaust heat transfer may be taken as the expedient limit of performance improvement with regard to heat leakage.

Another uncertainty of performance improvement is the optimal heat exchanger effectiveness. Unlike increases in compressor and turbine efficiency, which can only help engine performance, the optimal heat exchanger effectiveness for maximum overall cycle efficiency is less than 100 percent. This optimum is the point at which the benefits of increased heat transfer are outweighed by increasing heat exchanger pressure loss. It is worthwhile to verify the prudence of keeping the heat exchanger effectiveness at the reference value in any redesigns.

The heat exchanger pressure ratio may be related to the effectiveness as follows:

$$\pi_r = 1 - \alpha M_r^2 \left(\frac{\varepsilon}{1-\varepsilon} \right) \tag{3.32}$$

where α is bypass ratio, M_r is regenerator Mach number, and ε is regenerator effectiveness [31]. The value of αM_r^2 that matches the current Dynajet is 0.011. Using this value, Eq. (3.32) is plotted over a range of effectivenesses in Figure 3-64. Turbine inlet temperature is held constant at the reference value. The figure shows that the current effectiveness is already optimal, so no heat exchanger redesign is warranted. Figure 3-65 shows the variation of cycle power with effectiveness.

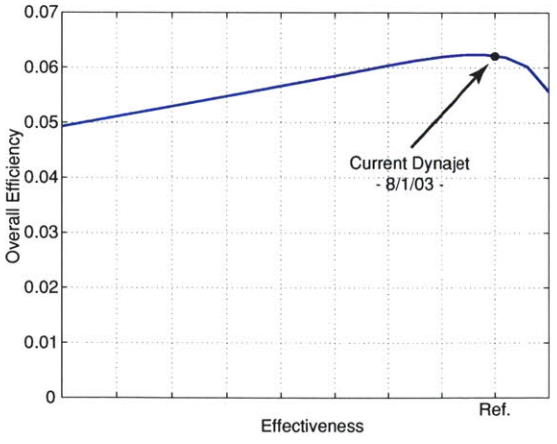

Figure 3-64: Impact of heat exchanger effectiveness on overall efficiency at constant turbine inlet temperature.

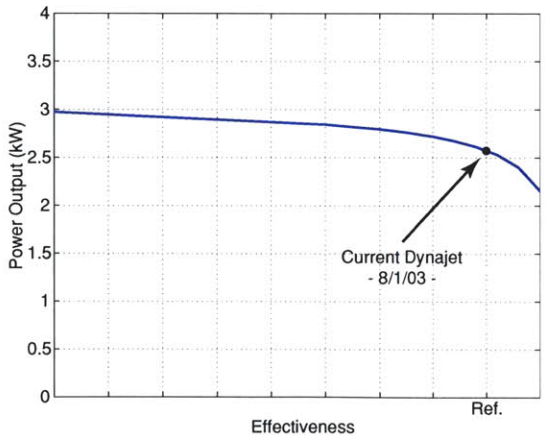

Figure 3-65: Impact of heat exchanger effectiveness on power output at constant turbine inlet temperature.

Considering the analysis just discussed, four scenarios or "packages" were examined for the expedient improvement of Dynajet performance:

Package A

- Flow leakage eliminated
- Turbine distortion eliminated
- 80% reduction in net heat transfer to compressor exhaust

Package B

- 50% reduction in flow leakage
- 50% reduction in turbine distortion
- 80% reduction in net heat transfer to compressor exhaust

Package C

- Flow leakage eliminated
- Turbine distortion eliminated

Package D

- 50% reduction in flow leakage
- 50% reduction in turbine distortion

Table 3.4 lists performance for each of these improvement packages under four limiting conditions: a power output of 5 kW, a turbine exit temperature of 923 K, an inverter limited power output of 3 kW (output beyond this level would require upgrading the inverter), and a current engine power output of 2.6 kW. The table also lists the Bill of Materials Dynajet performance for comparison. Figure 3-66 graphically shows improvement package performance over a range of fuel flows.

Package A gives the highest overall efficiency for each limiting condition, achieving significant improvement for all. At the lowest output of 2.6 kW, Package A increases overall efficiency by 2.5 points to 8.6 percent. At the highest output of 5 kW, the improvement is larger. At 13.5 percent, the overall efficiency is more than double that of the BOM Dynajet. Overall efficiencies for the inverter and turbine exit temperature limited cases are 9.5 and 10.6 percent, respectively.

At the same turbine exit temperature, Package B has higher output than Package A because of the aforementioned heat exchanger pressure ratio issue. With more leakage, Package B suffers less of a pressure loss through the heat exchanger. In fact, the BOM Dynajet with no flow leakage reduction and 80 percent reduction of heat transfer to the compressor exhaust has the highest power output potential. At a turbine exit temperature of 923 K, it produces 3.84 kW at an overall efficiency of 8.3 percent.

It should be noted that potential for improvement to turbine exit temperature limited power outputs and beyond may be complicated by matching, turbomachinery performance, and material considerations. The analysis performed to create Table 3.4 assumed that the turbine is able to pass the BOM engine mass flow at all turbine inlet temperatures. Unfortunately, this simplification may not be accurate. At an output of 5 kW,

the turbine inlet corrected mass flows for Packages A, B, C, and D are between 8 and 10 percent higher than the turbine design point shown in Figure 3-49. Since, at this time, a full turbine map does not exist for the BOM turbine, it is not possible to assess if a turbine redesign is needed. Analysis further assumed that the BOM Dynajet turbine efficiency of could be maintained under all improvement scenarios. However, this assumption gives no consideration to matching, which may influence efficiency. Finally, the turbine inlet temperatures required for 5 kW of power output are higher than current production limits.

Table 3.4: Expedient improvement package performance.

		Power (kW)	Overall Efficiency (%)	Fuel Flow (g/s)	Turbine Inlet Corr. Flow (% Design)
BOM Dynajet		2.53	6.1	0.961	98.5
Constant Power (5.0 kW)	A	5.00	13.5	0.856	109.6
	B	5.00	11.4	1.020	107.7
	C	5.00	12.9	0.896	110.5
	D	5.00	10.9	1.060	107.7
TET Limited	A	3.41	10.5	0.755	105.0
	B	3.65	9.3	0.911	103.1
	C	3.36	9.8	0.793	105.0
	D	3.62	8.9	0.943	103.1
Inverter Limited	A	3.00	9.5	0.730	103.1
	B	3.00	8.1	0.857	101.3
	C	3.00	9.0	0.770	104.1
	D	3.00	7.8	0.892	101.3
Constant Power (2.6 kW)	A	2.60	8.6	0.705	102.2
	B	2.60	7.3	0.824	99.4
	C	2.60	8.1	0.745	102.2
	D	2.60	7.0	0.859	100.4

As a result of neglecting the effects of matching, turbomachinery performance, and materials far from the design point, the turbine exit temperature limited and 5 kW results in Table 3.4 have the most uncertainty. Operating conditions for the inverter limited and 2.6 kW results stray less from engine design values, so inaccuracies stemming from modeling simplifications are likely to be smaller.

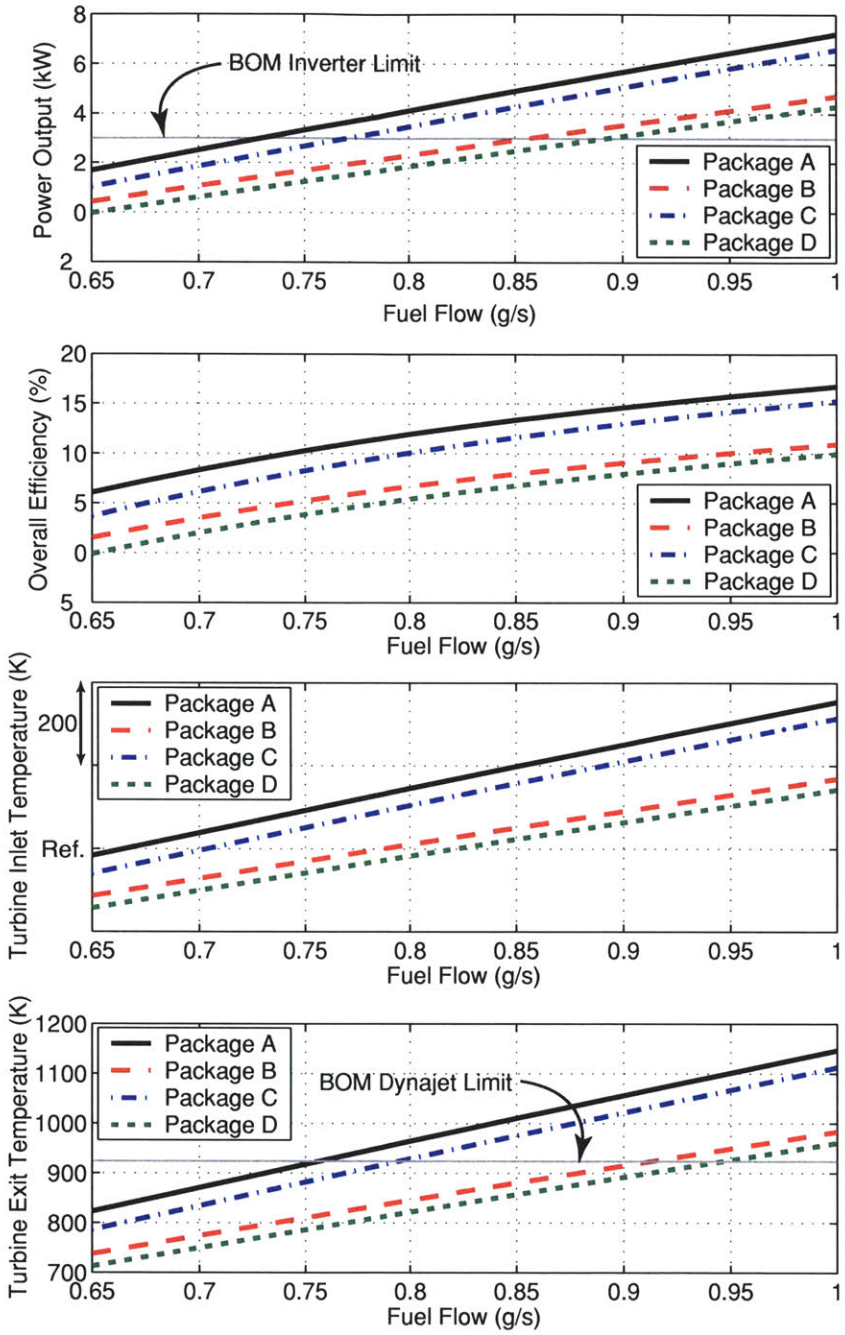

Figure 3-66: Expedient improvement package performance over a range of fuel flows.

3.8 Summary

An engineering study of the Dynajet identified several secondary nonidealities that cause the engine to perform below levels calculated by simple adiabatic cycle analysis. Major nonidealities include flow leakage, heat leakage, flow distortion, and turbomachinery

efficiencies below rig values. The identification of these issues enabled an estimate of the potential for Dynajet performance improvement, the primary goal of the study.

Various modeling methods were applied to quantify the effects of the cycle nonidealities on engine performance. The results of these efforts were combined to produce a cycle model of the Dynajet that closely matches engine data. In addition to producing an exact match to power output, the model matches five of eight station temperatures within 2 percent and matches the remaining three within 5 percent. The compressor effective efficiency, turbine efficiency, and heat exchanger effectiveness are within 8.4, 3, and 0 points of their respective reference values.

Among the nonidealities that affect the Dynajet, flow leakage incurs the greatest penalty. Its removal at constant fuel flow would enable a 138 percent increase in power output and an 8 point increase in overall efficiency. However, a consequence of flow leakage removal is increased heat exchanger pressure drop, which reduces power versus an unaltered Dynajet at constant turbine inlet temperature.

There is significant potential for improved Dynajet performance. Removal of all secondary nonidealities at constant power output would increase overall efficiency from 6.1 to 9.6 percent. Alternatively, removal of all secondary nonidealities at a turbine exit temperature of 923 K would enable increasing power output from 2.53 kW to 6.43 kW, a 154 percent increase. At the same time, overall efficiency would increase by 11.8 points to 17.9 percent.

Removing all Dynajet nonidealities may be relatively difficult; however, there is still potential for substantial performance improvement with less investment. For example, removing flow leakage (and the turbine distortion that accompanies it) and 80 percent of the heat transfer to the compressor exhaust enables power output of 3 kW at an overall efficiency of 9.5 percent. This improvement option allows continued use of the BOM inverter (limited to 3 kW) while increasing overall efficiency by 3.4 points.

Chapter 4

Summary and Conclusions

The market study presented in Chapter 2 identified the Dynajet's strengths and weaknesses in the civil and military markets. In doing so, strategies for Dynajet marketing and engineering improvements were revealed. The engineering study in Chapter 3 resulted in a detailed Dynajet cycle model accounting for all nonidealities. The potential for Dynajet improvement in light of these nonidealities was discussed. To conclude, the results of the market and engineering studies will be combined to judge the competitiveness of improved versions of the Dynajet.

4.1 Market Study Summary

The Dynajet's major competitive advantage in the civil market is very low emission of noise and pollutants. In the military market, advantages are reliability, low weight, and low noise. Major disadvantages in both markets include high purchase price and high power specific fuel consumption.

Purchase price is the largest contributor to Dynajet cost of ownership. As such, it also holds the greatest opportunity for reducing cost of ownership. This is particularly the case in the civil market where annual utilization is low and there is little recognition of other contributors to cost. Annual utilization in the military market is higher, resulting in more sensitivity to other cost contributors such as fuel consumption and maintenance.

Due to significant acquisition cost sensitivity, the U.S. civil market opportunity for the current Dynajet is relatively small. The best near term option is in the marine area, where price is less of a concern and a premium is paid for low noise. In the long term, increasing the power output, adapting the Dynajet for use with an absorption cooler, and/or leveraging its superior emissions characteristics could open other opportunities.

The Dynajet's potential in the military market is more favorable. The current engine is slightly more expensive than existing small military generators on a cost of ownership basis, but this is mitigated by superior reliability and noise characteristics. The best approaches to improving near term competitiveness in this market are increasing power output to 3 kW and reducing fuel consumption and maintenance costs as much as possible.

As in the civil market, adapting the Dynajet for use with an absorption cooler could open additional opportunities.

4.2 Engineering Study Summary

The Dynajet has several small nonidealities that together amount to a significant deviation from ideal performance. These effects are present in larger engines but are of a much smaller magnitude. In fact, removing all secondary nonidealities and setting fuel flow to give a turbine exit temperature of 923 K would result in a power output increase of 154 percent to 6.43 kW. At the same time, fuel flow would be 13 percent less than that of current Dynajet, resulting in an overall efficiency increase of 12 points to 18 percent.

Secondary nonidealities exhibited by the Dynajet include flow leakage, heat leakage, flow distortion, and turbomachinery efficiencies below rig values. Flow leakage contributes the most to performance degradation by inhibiting the heat exchanger's ability to conserve enthalpy. Heat leakage to the compressor exhaust has a similar effect on the heat exchanger, while heat leakage to the compressor inlet and flow path reduces the effective compressor efficiency. Flow distortion effects performance by reducing compressor and turbine efficiency.

Although removing all Dynajet nonidealities may be difficult, expeditious performance improvement is possible by making some of the easiest improvements. For example, removing flow leakage (and the turbine distortion that accompanies it) and 80 percent of the heat transfer to the compressor exhaust enables power output of 3 kW at an overall efficiency of 9.5 percent.

4.3 Competitiveness of an Improved Dynajet

Improvement Package A is the best expedient option for maximizing the Dynajet's overall efficiency. Described in Section 3.7.2, this improvement package includes the elimination of all flow leakage, 80 percent reduction in net heat transfer to the compressor exhaust, and elimination of turbine distortion. Figure 4-1 shows ownership cost of this improved Dynajet at 2.6, 3, and 5 kW power outputs. For comparison, the Bill of Materials Dynajet and competitor military generators are also shown.

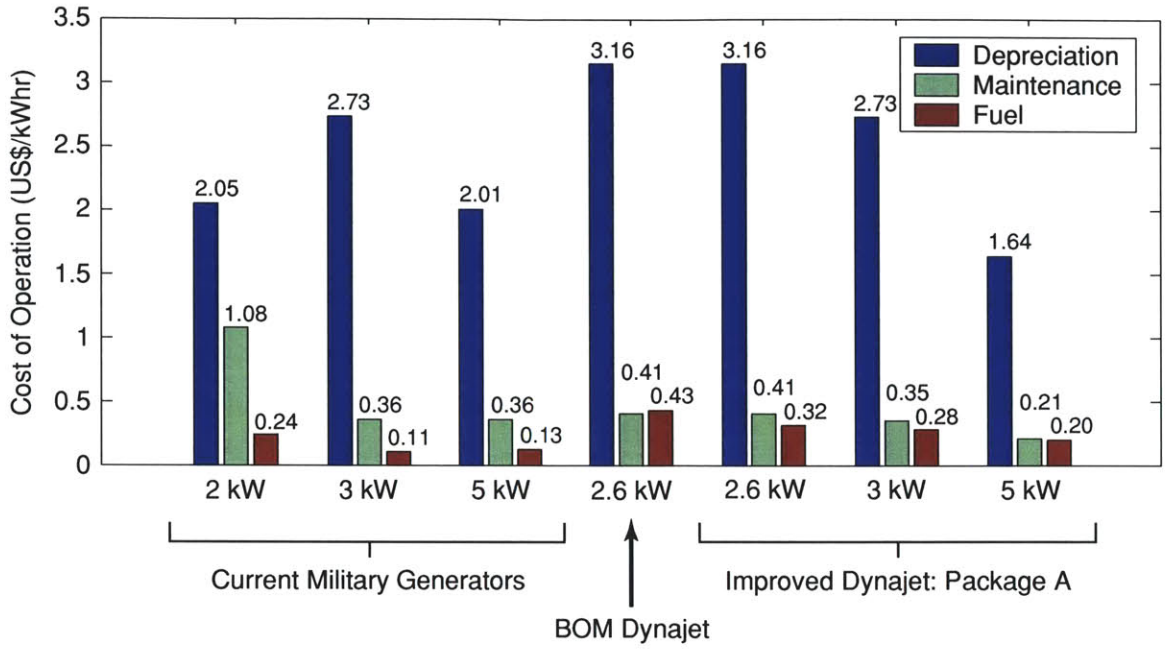

Figure 4-1: Improved Dynajet and military generator cost components at 280 hours annual output.

At a power output of 2.6 kW, the improved Dynajet is 22 percent more expensive per unit power than the current 3 kW TQG. Although the improved Dynajet fuel cost is reduced by 26 percent relative to the BOM Dynajet, the contribution of depreciation to overall cost is much greater and remains unchanged. As a result, the 2.6 kW improved Dynajet is still between 15 and 56 percent more expensive to own than the military generators.

A 3 kW improved Dynajet is much more favorable economically than a 2.6 kW version. At this output, the depreciation cost of the improved Dynajet exactly equals that of the military 3 kW TQG. Although fuel consumption is still high, its contribution to total cost of ownership remains low. The improved Dynajet is only 5 percent more expensive to own than the 3 kW TQG. Reducing Dynajet maintenance cost from \$1.06/hr to \$0.58/hr would set their ownership costs equal. A Dynajet with this power output would be very well positioned to fill generator needs in the U.S. military. Noise and reliability issues with the current 3 kW TQG may be a cause for replacement with an improved Dynajet; a quiet, reliable, competitively priced alternative.

A 5 kW improved Dynajet has the most competitive ownership cost. At this output, the depreciation cost per kilowatt is nearly half that of the BOM Dynajet, making the 5 kW improved Dynajet 18 percent less expensive to operate than the comparable 5 kW TQG.

Due to increased overall efficiency, the 5 kW improved Dynajet is also more competitive in terms of fuel consumption than lower output versions. Finally, output at this level would open the potential Dynajet market to higher power demand applications common in the U.S. civil market.

For additional comparison, Figure 4-2 (a) and (b) show the generator set plus fuel weight for the 3 and 5 kW improved Dynajets and military TQGs. Since 5 kW power output from the Dynajet would require a larger alternator and inverter, the dry weight for this version was arbitrarily increased from 143 pounds to 223 pounds. This increase assumes that the weight of these components is one-third of the BOM Dynajet weight and that their contribution scales with power output.

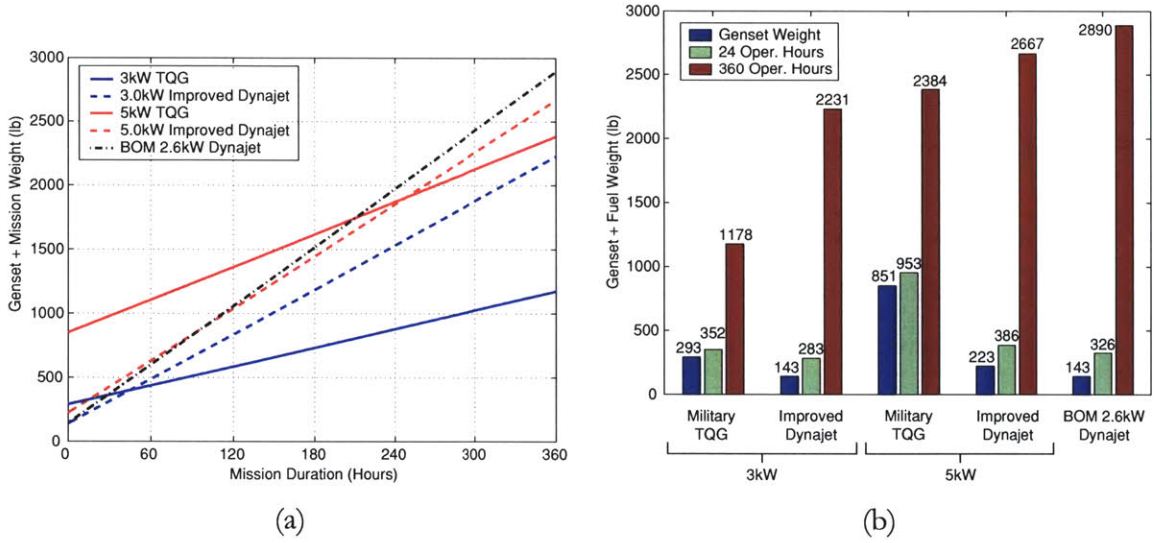

Figure 4-2: Mission weights for Package A improved Dynajets, BOM Dynajet, and militart TQGs.

The 3 and 5 kW improved Dynajets are both superior to their military counterparts for short duration missions. Compared to the 3 kW TQG, the 3 kW Dynajet is 51 percent lighter dry and 20 percent lighter with 24 hours of fuel. It is not until a mission duration of 45 hours that the 3 kW TQG becomes lighter due to lower fuel consumption. The 5 kW Dynajet is even more superior to its counterpart. It is 74 percent lighter dry and 59 percent lighter with 24 hours of fuel. The breakeven point for the 5 kW units is at 248 hours of operation.

From a market perspective, a Dynajet improved with Package A to 5 kW is certainly the best option. Assuming the purchase price can be maintained at $9000, it is 18 percent less expensive to own than the military's 5 kW TQG. It is also lighter for up to 10 days of

continuous operation. The only negative is that the military considers their 5 kW TQG reliable and may not be anxious to replace it (although the extreme quietness of the Dyanjet would be a strong selling point). Beyond the military, 5 kW output is appealing because it allows the Dynajet to accommodate a larger portion of the U.S. market.

From an engineering perspective, improving the Dynajet to 3 kW may be easier than improving it to 5 kW. No turbomachinery redesign is necessary and the current inverter can still be used. Incidentally, these engineering advantages also translate to economic advantages because costs are kept down. Although performances for the 5 kW engines in Table 3.4 are superior to the 3 kW engines, more analysis is needed to ascertain the relative levels of investment required to attain such power levels. The turbine inlet temperature necessary for 5 kW may require a turbine redesign.

Any decision to improve the Dynajet by removing nonidealities will be subject to verification by engine testing. Although it is not possible to judge the Dynajet's improvement potential with absolute certainty until such tests are done, the market and engineering studies suggest that promising results are likely.

Appendix A

MATLAB Cycle Analysis Program

A lumped parameter thermodynamic engine model, also known as a cycle deck, was created in MATLAB for analysis of the Dynajet cycle. The cycle deck can be used for performance prediction or data analysis, depending upon what quantities are known. Performance prediction is achieved from known component characteristics, while data analysis is used to deduce component characteristics from known engine performance.

In its most basic form, the MATLAB program emulates a commercial off-the-shelf program known as GasTurb and is an effective performance prediction tool. Inlet conditions, component characteristics, flow rate, and turbine inlet temperature are taken as inputs. Engine power and fuel flow rate are outputs. A full listing of inputs and outputs appears in Table A.1. The program models components by transfer functions that operate on pressure and temperature inputs. Flow specific heat is varied throughout the cycle as a function of the flow constituents and temperatures.

Table A.1: MATLAB cycle analysis program inputs and outputs.

Inputs	Outputs
Diffuser Inlet Temperature (K)	Station Temperatures (K) and Pressures (Pa)
Diffuser Inlet Pressure (Pa)	Electric Power (kW)
Ambient Pressure (Pa)	Shaft Power (kW)
Mass Flow Rate (kg/s)	Fuel Flow Rate (kg/s)
Intake Pressure Ratio	Power Spec. Fuel Consumption (kg/kW-hr)
Exit Pressure Ratio	Thermal Efficiency
Bearing Loss (W)	
Generator Efficiency	
Inverter Efficiency	
Power Offtake (W)	
Compressor Pressure Ratio	
Compressor Efficiency	
Turbine Inlet Temperature (K)	
Turbine Efficiency	
Burner Pressure Ratio	
Burner Efficiency	
Fuel Heating Value (J/kg)	
Air-Side Heat Exchanger Pressure Ratio	
Gas-Side Heat Exchanger Pressure Ratio	
Heat Exchanger Effectiveness	

The MATLAB program output was compared to GasTurb output for a number of cases to verify its accuracy. One particular comparison is shown in Table A.2. This case was produced to match the original IA model of the Dynajet. The MATLAB program output matches GasTurb output to within 1 percent for all relevant quantities.

Table A.2: Comparison of MATLAB program output to GasTurb output.

Quantity	Percent Error Between MATLAB and GasTurb Output
Tt1 (K)	0.00
Pt1 (kPa)	0.00
Tt2 (K)	0.01
Pt2 (kPa)	0.00
Tt4 (K)	0.17
Pt4 (kPa)	0.00
Tt7 (K)	0.00
Pt7 (kPa)	0.00
Tt8 (K)	0.06
Pt8 (kPa)	0.00
Tt12 (K)	0.27
Pt12 (kPa)	0.00
Power Output (kW)	0.39
Fuel Flow (g/s)	0.71
Thermal Efficiency	0.98

An example of the MATLAB program logic for data analysis to determine component efficiencies is shown in Figure A-1. This method was used to determine component efficiencies from engine data. More specifically, it was used to produce Figure 3-3. As discussed in Section 3.2, inlet conditions, fuel flow, mass flow, all station pressures, and two station temperatures are needed to fully define an adiabatic cycle. The example of Figure A-1 matches specified turbine inlet and exit temperatures. The analysis steps can be summarized as follows:

1. Start with conditions at Station 1.
2. Use compressor pressure ratio and an initial guess for compressor efficiency to attain Station 2/3 conditions.
3. Use air-side heat exchanger pressure ratio and an initial guess for air-side temperature change to attain Station 4/5 conditions.
4. Use fuel flow, burner efficiency, and burner pressure ratio to calculate turbine inlet

conditions.

5. Use turbine pressure ratio and specified turbine exit temperature to determine turbine efficiency and turbine exit pressure.
6. Use gas-side heat exchanger pressure ratio and an initial guess for heat exchanger effectiveness to calculate Station 12 conditions.
7. Calculate heat transfer to heat exchanger air-side and from heat exchanger gas-side using steady flow energy equation. If they match, continue to Step 8. If they do not match, modify air-side temperature change guess appropriately and return to Step 3.
8. Calculate power output.
9. If calculated power output and turbine inlet temperature match the data, continue to Step 10. If not, modify compressor efficiency and heat exchanger effectiveness and return to Step 2.
10. Finished. Current compressor efficiency, turbine efficiency, and heat exchanger effectiveness produce match to data.

Iteration is preformed using the Newton-Raphson method and terminates after specified tolerances are met.

In addition to the two MATLAB program variants described here, several more were created for other tasks such as modeling cycle nonidealities.

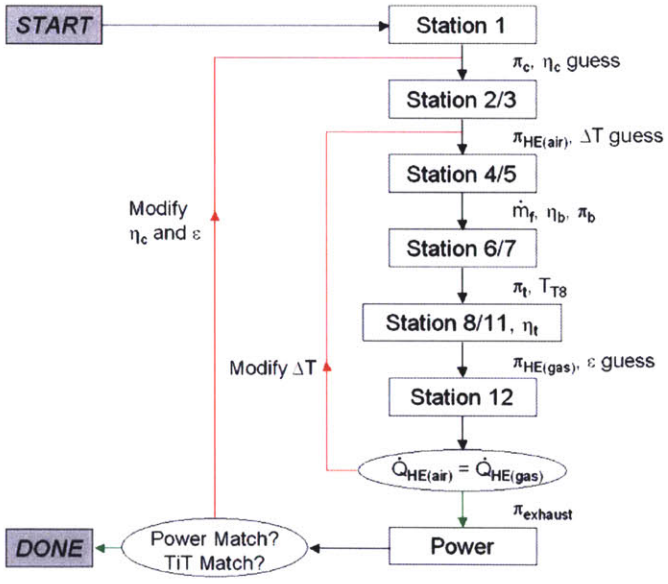

Figure A-1: Matlab program logic for data analysis.

Appendix B

NGV Thermocouple Conduction Loss

Figure B-1 shows the turbine nozzle guide vane leading edge thermocouples. Due to their very small exposed length, these thermocouples are subject to conduction loss to the wall through which the rods pass. This loss causes the thermocouples to indicate temperatures lower than the flow stagnation temperature. This appendix describes the approach taken to estimating the error.

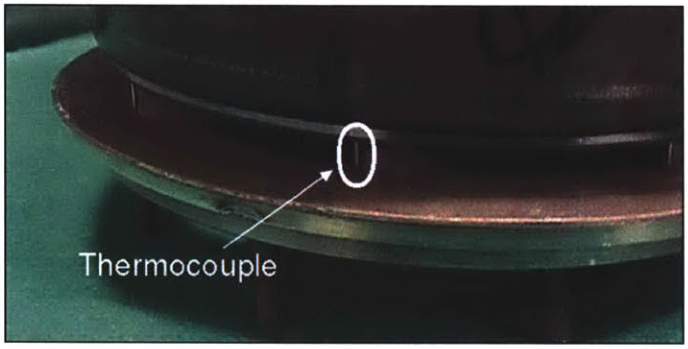

Figure B-1: Nozzle guide vane thermocouples.

The equation from Doebelin for thermocouple conduction loss is as follows [32]:

$$\text{Error} = T_r - T_f = \frac{T_w - T_f}{\cosh(mL)} \tag{B.1}$$

where T_r is the thermocouple rod temperature, T_f is the flow stagnation temperature, T_w is the wall temperature, and L is the exposed thermocouple length. The variable m is given by:

$$m = \sqrt{\frac{h_{rod} C}{kA}} \tag{B.2}$$

where h_{rod} is the rod film coefficient, C is the rod circumference, k is the rod thermal conductivity, and A is the rod cross-sectional area.

Table B.1 summarizes the values used to evaluate Eqns. (B.1) and (B.2). The rod film coefficient was calculated using the Churchill and Bernstein correlation for cylinder cross flow based on the known NGV geometry and mass flow [33]. The wall temperature was estimated as follows:

$$T_w = T_f - \frac{\dot{q}}{h_{wall}} \tag{B.3}$$

The wall heat transfer rate per unit area, $\dot{q}$, was estimated by dividing the total scroll heat transfer calculated in Section 3.3.3 by the surface area of the scroll. The wall film coefficient, h_{wall}, was estimated using a turbulent flat plat correlation, again based on the known NGV geometry and mass flow. The flow temperature was assumed to be the reference turbine inlet temperature plus 16 K to match the best engine model presented in Section 3.6.2.

Table B.1: Thermocouple conduction error analysis values.

Conduction Error Variable	Value
Flow Temperature, T_f (K)	Ref. + 16
Wall Temperature, T_w (K)	Ref. - 1
Exposed Rod Length, L (mm)	2.3
Rod Film Coefficient, h_{rod} (W/m^2K)	1441
Rod Circumference, C (mm)	2.5
Rod Thermal Conductivity, k (W/mK)	16
Rod Cross-Sectional Area, A (mm^2)	0.471
Wall Heat Transfer Rate per Unit Area, q (W/m^2)	6134
Wall Film Coefficient, h_{wall} (W/m^2K)	352

Figure B-2 shows the conduction error calculated over a range of flow/wall temperature differentials. The dashed red line indicates the 17 K differential that results from the wall temperature estimate of the reference temperature minus 1 K in Table B.1. At this differential, the conduction error is approximately 6.8 K. Note, however, that this is a lower bound on the error. Due to high velocities, the heat transfer at the wall adjacent to the NGVs is likely to be substantially higher than the scroll average, the value upon which the 17 K differential is based. That being the case, the flow/wall temperature differential is likely to be significantly larger, as is the conduction error.

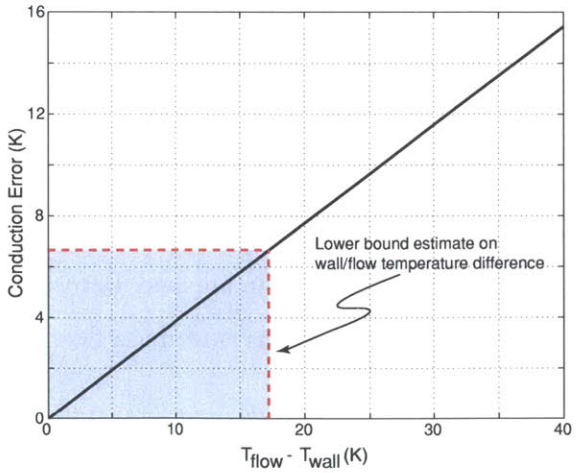

Figure B-2: NGV thermocouple conduction error.

Bibliography

[1] Nakajima, T. et al. "The Development of the Micro Gas Turbine Generator." Yokohama International Gas Turbine Conference, 1995.

[2] Freedonia Group. "Portable Power Supplies to 2005." Report# 1471, 2000.

[3] U.S. Department of Commerce. "Current Industrial Report: Motors and Generators." Year 2000, Issued Sept. 2001.

[4] Electrical Generating Systems Association. "Quarterly Generator Shipment Survey." Quarter Ending December 31, 2001, Issued Feb. 11 2002.

[5] *The Economist*, November 2000.

[6] California Air Resources Board. "Public Meeting to Consider Approval of the California's Off-Road Large Spark-Ignited Engine Emissions Inventory." Appendix B, October 1998.

[7] Oak Ridge National Laboratory. "Advanced Power Generation Systems for the 21st Century: Market Survey and Recommendations for a Design Philosophy." Report# ORNL/TM-1999/213.

[8] DoD Project Manager Mobile Electric Power web site: http://www.pmmep.org.

[9] Phone conversation with Terry Dean, Marine Corps Light Armored Vehicle Program Managers Office. April 29, 2002.

[10] Phone conversation with James Flynn, General Motors Defense. May 1, 2002.

[11] Recreational Vehicle Industry Association. "RV Shipments Data." July 2003.

[12] Recreational Vehicle Industry Association. "Recreation Vehicle Shipments." February 2002.

[13] Carver Yachts promotional CD, 2002.

[14] National Marine Manufacturer's Association. "Boating 2001: The Boating Market." http://www.nmma.org/facts/boatingstats/2001/files/boatingmarket.asp.

[15] Disclosure Global Access Research Database, http://www.primark.com/ga/dga.asp, Thomson Financial, 2001.

[16] Dutch Gas Turbine Association. "Small Gas Turbines, State of the Art and Market Potential, with a Special Focus on the Netherlands Market." January 2001.

[17] Capstone Turbine Annual Report, 2002.

[18] Environmental Protection Agency. "Control of Emissions from Nonroad Spark-Ignition Engines." http://www.epa.gov/otaq/regs/nonroad/equip-ld/hhsnprm/hh-regs3.pdf.

[19] California Air Resources Board. "Small Off-Road Engines." http://www.arb.ca.gov/regact/sore/regs_fin.pdf.

[20] Environmental Protection Agency. "Control of Emissions of Air Pollution from Nonroad Diesel Engines." http://www.epa.gov/otaq/regs/nonroad/equip-hd/frm1998/nr-fr.pdf.

[21] Environmental Protection Agency. "Technical Highlights: Blue Sky Series Engines." http://www.epa.gov/otaq/regs/nonroad/marine/ci/fr/f99048.pdf.

[22] Email from Alan Stout, EPA Engine Programs and Compliance Division. February 20, 2002.

[23] California Air Resources Board. "Proposed Regulation Order: Establish a Distributed Generation Certification Program." http://www.arb.ca.gov/regact/dg01/dg01staffmodification.pdf.

[24] California Public Utilities Commission. "Decision Adopting Interconnection Standards." http://www.cpuc.ca.gov/word_pdf/FINAL_DECISION//4117.pdf.

[25] Gong, Yifang et al. "A Model for Estimating Impeller Performance with Heat Addition." MIT Gas Turbine Laboratory Internal Document, 2002.

[26] Koschel, W. et al. "Effect of Steady State Inlet Temperature Distortion on the Engine Compressor Flow." AGARD Engine Response to Distorted Inflow Conditions, 1987.

[27] Greitzer, E.M. "A Note on Compressor Exit Static Pressure Maldistributions in Asymmetric Flow." CUED/A-TURBO/TR-79, 1979.

[28] Japikse, D. "Turbocharger Turbine Design and Development." Technical Memorandum 265, July 1979.

[29] Meyer, C. and Lowrie III, J. "The Leakage Through Straight and Slant Labyrinths and Honeycomb Seals." Journal of Engineering Power, October 1975.

[30] Kurzke, J. "GasTurb Help File." 2001.

[31] Kerrebrock, Jack L. Aircraft Engines and Gas Turbines. MIT Press: Cambridge, MA, 1992.

[32] Doebelin, Ernest. Measurement Systems: Application and Design. McGraw-Hill: New York, 1983.

[33] Incropera, F. and DeWitt, D. Fundamentals of Heat and Mass Transfer. John Wiley & Sons: New York, 1990.